

## Bone Bioengineering for Mandibular Reconstruction

Kurt Busuttil Naudi BChD (Malta) MFDS RCPS (Glas) MSurgDent (Edin)

This thesis is submitted by the author as the requirement towards the degree of  
Doctor of Dental Surgery in the School of Medicine at the University of  
Glasgow September 2010.

To my parents and my brother, and especially to my wife Antoniella and son Isaac for their patience throughout this project.

## Table of Contents

Reference for Figures.....	- 6 -
Reference for Tables.....	- 12 -
Acknowledgements.....	- 13 -
Declaration.....	- 16 -
Abbreviations.....	- 17 -
Synopsis.....	- 19 -
Literature Review.....	- 22 -
1 Bone.....	- 23 -
1.1 Introduction.....	- 23 -
1.2 Composition.....	- 23 -
1.2.1 Inorganic Salts.....	- 24 -
1.2.2 Organic Matrix.....	- 24 -
1.3 Bone Structure.....	- 24 -
1.3.1 Compact Bone.....	- 24 -
1.3.2 Cancellous (Spongy) Bone.....	- 25 -
1.3.3 Bone cell Types.....	- 27 -
1.3.4 Bone Marrow.....	- 28 -
1.4 Bone Functions.....	- 28 -
1.4.1 Calcium Homeostasis.....	- 29 -
1.4.1.1 Parathyroid hormone.....	- 29 -
1.4.1.2 Calcitonin.....	- 30 -
1.5 Bone Development.....	- 30 -
1.6 Bone Fracture Repair.....	- 35 -
2 Cytokines in the repair of critical-size bone defects of the mandible.....	- 39 -
2.1 Discussion.....	- 39 -
2.1.1 Vascular Endothelial Growth Factor.....	- 39 -
2.1.2 Transforming Growth Factor $\beta$ .....	- 40 -
2.1.3 Fibroblast Growth Factor.....	- 42 -
2.1.4 Prostaglandin E1.....	- 44 -
2.1.5 Bone Morphogenetic Protein.....	- 44 -
2.1.5.1 Bone Morphogenetic Protein 9.....	- 45 -
2.1.5.2 Bone Morphogenetic Protein 4.....	- 45 -
2.1.5.3 Bone Morphogenetic Protein 3.....	- 46 -
2.1.5.4 Bone Morphogenetic Protein 2.....	- 47 -
2.1.5.4.1 BMP-2 use in Primates.....	- 47 -
2.1.5.4.2 BMP-2 use in Dogs.....	- 50 -
2.1.5.4.3 BMP-2 use in Rats.....	- 51 -
2.1.5.4.4 BMP-2 use in Pigs.....	- 53 -
2.1.5.4.5 BMP-2 use in Rabbits.....	- 53 -
2.1.5.5 Bone Morphogenetic Protein 7.....	- 56 -
3 Scaffoldings used for bone regeneration in critical-size bone defects.....	- 59 -

3.1 Discussion .....	- 59 -
3.1.1 Natural scaffolds .....	- 59 -
3.1.1.1 Collagen .....	- 59 -
3.1.1.2 Fibrin .....	- 61 -
3.1.1.3 Alginate .....	- 62 -
3.1.1.4 Silk, Hyaluronan, Chitosan and Agarose .....	- 63 -
3.1.2 Synthetic Scaffolds .....	- 66 -
3.1.2.1 Ceramics .....	- 66 -
3.1.2.1.1 Calcium Phosphate Cements.....	- 66 -
3.1.2.1.2 Bioactive Glasses .....	- 67 -
3.1.2.1.3 Hydroxyapatite.....	- 68 -
3.1.2.1.4 $\beta$ -tricalcium phosphate.....	- 73 -
3.1.2.2 Titanium.....	- 75 -
3.1.2.3 Polymeric materials .....	- 76 -
3.1.2.3.1 Poly( $\alpha$ -hydroxy esters).....	- 76 -
3.1.2.3.1.1 Poly(L-lactic acid) .....	- 76 -
3.1.2.3.1.2 Poly(glycolic acid) .....	- 79 -
3.1.2.3.1.3 Poly(lactic-co-glycolic acid).....	- 81 -
3.1.2.3.1.4 Poly(propylene fumarate) .....	- 83 -
3.1.2.3.1.5 Poly(anhydride).....	- 84 -
3.1.2.3.1.6 Poly(phosphazene).....	- 85 -
3.1.2.3.1.7 Polyethylene glycol.....	- 85 -
Aim .....	- 88 -
4.1 Aim of the study.....	- 89 -
Materials and Methods.....	- 90 -
5.1 Preclinical investigations .....	- 91 -
5.1.1 Rabbit mandible anatomy .....	- 91 -
5.1.2 Dry mandible specimens.....	- 95 -
5.1.2.1 Surgical site creation.....	- 95 -
5.1.2.2 Surgical site support.....	- 95 -
5.1.3 Cadaveric work .....	- 101 -
5.1.3.1 Plain film radiography .....	- 104 -
5.2 Clinical cases .....	- 104 -
5.2.1 Cases .....	- 104 -
5.2.2 Surgical procedure .....	- 107 -
5.2.3 Cone beam computed tomography .....	- 116 -
5.2.4 Mechanical testing .....	- 118 -
5.2.4.1 Preliminary investigations .....	- 118 -
5.2.4.1.1 Selection of testing method.....	- 118 -
5.2.4.2 Clinical case testing .....	- 120 -
5.2.4.2.1 Specimen preparation.....	- 120 -
5.2.4.2.2 Specimen mounting .....	- 120 -
5.2.4.2.3 Mechanical testing machine.....	- 125 -
5.2.5 Quantitative histological assessment .....	- 125 -
5.2.5.1 Quantitative analysis of bone content.....	- 127 -
5.2.5.2 Statistical analysis.....	- 129 -

Results.....	- 130 -
6.1 Clinical Findings .....	- 131 -
6.2 Gross appearance of surgical site.....	- 131 -
6.3 Radiographic assessment .....	- 131 -
6.3.1 Plain Films .....	- 131 -
6.3.2 Cone beam computed tomography .....	- 137 -
6.4 Mechanical testing .....	- 142 -
6.4.1 Treatment side.....	- 144 -
6.4.2 Untreated side .....	- 144 -
6.5 Quantitative histological assessment .....	- 146 -
6.5.1 Gross histological appearance.....	- 146 -
6.5.2 Binary image analysis .....	- 150 -
Discussion.....	- 152 -
7.1 Discussion on the study rationale .....	- 153 -
7.2 Radiographic assessment .....	- 155 -
7.3 Mechanical assessment .....	- 157 -
7.4 Quantitative histological evaluation .....	- 159 -
7.5 Future Study.....	- 163 -
7.6 Clinical implications of the study .....	- 163 -
Conclusions.....	- 165 -
References.....	- 167 -
Abstracts .....	- 182 -

## Reference for Figures

- Figure 1.1 Compact & Cancellous Bone in cross section. (SEER Program)
- Figure 1.2 Flowchart showing the effects of low blood calcium ion concentration on the parathyroid gland
- Figure 1.3 Flowchart showing the effects of high blood calcium ion concentration on the thyroid gland
- Figure 1.4 Diagram of the intramembranous model of bone ossification. (Gartner and Hiatt, Colour Textbook of Histology, p. 122, Figure 7-12. Saunders Co Ltd, Jan 1997)
- Figure 1.5 Diagram of the endochondral model of bone ossification. (Moyer, University of Virginia School of Medicine, Bone and bone formation, CTS/Physiology, Lecture 14, September 30, 2004)
- Figure 1.6 Diagram illustrating the phases of bone remodelling. (F. Hoffmann-La Roche Ltd)
- Figure 5.1 Lateral view of the anatomy of the skull and mandible of the rabbit
- Figure 5.2 Lateral view of skull and mandible with muscles of mastication still attached
- Figure 5.3 Lateral plain radiographic film of an explanted rabbit mandible showing the long roots of the incisor, premolar and molar teeth
- Figure 5.4 Lateral view of dry explanted rabbit mandible
- Figure 5.5 Superior sagittal view of dry explanted rabbit mandible
- Figure 5.6 Close up view of first tested method for mandibular support using Kirshner Wire and titanium screws

- Figure 5.7 Superior view of surgical defect
- Figure 5.8 Inferior view of surgical defect
- Figure 5.9 Superior view of titanium screw in place
- Figure 5.10 Inferior view of titanium screw in place
- Figure 5.11 Posterior view of titanium screw in place in the dry mandible
- Figure 5.12 Inferior close-up view of the titanium screw in place in the dry explanted rabbit mandible
- Figure 5.13 Exposure of mandible and mental nerve in cadaveric case
- Figure 5.14 Placement of titanium screw for reinforcement of the mandible
- Figure 5.15 Titanium screw in place
- Figure 5.16 Segment of bone removed with incisor
- Figure 5.17 Unilateral critical-size surgical defect created
- Figure 5.18 Size 1 E/F speed AGFA Dentus M2 radiographic film
- Figure 5.19 X-ray machine with attached objective measuring tool
- Figure 5.20 Plain film of TCP scaffolding in surgical defect in cadaveric case
- Figure 5.21 Draping method on one of the clinical cases
- Figure 5.22 Titanium screw in place in one of the clinical cases
- Figure 5.23 Unilateral critical-size surgical defect in one of the clinical cases
- Figure 5.24 Placement of TCP scaffolding into surgical site in the clinical case
- Figure 5.25 Closure of the surgical site with resorbable sutures
- Figure 5.26 Dissection of a case, 3 months after placement of graft
- Figure 5.27 Explanted mandible of case 10 before removal of attached soft tissue, superior view

- Figure 5.28 Explanted mandible of case 10 before removal of attached soft tissue, inferior view
- Figure 5.29 Close-up of the superior view of the surgical site of case 10 after removal of most of the soft tissue
- Figure 5.30 Close-up of the inferior view of the surgical site of case 10 after removal of most of the soft tissue
- Figure 5.31 Labelled, explanted mandibles of cases 6, 7 and 8 in formalin on ice
- Figure 5.32 Explanted mandibles of all cases in freezer at -80°C
- Figure 5.33 i-CAT® scanner, with the explanted mandible on the custom made platform
- Figure 5.34 Close-up of the explanted mandible on the acrylic platform in the i-CAT® scanner
- Figure 5.35 Dry rabbit mandible specimen showing failure along the first premolar tooth socket
- Figure 5.36 Specimen in the aluminium box frame
- Figure 5.37 Aluminium box frame
- Figure 5.38 “L” shaped sections of extruded aluminium
- Figure 5.39 Specimen in the box frame covered in tape
- Figure 5.40 Specimen in the larger aluminium frame
- Figure 5.41 Lateral view of the large aluminium frame
- Figure 5.42 Specimen loaded into mechanical testing machine
- Figure 5.43 Loading jig
- Figure 5.44 BOSE Electroforce® 3300 test instrument with VDU of the control computer which displays the load and displacement



- Figure 5.45 H&E stained sagittal section across one of the surgical specimens at x10 magnification
- Figure 5.46 H&E stained section of the regenerate under x20 magnification, showing bone and intervening fibrous tissue
- Figure 5.47 Same image converted into binary format after clean up, leaving the bone coloured black (x20)
- Figure 6.1 Case 10, one week post-operatively
- Figure 6.2 Clinical image of explanted mandibular specimen in one of the cases treated with TCP and rhBMP-7
- Figure 6.3 Case 4, TCP scaffolding alone, at 0, 4 and 8 weeks
- Figure 6.4 Case 5, TCP and rhBMP-7, at 0, 4 and 8 weeks
- Figure 6.5 Case 6 TCP alone at 8 wks
- Figure 6.6 Case 10 with BMP-7 at 8 weeks
- Figure 6.7 Panoramic reconstruction from the i-CAT<sup>®</sup> scan of the mandible in case 10, treated with TCP and BMP-7
- Figure 6.8 Axial (1.00), and coronal sections (2.00 – 20.00) of the surgical site reconstructed from the i-CAT<sup>®</sup> scan of a case treated with TCP and BMP-7. The sites for the various coronal sections are marked on the axial scan in yellow
- Figure 6.9 Panoramic reconstruction from the i-CAT<sup>®</sup> scan of the mandible in a case treated with TCP alone
- Figure 6.10 Axial (1.00), and coronal (6.00 – 22.00) sections of the surgical site reconstructed from the i-CAT<sup>®</sup> scan of a case treated with TCP alone. The sites for the various coronal sections are marked on the axial scan in yellow

- Figure 6.11 A typical mechanical test result showing an abrupt fall in load at the failure point
- Figure 6.12 Histogram of the failure moments of the non-rhBMP-7 specimens (denoted by \*) that were weaker than the specimens treated with rhBMP-7
- Figure 6.13 Histogram of the failure moments of the untreated sides, showing lower values for the specimens that failed across the incisor tooth (denoted by \*)
- Figure 6.14 H&E stained section of a case that received TCP alone showing minimal bone formation (x10)
- Figure 6.15 H&E stained section of a case that received rhBMP-7 showing woven and lamellar bone formation (x40)
- Figure 6.16 H&E stained section of a case that received rhBMP-7 showing minimal amounts of scaffolding (x20)
- Figure 6.17 H&E stained section of a case that received TCP alone showing no bone and large amounts of retained scaffold (x40)
- Figure 6.18 H&E stained section of the mid-surgical field of one of the cases treated with TCP alone. Minimal bone formation is evident (x20)
- Figure 6.19 Inflammation in relation to the scaffold in a case that received TCP alone (x40)
- Figure 6.20 The percentage overall mean bone volume in the two groups and the standard error. The difference in mean bone formation was significant ( $p = 0.014$ )

Figure 6.21 The percentage mean bone volume in mid surgical field of the two groups and the standard errors. The difference in mean bone formation was significant ( $p = 0.009$ )

## **Reference for Tables**

Table 3.1	Types of scaffolding materials used in the repair of bone defects
Table 5.1	Rabbit muscles of mastication
Table 6.1	Magnitude of failure moments for all specimens

## **Acknowledgements**

I would like to thank Dr Helen Marlborough for her help and advice during the early stages of my research.

Thank you to Professor Joseph Barbenel for performing the mechanical testing for the specimens used in this project and for regularly giving useful advice.

Thanks to Dr Malgorzata Rosochowska and Dr David Smith from Strathclyde University, Glasgow for allowing us to use their mechanical testing machine and for their help with the testing.

Thank you to Mr Jeremy McMahon from the Southern General Hospital, Glasgow for his keen participation in the operative sessions during the project.

Thanks to Mr Fraser Walker from the Maxillofacial Laboratories in the Southern General Hospital, Glasgow for his significant help during the early stages of this project.

Special thanks to Dr Lucy Di Silvio from Guy's, King's & St Thomas' Hospital, London for her advice and for providing us with the scaffolding material. Thanks also to Dr Kenny Ade and Dr Lertrit Sarinnaphakorn for helping with the addition of the cytokine onto the scaffolding.

A special thank you to Christine Stirton from Biological Services Glasgow for tolerating our several requests and for providing us with such state of the art facilities.

Thanks to Dr Michael Wilkinson and Mr David McLaughlin from Biological Services Glasgow for their help and support during the project.

A very special thank you to Dr David Lappin for his dedication, perseverance and help.

Thank you to Ms Laetitia Brocklebank from Glasgow Dental School for allowing us to use the cone-beam CT scanner for the analysis of the specimens, and a special thank you to Ms Elizabeth Weldon for her very significant support.

Thanks to Ms Audrey Maguire for her help in the early scheduling of the project.

Thanks to Mr Neil Nairn for allowing me to use his custom-made stand for the radiographic analysis of the specimens.

A special thank you to Ms Alison McCormack for giving general support and advice.

Very special thanks to Dr Keith Hunter from the University of Sheffield for all the work and support given during the histological analysis of the specimens.

A very special thanks to Professor Ayoub my mentor and advisor and the person without whom this project would have never taken place.

A special thank you to Professor Moos for his frequent and very useful advice and words of wisdom.

Finally, last but by no means least, a very big thanks to my wife Antoniella and my son Isaac for tolerating me staying for hours on end on the computer.

## **Declaration**

This thesis represents the original work of the author.

KURT BUSUTTIL NAUDI BChD (Malta) MFDS RCPS (Glasg) MSurgDent (Edin)

September 2010

© KURT BUSUTTIL NAUDI 2010



## Abbreviations

- ACS – absorbable collagen sponge
- BMD – bone mineral density
- BMP – bone morphogenetic protein
- Ca<sup>++</sup> - calcium ion
- CaCO<sub>3</sub> – calcium carbonate
- CAF – calcium alginate film
- CBD – collagen-binding domain
- CBM – collagenous bone matrix
- cc – cubic centimetres (cm<sup>3</sup>)
- cDNA – complementary deoxyribonucleic acid
- CHA – coral-based porous HA
- CMC – carboxymethylcellulose
- CMV – cytomegalovirus
- CT – computed tomography
- DBM - demineralised bone matrix
- EC – endochondral
- FGF – fibroblast growth factor
- H&E - haematoxylin and eosin
- HA – hydroxyapatite
- IGF – insulin-like growth factor
- IM – intramembranous
- MPa – megapascals
- MSC - mesenchymal stem cell
- MuCT – micro-computed tomography

OP-1 – osteogenic protein 1

PBS – phosphate buffered saline

PEO/PBT – poly(ethylene oxide)-p-bromotoluene

PGA – polyglycolic acid

PGE1 – prostaglandin E1

PGS – PLGA-coated gelatin sponge

PLA – polylactic acid

PLGA – poly D, L lactic-co-glycolic acid

PPF – poly(propylene glycol-co-fumaric acid), Poly(propylene fumarate)

PTH – parathyroid hormone

rhBMP-7 – recombinant human bone morphogenetic protein 7

SF – silk fibroin

TCP – tricalcium phosphate

TGF- $\beta$  – transforming growth factor beta

VEGF – vascular endothelial growth factor

## Synopsis

The reconstruction of critical-size bone defects following tumour resection or bone loss due to trauma is topical today and relates to the complexity of the treatment involved and poor healing outcomes. In bone bioengineering, the current trends are to explore novel methods of repairing these defects by using various bone substitutes. Various graft materials have been used for the restoration of these defects. A graft ideally needs to promote osteogenesis, osteoinduction and osteoconduction.

The aim of this investigation was to assess the histological, radiographic and mechanical properties of the tissue regenerate following the application of tricalcium phosphate (TCP) scaffolding and recombinant human bone morphogenetic protein 7 (rhBMP-7) for the reconstruction of a critical-size osteoperiosteal mandibular continuity defect in the rabbit model.

Highly purified and freeze dried recombinant human BMP-7 was used. It was produced by Chinese hamster ovary cells in culture and purified from the culture media.

All the TCP samples had a porosity of 80% and average pore size of 100 – 500µm. For the rhBMP-7 loaded scaffolds; rhBMP-7 was reconstituted according to a recommended specification and 400ng were loaded by adsorption into the TCP scaffolds.

Nine adult New Zealand white rabbits (3.0-4.0kg) were used for the planned study. In each case a unilateral osteoperiosteal mandibular body critical-size defect was created. In six cases the critical-size defect was filled with the rhBMP-7 on the TCP scaffolding, and in three cases the TCP was used alone. Assessments were made with plain radiographs at 0, 4, 8, and 12 weeks follow-up. Three months post-operatively the animals were sacrificed, the mandibles removed and the surgical sites were assessed with cone beam CT radiography, tested mechanically and analysed histologically.

More bone regeneration was seen radiographically and histologically within the mandibles that received rhBMP-7 in the TCP, with evidence of both woven and lamellar bone formation. Union was obtained at the surgical site with no cartilage formation. The regenerated bone was confined to the area that had received the scaffold, with no calcification of the surrounding soft tissues. The TCP was also resorbed more completely in this experimental group. Very little bone was formed in the cases where the defect was filled with TCP alone. The mechanical properties of the regenerate in the group that received the rhBMP-7 and TCP were also significantly superior to those of the cases that received TCP alone.

Histologically the overall mean of the percentage regenerated bone volume in the rhBMP-7 and TCP cases was  $29.41\% \pm 6.25$ , while that for the TCP alone cases was  $6.35\% \pm 3.08$ . The difference between the groups was statistically significant ( $p = 0.014$ ).

Mechanically the failure moments for the TCP alone cases were found to be very low (0-48mNm) while those for the rhBMP-7 and TCP cases were higher but there was considerable variation between the cases (55-2115mNm). Some of the cases in this group achieved failure moments comparable to normal untreated bone.

In conclusion TCP scaffolding and rhBMP-7 can be used successfully for the reconstruction of critical-size mandibular defects in the rabbit model and TCP loaded with rhBMP-7 was significantly superior in its capacity for bone regeneration histologically when compared to TCP alone. The resultant bony regenerate could also at times have mechanical properties similar to those of natural bone. But due to the variability of the mechanical properties further investigations are required before clinical application.

## **Literature Review**

# 1 Bone

## 1.1 Introduction

Bone is a unique hard form of connective tissue as a result of its heavily calcified extracellular components. Like all other connective tissue it consists of cells, fibres and extracellular matrix, with the calcified matrix being the most abundant. The resulting strength enables bone to perform its functions as a frame for the locomotion of the musculoskeletal system and to protect vital organs. Bone has a tensile strength nearly equal to that of cast iron but at less than one third its weight (Thibodeau and Patton, 2007). These material properties together with the general design of bone result in exceptional stiffness and strength that give bone the ability to withstand physiological loads without breaking (Currey, 2002) also due to a degree of intrinsic flexibility.

## 1.2 Composition

The extracellular matrix of bone (bone matrix) is composed of two main chemical components:

- Inorganic salts
- Organic matrix

About 66% of the matrix by dry weight is composed of inorganic salts while the remaining 34% is organic. *In vivo*, water forms 10% of the bone mass (Athanasίου, et al., 2000).

### 1.2.1 Inorganic Salts

Bone hardness is the result of the deposition of calcium and phosphate crystals (hydroxyapatite). These crystals form 85% of the total inorganic matrix, with the remaining 15% being mostly calcium carbonate (10%) as well as small amounts of magnesium, sodium, sulphate and fluoride (5%).

### 1.2.2 Organic Matrix

Collagen fibres and ground substance are the main constituents of the organic matrix. The ground substance, a mixture of protein and polysaccharides released by connective tissue cells, is actively involved in the metabolic functions of bone cells including growth and repair; it also acts as an adhesive between the cellular and fibrous components of the bone.

Chondroitin sulphate, a large protein, and glucosamine, an amino sugar, are examples of ground substance materials found in bone. Due to the chemical and physical properties of these constituents, ground substance adds to the overall strength of bone and helps increase its resilience to compressive forces.

## 1.3 Bone Structure

### 1.3.1 Compact Bone

In the adult skeleton, compact bone forms 80% of the total bone mass (Thibodeau and Patton, 2007). It is hard and dense, with only 10% porosity thus containing minimal amounts of cells and blood vessels (Sikavitsas, et al., 2001).



The main structural unit of cortical bone is the cylindrically shaped osteon or Haversian system (Havers, 1691). Each osteon surrounds a Haversian canal that runs lengthwise through the bone. These canals contain blood vessels, lymphatics and nerves thus providing nutrients and a method for removal of any waste products of the bone cells.

Each osteon is made up of up to 4 different structures (Figure 1.1):

- Lamellae – concentric, cylinder-shaped layers of calcified matrix
  - Interstitial lamellae are islands of calcified matrix between osteons, remnants of previous osteons than have been remodelled
- Lacunae – small spaces between lamellae containing bone cells and tissue fluid
- Canaliculi – very small interconnecting canals between lacunae and Haversian canals
- Haversian (central) canal
  - Volkmann canals are transverse canals connecting Haversian canals

Due to the longitudinal arrangement of the osteons the tensile and compressive strength of compact bone in the longitudinal direction have been reported to range between 79-151 MPa and 131-224 MPa respectively (Yaszemiski, 1996).

### 1.3.2 Cancellous (Spongy) Bone

20% of the adult skeleton bone mass is composed of cancellous bone with trabeculae (bony trusses), not osteons, as the structural units (Thibodeau and Patton, 2007). Trabecular bone has a porosity ranging between 50-90% with the

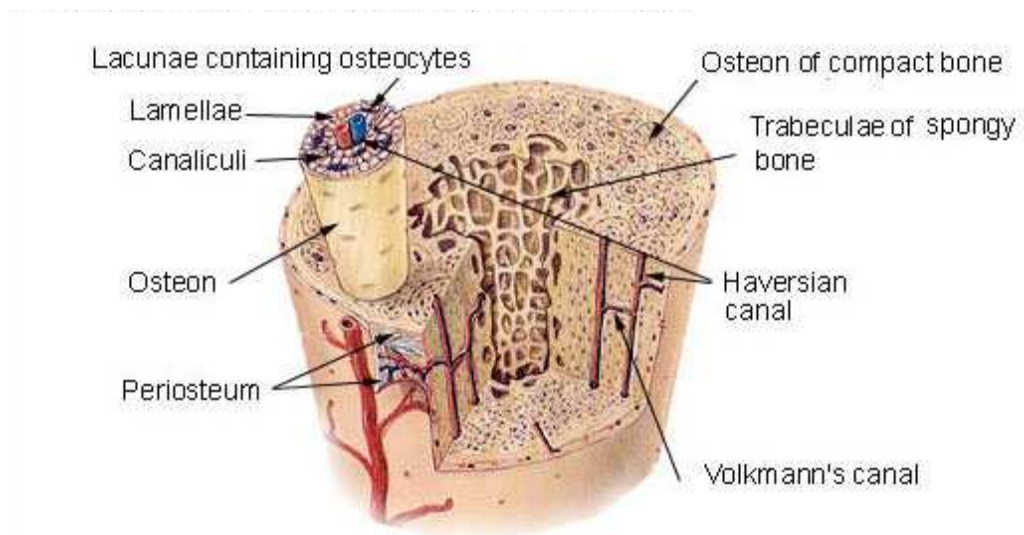


Figure 1.1 Compact & Cancellous Bone in cross section. (U.S. National Cancer Institute's Surveillance, Epidemiology and End Results (SEER) Program [<http://training.seer.cancer.gov/anatomy/skeletal/tissue.html>] Last accessed 11/09/2010)

trabeculae aligned in the direction of stress application, thus varying between different bones (Sikavitsas, et al. 2001). Bone cells and vasculature are found within the trabecular spaces. The tensile and compressive strength of trabecular bone vary with density but have been reported to range between 5-10MPa (Yaszemiski, 1996).

The cells in both cortical and cancellous bone derive their nutrients and excrete their waste products into the surrounding vasculature. This vasculature is derived from feeder arteries that supply the medullary cavity (in the cancellous bone) of the bone directly, and from blood vessels in the periosteum that branch off into the cortical bone.

### 1.3.3 Bone cell Types

There are three main types of cell in bone:

- Osteoblasts (Bone formers)
- Osteoclasts (Bone resorbers)
- Osteocytes (Mature bone cells)

*Osteoblasts* are small cells, derived from mesenchymal stem cells, which synthesise and secrete osteoid. Osteoid forms part of the bone ground substance (i.e. the organic component of bone), and consists of collagenous proteins. The osteoid collagen molecules align into triple helices that bundle into fibrils (1.5-3.5nm diameter), which then bundle up into collagen fibres (50-70nm diameter) (Rho, et al. 1998). These fibres line up in regular patterns serving as a framework for the deposition of calcium and phosphate crystals (Thibodeau and Patton, 2007).

*Osteoclasts* are large multinucleate giant cells derived from haematopoietic cells of the bone marrow. They are formed by the fusion of several precursor cells and contain large numbers of mitochondria and lysosomes (Thibodeau and Patton, 2007). These cells secrete acids and proteolytic enzymes which dissolve mineral salts and digest the organic matrix of bone.

*Osteocytes* are mature, nondividing osteoblasts surrounded by osteoid that have stopped secreting matrix and lie in lacunae within the bone.

#### 1.3.4 Bone Marrow

Bone marrow is found within trabecular bone and the medullary cavity of long bones and is a specialised type of connective tissue called myeloid tissue.

Two types of marrow exist, *red marrow*, which is virtually the only type of marrow found in children, is mainly involved in the production of red blood cells. Yellow marrow gradually replaces red marrow as the person gets older, due to the fatty deposits in the marrow cells. This process results in the gradual cessation of production of red blood cells in marrow, but these cells still maintain their potential for red blood cell production if required to do so, as in periods of prolonged anaemia (Thibodeau and Patton, 2007).

#### 1.4 Bone Functions

Bone has five primary functions within the body:

- *Support* – the skeleton acts as a support for the various body parts

- *Protection* – the body’s delicate vital organs are encased in a bony protective ‘shield’ created by the cranial vault and the rib cage for example
- *Movement* – together with their joints and the attached muscles, bones bring about movement
- *Mineral Storage* – Bones are an excellent natural reservoir of calcium, phosphorus and various minerals. They are therefore intimately associated with the body’s homeostatic mechanisms that control blood calcium levels
- *Haematopoiesis* – that is the production of red blood cells by red bone marrow, which is located primarily in the pelvis, ribs, sternum, flat bones of the skull and some long bone epiphyses in the adult

#### 1.4.1 Calcium Homeostasis

The skeleton stores 98% of the body’s calcium. Control of calcium ion concentration in the blood is essential for bone formation, blood clotting, transmission of nerve impulses, and maintenance of skeletal and cardiac muscle contraction (Thibodeau and Patton, 2007). Two hormones control the blood calcium levels:

- Parathyroid hormone – secreted by the parathyroid glands
- Calcitonin – secreted by the thyroid gland

##### 1.4.1.1 Parathyroid hormone

Parathyroid hormone is a polypeptide containing 84 amino acids. When the calcium ion levels in the blood flowing through the parathyroid gland fall below

physiologic limits it releases parathyroid hormone (PTH) which stimulates an increase in the activity of osteoclasts. This results in bone matrix breakdown releasing calcium into the blood (Figure 1.2). PTH also increases renal absorption of calcium from urine & stimulates vitamin D synthesis, which increases calcium absorption from the intestine (Thibodeau and Patton, 2007).

#### 1.4.1.2 Calcitonin

Calcitonin is a 32-amino acid linear polypeptide hormone that is produced primarily by the parafollicular (C-cells) of the thyroid gland. It is released when high calcium ion levels are detected in the blood and it stimulates osteoblasts to deposit calcium in bone (Figure 1.3). Calcitonin also has an inhibitory effect on osteoclasts (Thibodeau and Patton, 2007).

#### 1.5 Bone Development

Osseous development can take place through one of two methods; intramembranous ossification or endochondral ossification. *Intramembranous ossification* occurs within a connective tissue membrane. Mesenchymal stem cells within the membrane differentiate into osteoblasts and these start to secrete the organic matrix composed of collagen (protein) & ground substance (mucopolysaccharides). Calcification then commences once hydroxyapatite crystals are released by the osteoblasts and are deposited onto the organic bone matrix (Figure 1.4). Bone formed in this way is generally quite flat and cannot grow by interior expansion but only by appositional growth and remodelling, the skull would be an example of such a bone (Thibodeau and Patton, 2007).

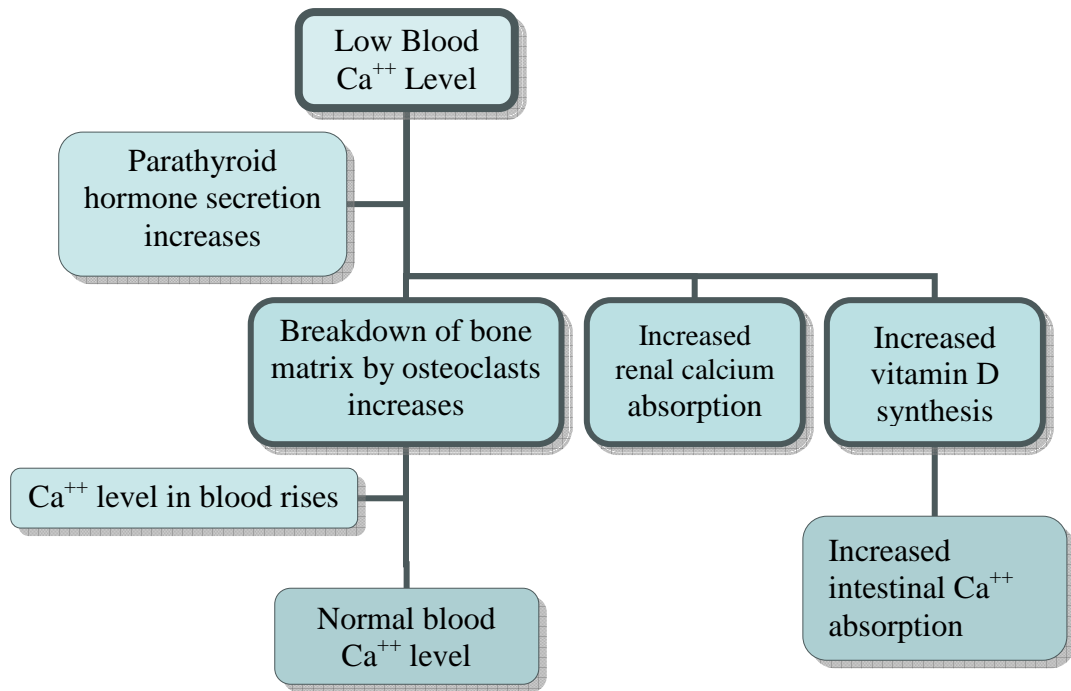


Figure 1.2 Flowchart showing the effects of low blood calcium ion concentration on the parathyroid gland.

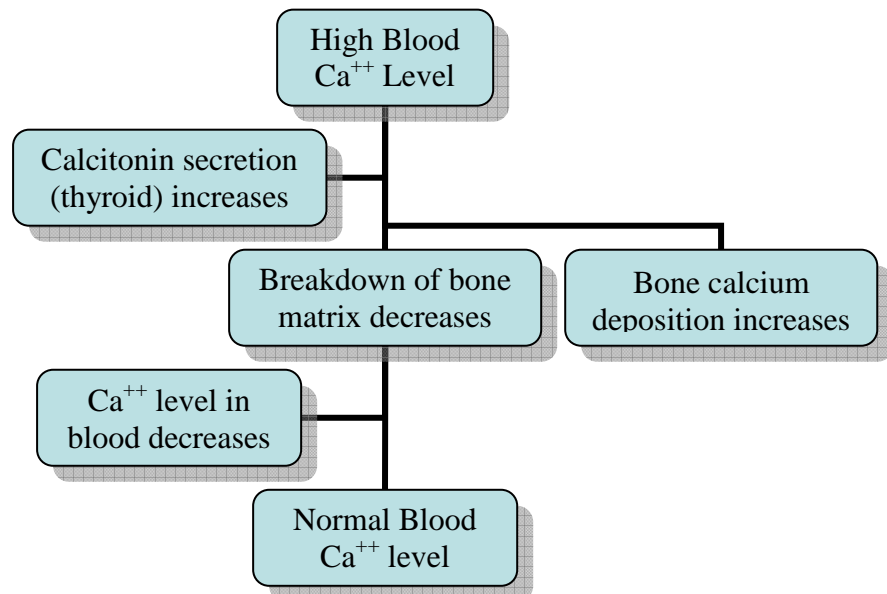


Figure 1.3 Flowchart showing the effects of high blood calcium ion concentration on the thyroid gland.

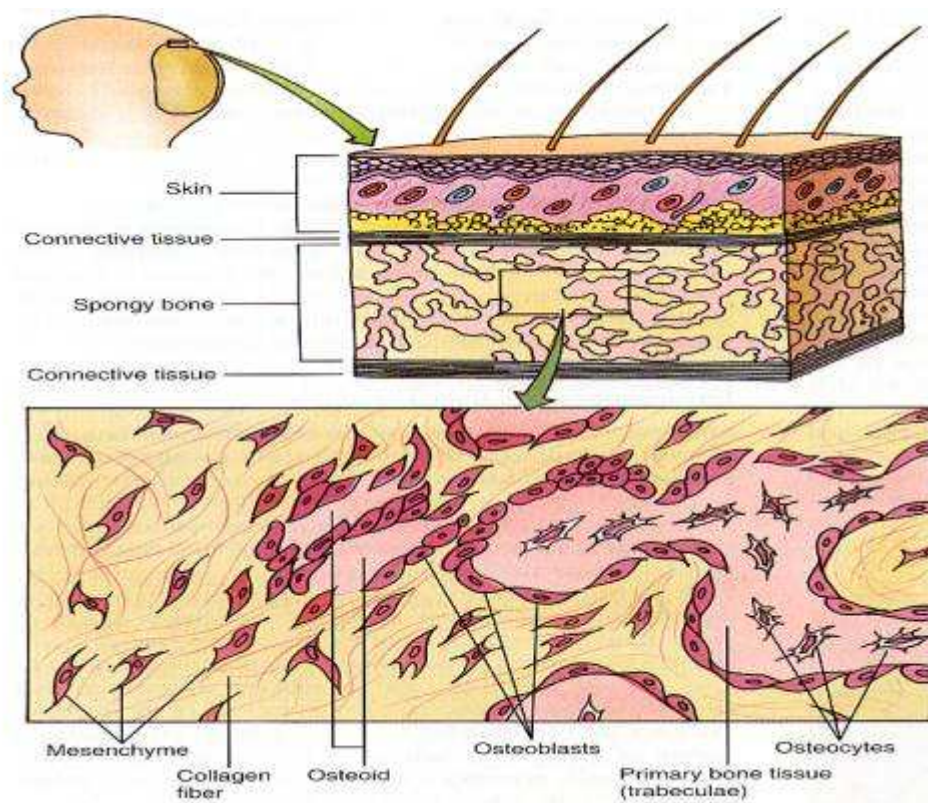


Figure 1.4 Diagram of the intramembranous model of bone ossification.  
 (Gartner and Hiatt, Colour Textbook of Histology, p. 122, Figure 7-12. Saunders  
 Co Ltd, Jan 1997)



Most bones are formed by *endochondral ossification*. This involves the gradual calcification of a cartilaginous model starting from the centre and spreading to the ends of the developing bone (Figure 1.5). Periosteum forms around the cartilaginous model, osteoblasts differentiate from mesenchymal stem cells within it and start to deposit a collar of bone around the diaphysis. The adjacent cartilage immediately starts to calcify and once a blood vessel enters the changing cartilage a primary ossification centre is formed (Figure 1.5, stage D). The bone formed is weak, immature woven bone that slowly remodels into stronger lamellar bone over time (Mistry and Mikos, 2005). Secondary ossification centres eventually form in the epiphyses (Figure 1.5, stage G) and these grow to meet the ossification progressing from the diaphysis (Figure 1.5, stage J).

Bone grows in diameter by remodelling (Figure 1.6), that is by resorption of its inner (medullary) surface by osteoclasts and deposition of new bone on its outer (periosteal) surface. There are five phases in the remodelling process (Parfitt, 1984):

- *Quiescence* – inactive cells present on the bone surface (80% of bone is in this state at any one time)
- *Activation* – biochemical or physical signals, released for example due to increased demand from exercise, attract cells (e.g. macrophages) to the site, these differentiate into osteoclasts
- *Resorption* – by osteoclasts of the inorganic and organic components of the bone (Howship's lacunae formation)

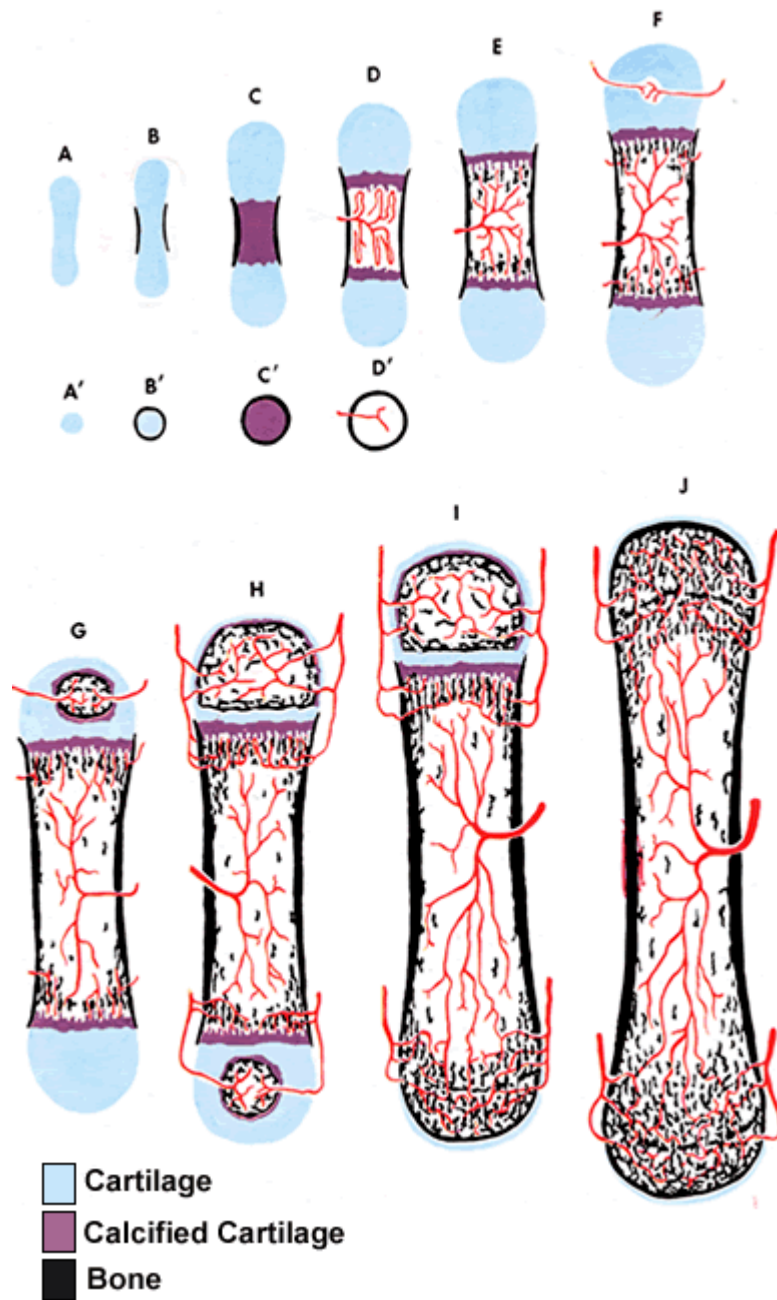


Figure 1.5 Diagram of the endochondral model of bone ossification. (Moyer D, University of Virginia School of Medicine, Bone and bone formation, CTS/Physiology, Lecture 14, September 30, 2004 [[http://www.med-ed.virginia.edu/courses/cell/BoneSample/MMHndt\\_Bone.html](http://www.med-ed.virginia.edu/courses/cell/BoneSample/MMHndt_Bone.html)] last accessed 11/09/2010)

- *Reversal* – osteoclasts leave and mononuclear macrophage-like cells secrete a cement-like substance on the bone surface
- *Formation* – Osteoblasts fill the lacunae with bone matrix and bone minerals to induce osteon formation

During childhood and adolescence bone deposition occurs at a faster rate than bone resorption so bones become larger. Up to the age of 35 the rate of deposition and resorption occur at similar rates but after 40 years of age the rate of resorption outstrips the rate of deposition so bone strength starts to reduce.

### 1.6 Bone Fracture Repair

Bone fracture results in loss of function and damage to adjacent structures, usually blood vessels. This vascular damage triggers a cascade of healing events that, in a fit & healthy person, result in complete repair of the fracture. Fractures can be compound into the mouth or through the skin, comminuted or simple and may be displaced or undisplaced. Fracture healing can be divided into four stages:

- Initial haemorrhage into the site and clot formation
- Haematoma formation and organization

Neutrophils are the first cells to arrive in the fracture site. These are followed by macrophages and together these remove any necrotic bone

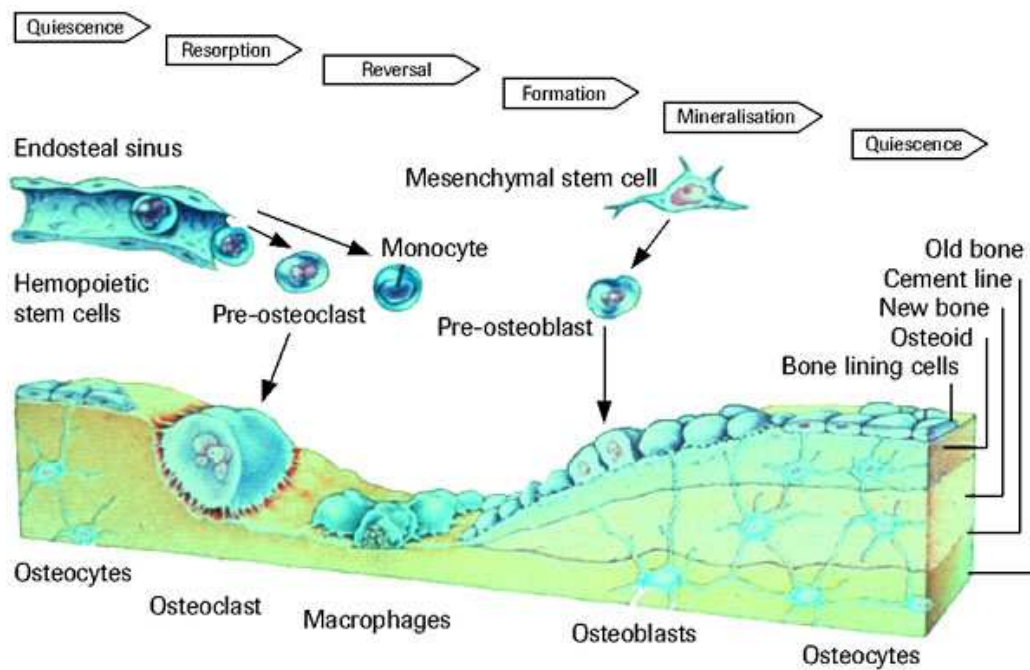


Figure 1.6 Diagram illustrating the phases of bone remodelling. (F. Hoffmann-La Roche Ltd, [<http://www.roche.com/pages/facets/11/ostedefe.htm>] last accessed 11/09/2010)

fragments. Fibroblasts and capillaries then proliferate into the injury site from the adjacent undamaged vessels. This forms loose connective tissue (granulation tissue) in the fracture site

- Callus formation

Osteoblasts migrate to the site from the adjacent periosteum and bone and together with the fibroblasts start to deposit collagen to form a callus which covers the whole fracture. The part of the callus within the medullary cavity of the bone is the internal callus, this will be remodelled to form the new bone; the external callus acts as a splint and will be resorbed eventually after healing. The callus is then ossified by both endochondral ossification and bone matrix deposition on its outer surface by the osteoblasts, forming woven (spongy) bone.

- Callus remodelling

The woven bone is gradually replaced by lamellar (compact) bone and is remodelled by osteoclasts according to the direction of mechanical stress to restore the original shape.

The whole healing process takes approximately 6 weeks depending on the severity of the break and the age & health status of the individual.

Physiologically, mechanical stresses have an important effect on the healing of the fracture. This is because physiological stress and compression result in a greater rate of bone deposition producing quicker healing. This is the rationale

behind early return to function following open reduction and internal fixation. The size of the external and internal callus is also reduced if the fracture ends are apposed more closely by the fixation method.

Several factors may affect the healing processes involved in fracture repair:

- Fracture ends movement – Movement between the two ends results in excessive callus formation and slows tissue union, which in the long term may result in fibrous union (non-union) due to collagen deposition.
- Interposed soft tissues – These too delay healing and can result in non-union.
- Gross misalignment – Delayed healing may also result from misalignment of the fractured ends.
- Infection – Infection of the fracture site will delay healing, may progress into chronic osteomyelitis and may result in non-union.
- Pre-existing bone disease – Osteomyelitis, osteoporosis, osteopetrosis, diabetes, steroid medications and bisphosphonates can all result in less effective bone healing either due to reduced bone density, reduced bone quality, reduced osteoclast/osteoblast function or reduced blood supply.

## 2 Cytokines in the repair of critical-size bone defects of the mandible

### 2.1 Discussion

Cytokines are signalling polypeptide molecules that regulate a multitude of cellular functions including differentiation, proliferation, migration, adhesion and gene expression (Mistry and Mikos, 2005). For example; bone morphogenetic proteins are cytokines that stimulate mesenchymal stem cell differentiation into osteoblasts as well as aiding the function of osteoblasts directly. Bone morphogenetic proteins therefore have *osteoinductive* properties.

A review of the literature demonstrated the use of six main types of cytokine in the induction of bone in critical-size bone defects in the mandible, these are:

- Vascular Endothelial Growth Factor (VEGF)
- Transforming Growth Factor  $\beta$  (TGF-  $\beta$ )
- Insulin-like Growth Factor (IGF)
- Fibroblast Growth Factor (FGF)
- Prostaglandin E1 (PGE1)
- Bone Morphogenetic Protein (BMP)

#### 2.1.1 Vascular Endothelial Growth Factor

Only one study reported the use of VEGF in the repair of critical-size mandibular defects. Kleinheinz J, et al. (2002) used VEGF165 in a collagen type I carrier in the repair of bicortical holes in the rabbit mandible. 56 rabbits were operated and the defects were filled with collagen type I implants, collagen implants complexed with 0.8 $\mu$ g VEGF165, or left without any filling.

Specimens were taken at 3, 7, 14, and 28 days post-operatively and analysed histologically and histomorphometrically looking at the blood vessel density, total blood vessel surface area, bone surface area and bone density. This showed persistently high numbers of blood vessels 14 days post-operatively in the group that received VEGF165 in a collagen carrier when compared to controls. The density of the regenerated bone was also significantly higher in the study group that received the VEGF. It was concluded that the activation of angiogenesis using VEGF165 leads to more intensive angiogenesis and bone regeneration. The large number of cases used in this report strengthens the values of the results obtained but the defect created even though described as a critical-size defect was not a continuity defect as holes were simply created in the mandible. This type of defect can heal more easily than a complete continuity defect.

### 2.1.2 Transforming Growth Factor $\beta$

In 1998 Sherris, et al. used TGF- $\beta$ 1 together with demineralised bone matrix (DBM) to reconstruct a critical-size mandibular defect, devoid of periosteum, in a canine model. The study was a randomized, blinded, placebo-controlled, prospective animal pilot study performed on 6 cases. In group 1 (n=3) the defect was reconstructed with DBM alone and while in group 2 (n=3) DBM plus TGF- $\beta$ 1 (250  $\mu$ g TGF- $\beta$ 1/g DBM) was used. Radiographic, histological, and biomechanical (four-point bending) testing performed 12 weeks after graft implantation showed that the group which received TGF- $\beta$ 1 and DBM in the defect had significantly stronger bone when compared to the control group that only received DBM (P < 0.02). In fact only fibrous union, as opposed to the



bony union in the TGF-  $\beta$ 1/DBM group, occurred in the control group. The difference between the groups was very large, bony as opposed to fibrous union, so this partially makes up for the small sample size (6 cases).

Also in 1998, Zellin, et al. showed that the amount of bone regeneration in critical-size defects in the rat mandible repaired with recombinant human TGF-  $\beta$ 1 (rhTGF- $\beta$ 1) was dose dependent, when the periosteum was left intact. The results were the same no matter what type of carrier was used for the rhTGF- $\beta$ 1 (3% methyl cellulose gel, porous CaCO<sub>3</sub> particles, or poly(lactide-co-glycolide) beads). However, when the periosteum was removed from the surgical site (with microporous expanded polytetrafluoroethylene barrier membranes), rhTGF- $\beta$ 1 inhibited bone regeneration. These results suggest that TGF- $\beta$ 1 has a proliferative effect on cells already committed to the osteoblastic lineage, but may actually be inhibitory to the induction of osteogenic cells in vivo. Again the defects created were not continuity defects but bur holes, but useful information was still obtained from the results.

Shigeno, et al. (2002) reported the use of TGF- $\beta$ 1 in a collagen sponge carrier in the repair of critical-size defects in the mandibles of 12 adult beagle dogs (9.0-12.0 kg). The 2<sup>nd</sup>, 3<sup>rd</sup> and 4<sup>th</sup> premolar teeth on both sides of the mandible were extracted. After the extraction sites healed, a bone defect (10.0 x 15.0 x 10.0mm or 10.0 x 10.0 x 10.0mm) was created. A collagen sponge (10.0 x 10.0 x 10.0mm) containing TGF- $\beta$ 1 in saline at concentrations of 1.0 $\mu$ g, 5.0 $\mu$ g, or 10.0 $\mu$ g was placed at the bottom of the defects. The animals were killed four, six, or eight weeks post-operatively. Soft X-ray and bone-salt measurement

analyses of the surgical sites showed greater bone formation in the defects into which TGF- $\beta$ 1 had been incorporated than with the control defects, which only received the collagen sponge loaded with saline. The bone had in fact regenerated in defects that had received the TGF- $\beta$ 1 by four weeks. The authors used too many variables with a small number of cases. It probably would have been better if a single dose strength of TGF- $\beta$ 1 was used. The defect was again not a continuity defect which this time was not even a true-and-true defect since there was bone at the base of the hole.

More recently, in 2005, Srouji, et al. reported the use of TGF- $\beta$ 1 and/or insulin-like growth factor 1 (IGF-1) in a hydrogel carrier in the repair of critical-size mandibular defects in twenty-five 3-month-old Sprague–Dawley rats (300g). 3 x 4mm mandibular lower border bone defects were created. Bone defect healing was tested after 3 and 6 weeks radiographically (Soft X-ray & Three-dimensional computerized tomography) and morphologically. Histologically, significantly more bone formation was noted after 6 weeks in the groups that received either TGF- $\beta$ 1, IGF-1 or TGF- $\beta$ 1+IGF-1. The percentage of radiographic defect closures was greatest in the groups that received either TGF- $\beta$ 1 or TGF- $\beta$ 1+IGF-1 (38% & 37%). Again the defects created in this project were not continuity defects.

### 2.1.3 Fibroblast Growth Factor

The use of FGF in the repair of critical-size mandibular defects was reported in 1999 by Xu, et al. They looked at the effect of basic fibroblast growth factor (bFGF) on bone formation induced by recombinant human bone morphogenetic

protein-2 (rhBMP-2) in the repair of mandibular defects in 56 rabbits. Polylactic acid (PLA) was used as a carrier. The rabbits were divided into five groups. Mandibular three-walled defects (1.5 cm x 0.5 cm, full thickness) were created in right side in each case. The defects in each group were then filled with grafts as follows; PLA/rhBMP-2/bFGF, PLA/rhBMP-2, PLA/bFGF, PLA and nothing as control. Healing was assessed radiographically and histologically at 2, 4 and 8 weeks post-operatively. The group that received a composite graft of bFGF and rhBMP-2 on the PLA carrier had the best bone growth at 4 weeks post-operatively ( $P < 0.05$ ), when compared all the other groups.

Lu and Rabie (2002) compared the healing of critical-size mandibular defects in 42 rabbits repaired in six different ways; autogenous endochondral (EC) bone, autogenous intramembranous (IM) bone, fresh-frozen allogenic IM bone only, fresh-frozen allogenic IM bone and demineralized bone matrix powder prepared from intramembranous bone (DBM(IM)) only, and fresh-frozen allogenic IM bone and basic fibroblast growth factor (bFGF) mixed with DBM(IM) powder, non-grafted controls. The cases were killed after 3 weeks. The amount of new bone formation was quantified by image analysis of the histological slides. The group that received the composite allogenic IM bone/bFGF/DBM(IM) graft had bone regeneration that was superior to all other grafts (including autogenous endochondral bone) and nearly as good as the group that received autogenous IM bone. Though the bone defects created were large ( $15 \times 10$ mm ostectomy), the authors clearly stated that a continuity defect of the mandible was not created.

#### 2.1.4 Prostaglandin E1

The bone inducing capabilities of prostaglandin E1 (PGE1) and BMP-5 were compared by Arosarena and Collins (2003). The study was a prospective controlled trial. Bilateral critical-size mandibular defects were created in 29 Sprague-Dawley rats with each hemimandible assigned to an experimental group, which were filled in one of seven ways; with collagen/polylactic acid (PLA) (group 1), PLA with BMP-5 (group 2), PLA with PGE1 (group 3), collagen/calcium hydroxyapatite cement (HAC) (group 4), HAC with BMP-5 (group 5), or HAC with PGE1 (group 6). The control group (group 7) had unfilled defects. The animals were sacrificed after 12 weeks, and the surgical sites were analysed histologically using stereologic techniques that provided quantitative estimates of the three-dimensional composition of the defects. The HAC/BMP-5 group contained significantly more new bone and less fibrous tissue than all the other groups ( $p \leq 0.02$  and  $p < 0.01$ , respectively). The groups containing PGE1 (groups 3 & 6) demonstrated significantly more osteoid development than the other experimental groups ( $p < 0.001$ ) suggesting it actually delayed bone healing.

#### 2.1.5 Bone Morphogenetic Protein

BMP has been extensively used for the repair of critical-size mandibular defects. There are over 20 sub-types of BMP, these all forming part of the transforming growth factor  $\beta$  superfamily. Six main sub-types of BMP have been used in the literature:

- BMP-2
- BMP-3

- BMP-4
- BMP-5 – described in the section of Prostaglandin E1 above
- BMP-7 – also known as osteogenic protein 1 (OP-1)
- BMP-9

#### 2.1.5.1 Bone Morphogenetic Protein 9

Alden, et al. in 2000 reported on the use of BMP-9 and BMP-2 adenoviral vectors (CMV promoters) in the repair of critical-size mandibular defects in athymic nude rats. 13 rats had bilateral 4mm diameter holes created in the body of the mandible and the 26 surgical sites were filled in three different ways; 9 with BMP-9 with the CMV promoter, 9 with BMP-2 and the CMV promoter and 8 with the CMV promoter alone. Gross tissue examination, radiographic analysis and histological analysis showed significantly better bone regeneration in the both the group receiving BMP-9 adenoviral vectors and BMP-2 adenoviral vectors compared to the control that only received  $\beta$ -galactosidase gene adenoviral vectors ( $p < 0.05$ ). One of the sites treated with BMP-2 showed near complete healing at 12 weeks post-operatively. The weakness of this study is that the defects created again were not continuity defects; they in fact were just 4mm diameter circular defects created at the angle of the mandible with a bur.

#### 2.1.5.2 Bone Morphogenetic Protein 4

Arosarena and Collins (2005) compared the effectiveness of BMP-4 and BMP-2 at varying doses in the repair of unilateral critical-size mandibular defects in 82 Sprague-Dawley rats. Hyaluronic acid polymer carrier was loaded with 0.01,

0.1, 1, or 10µg of BMP-2 or BMP-4, while in the controls the defect received either hyaluronic acid sponges loaded with growth factor dilution buffer or was left unfilled. The animals were sacrificed after 8 weeks, and the surgical sites were analysed histologically using stereologic techniques that provided quantitative estimates of the three-dimensional composition of the defects. Carriers containing BMP-2 or BMP-4 at a concentration of 10µg, induced significantly more bone production in the defects compared to the controls ( $p = 0.01$  and  $p = 0.0001$ , respectively). BMP-4 induced thicker cortical bone and more trabecular bone while BMP-2 resulted in more partial defect bridging. They concluded that, in the rat model, doses between 1 and 10µg of BMP-2 and  $\geq 10\mu\text{g}$  of BMP-4 would result in bony union. The large number of cases used and the clear description of the method and results, which were very significant, make the conclusions made by the authors particularly strong; but the defect created (5mm x 5mm) again did not result in loss of the continuity of the mandible.

#### 2.1.5.3 Bone Morphogenetic Protein 3

In 2003 Arosarena, et al. investigated the repair of critical-size defects created in the left mandibular bodies of thirty-seven male Fischer rats. The defects were filled with a bone marrow cell suspension (group 1), a synthetic bone matrix consisting of bovine collagen and calcium hydroxyapatite cement (group 2), the matrix and marrow cells (group 3), the matrix with 100µg of bone growth factor mixture (group 4), or the matrix with bone growth factor mixture and marrow cells (group 5). The animals were sacrificed after 8 weeks, and the nondemineralized specimens were processed histologically. The bone growth

factor mixture consisted mostly of BMP-3 and TGF- $\beta$ . Stereologic techniques were used to determine and compare the volume fractions and volume estimates of mature bone, new bone, osteoid, marrow, remaining cement, and fibrous tissue in each defect. Volumes of mature bone, new bone, and remaining cement did not differ significantly among the groups ( $p = 0.30$  for mature bone,  $p = 0.17$  for new bone, and  $p = 0.34$  for cement). However, group 4 and 5 specimens contained significantly more osteoid and larger marrow spaces than did the group 2 and 3 specimens ( $p < 0.001$  for both). The specimens in groups 2 and 3 contained significantly more fibrous tissue ingrowth than did those in groups 4 and 5 ( $p < 0.001$ ). The authors thus concluded that the synthetic bone substitute containing bone growth factor mixture (groups 4 & 5) was effective in stimulating new bone and osteoid development in the rat mandibular model. A good number of cases were used and the results were well presented and explained. The combination of the BMP-3 and TGF- $\beta$  did not allow the determination of whether each would have been as effective alone.

#### 2.1.5.4 Bone Morphogenetic Protein 2

##### 2.1.5.4.1 BMP-2 use in Primates

In 1996 Boyne started a pilot study looking at the repair of bilateral critical-size mandibular defects (2.2cm resections through the entire thickness of the mandible) in the adult male *Macaca fascicularis* (rhesus) monkeys using BMP-2 on a collagen type-I sponge (Helistat) as a carrier. In three animals 0.8mg BMP-2 per cc was placed in one side and 0.2mg BMP-2 per cc was placed in the contralateral side. In another 4 animals 0.4mg BMP-2 per cc was placed in the

defect on one side while the contralateral defect was filled with a particulate autogenous graft of cortical cancellous bone which was used as a control. In all seven animals, the alveolar ridges were regenerated completely with restoration of contour and cortical bone, and histomorphometric analyses revealed excellent calcified bone matrix to marrow spaces ratios. From these results the authors concluded that BMP-2 can bring about bony regeneration in critical-size mandibular defects in rhesus monkeys.

Again in 2001, Boyne looked at the repair of critical-size mandibular defects in primates using BMP-2 in a collagen carrier. Three groups were assessed; mandibular resection defects in middle-aged *Macaca fascicularis* animals, mandibular resection defects in *Macaca fascicularis* animals over 20 years of age, and (c) simulated bilateral clefts in *Macaca mulatta* animals 1 1/2 years of age. In the simulated bilateral cleft cases one side was filled with BMP-2 while the contralateral side was filled with autogenous particulate bone and marrow. Histomorphometric analysis of all the cases showed excellent bone regeneration in all the defects confirming that BMP-2 was as effective as autogenous particulate bone and marrow.

Also in 2001, Boyne and Shabahang evaluated the healing of critical-size mandibular defects in monkeys using BMP-2 on 3 different carriers; calcium carbonate coral (BioCoral), poly(methylethyl methacrylate) material (HTR) and porous bone mineral (Bio-Oss). 20mm defects were created in both the mandible and the maxilla and implants were placed in each defect. All carriers produced the same amount of implant osseointegration but the calcium



carbonate coral did not induce alveolar bone regeneration unlike HTR and Bio-Oss with BMP-2 that produced near complete regeneration.

In 2001 and 2002 Marukawa, et al. also reported on the repair of critical-size mandibular defects in the rhesus monkey (*Macaca mulatta*) with BMP-2 but using poly-D, L-lactic-co-glycolic acid-coated gelatin sponge (PGS) as a carrier. 20mm and 30mm size defects were created in the respective studies and in all cases there was excellent bone regeneration both radiographically and histologically. No controls were used in the 2002 study but in the 2001 paper some of the defects were filled with either PGS alone or left empty. These sites only showed a little bone deposition on the periphery of the surgical site and were otherwise filled with fibrous tissue.

Boyne, et al. in 2006 repeated the work he had done on young and middle-aged primates but this time used aged monkeys (20 years old), as these are comparable to 80 year old humans, to assess whether old age reduced the effectiveness of the BMP-2 due to reduced availability of mesenchymal stem cells. Bilateral critical-size mandibular defects were created and rhBMP-2 in a collagen sponge (Helistat) was placed in the defects. There was complete regeneration of the defects by four months post-operatively showing that aged primates had a potential for bone regeneration comparable to that of younger primates, as in fact the first author had already demonstrated in previous work (Boyne, 2001).

#### 2.1.5.4.2 BMP-2 use in Dogs

Toriumi, et al. in 1999 reported on the repair of 3cm, full-thickness critical-size defects in the canine mandible using rhBMP-2 in a poly(lactide-co-glycolide) particle carrier. Six dogs received the carrier with the rhBMP-2 while 3 controls received the carrier alone. Radiographic photodensitometry was performed on serial dental radiographs of the reconstructed segments to determine bone density and the degree of bone resorption over 30 months. After animal sacrifice histological and histomorphometric analyses were performed on the surgical sites. Controls, that received only the carrier in the surgical defect, did not produce any bone in the defect. The animals treated with rhBMP-2 demonstrated good bone formation that was comparable radiographically to that of normal host bone by 3 months. Radiographic photodensity measurements showed some evidence of early bone resorption (thinning of the cortical bone and decrease in height) in the rhBMP-2-induced bone. But no further resorption was noted in the induced bone by 11 months after reconstruction. The bone density of the induced bone increased over the 30 months.

In 2000, Barboza, et al. also reported on the repair of critical-size mandibular defects in the dog. RhBMP-2 in an absorbable collagen sponge (ACS) carrier  $\pm$  hydroxyapatite (HA) was used to repair bilateral, Class III alveolar defects surgically created in 4 adult mongrel dogs by extracting the mandibular fourth premolars and reducing the alveolar ridge. Histological evaluation 12 weeks after the repair of the defects showed limited bone augmentation in the sites that received rhBMP-2/ACS (0.7  $\pm$  0.6mm), while the sites that received rhBMP-2/ACS/HA exhibited clinically relevant ridge augmentation (5.5 $\pm$  1.6mm).

However, the bone that formed in the former was of poorer quality as it contained sparse bony trabeculae amidst HA particles, fibrovascular tissue, and marrow. The created defect was again large but not a continuity defect.

Critical-size defect repair in the canine mandible was again assessed by Nagao, et al. in 2002. RhBMP-2 in a poly D, L lactic-co-glycolic acid (PLGA)/gelatin sponge complex (PGS) carrier was used to repair bilateral rectangular bone defects (10 x 8 x 7 mm) in the premolar region of twelve adult beagle dogs. On examining the surgical sites with soft x-rays, three-dimensional computed tomography, histologically and peripheral quantitative computed tomography, the control group that received only PGS showed no bone regeneration. In contrast, in the group that received the BMP-2, newly formed bone was found in all defects from 4 weeks onward and was marked at 12 weeks, and the density of the newly formed bone was similar to that of the surrounding cortical bone at 12 weeks.

#### 2.1.5.4.3 BMP-2 use in Rats

Higuchi, et al. (1999) looked at the repair of bilateral round through-and-through bone defects (5 mm in diameter) in the angle of the mandible in eight Long-Evans rats, using rhBMP-2 in a PLGA/gelatin sponge (PGS) carrier. The control side received only the PGS carrier. The rats were sacrificed after 4 weeks and the surgical sites analysed histologically and histomorphometrically. In the control group, bone formation was present only along the border of the surgical site. In all cases in the BMP-2 group, a significantly larger quantity of newly formed bone was observed, with the bone defect being completely filled

with new bone in 4 of 8 rats ( $P < 0.0001$ ; paired t-test). The authors thus concluded that rhBMP-2/PGS induced effective bone regeneration on mandibular defects in rats.

Also in 1999, Kubler, et al. reported the use of a non natural BMP-variant (EHBMP-2) in the repair of critical-size defects in rats' mandibular angles. Complete repair was achieved with the use of a combination of granular collagenous bone matrix (ICBM) with EHBMP-2. The EHBMP-2 was produced by expression in *E. coli* through specific mutation of the amino acid sequence. The substitution of 12 N-terminal amino acids by a nonsense sequence results in a negligible affinity of EHBMP-2 to the extracellular matrix.

Park, et al. (2003) reported on the use of liposome-mediated and adenoviral gene transfer for the generation of autologous BMP-2-producing mesenchymal stem cells (BMSC). Primary BMSCs isolated from the rat femur were treated *ex vivo* with either an adenovirus or a liposome carrying human BMP-2 cDNA. These cells were then placed in critical-size mandibular defects in the rat. BMSCs treated with a reporter gene vector or untreated BMSCs served as controls. After healing the surgical sites were analysed by *in situ* hybridization, radiography and immunohistochemistry. Both groups of genetically modified cells produced BMP-2 for at least 2 weeks. In the liposome group, the critical-size defects were completely repaired by 6 weeks after surgery, while in the adenoviral gene transfer group complete bone healing occurred in 4 weeks. None of the control groups showed bone healing after 8 weeks. The authors

concluded that both gene transfer methods may represent the best vector systems for future clinical trials of bone regeneration by BMP-2 gene therapy.

#### 2.1.5.4.4 BMP-2 use in Pigs

Wurzler, et al. (2004) compared mandibular regeneration with an autologous bone transplant or rhBMP-2 in a collagen carrier, following the creation of a 5cm critical-size defect in the mandible of nine Göttingen mini-pigs. Bone regeneration and consolidation of the defects was analysed radiographically and histologically. Complete regeneration of the surgical defect with functional stability was observed in the group that received the rhBMP-2, while in the bone transplant group the bone bridging took longer and therefore functional stability was achieved more slowly. As a result the authors concluded that the rhBMP-2 implant was superior to autologous bone transplant for the repair of critical-size defects in the Göttingen mini-pig.

#### 2.1.5.4.5 BMP-2 use in Rabbits

Mao, et al. in 1998 reported on the use of rhBMP-2 in the repair of critical-size defects in the rabbit mandible and calvarium using four carriers, namely chitin, coral, coral-based porous HA (CHA), and xenogenic cancellous bone. The repaired defects were examined radiographically, histologically (under light microscope and scanning electron microscope), by immunohistochemistry, and biomechanically 2, 4, 8, and 12 weeks post-operatively. In all composite graft groups, except in the CHA group (HA takes longer to resorb) by 12 weeks the graft had been replaced completely by bone. Only fibrous tissue and a little peripheral new bone formed in the defects in the control groups that had

received only the carrier materials. The authors concluded that all the carriers used in this study would be effective for the use of BMP-2 in the repair of critical-size bone defects in the rabbit.

In 2003, Ueki, et al. looked at the effectiveness of polylactic acid/polyglycolic acid copolymer and gelatin sponge complex (PGS) carrier with or without rhBMP-2 in the repair of condylar defects in sixty adult male Japanese white rabbits. Unilateral defects were created in all animals, in twenty animals the defect was repaired with rhBMP-2 in the PGS carrier, in another twenty the defect was repaired with PGS alone and in the remaining twenty no graft was placed. Once the animals were sacrificed the surgical sites were assessed histologically. Four weeks after implantation, growth of bone and cartilage-like tissue was observed in all rabbits that received PGS grafts (with and without rhBMP-2), this was significantly better ( $p < 0.05$ ) than the control group where there was no growth of bone tissue, but the latter also developed a cartilage-like layer covering the operated surface. The authors concluded that PGS with or without rhBMP-2 could induce the regeneration of new bone and cartilage-like tissue in the rabbit condyle.

Okafuji, et al. (2006) and Kimura, et al. (2006) discussed the repair of a critical-size mandibular defect in rabbits using rhBMP-2 on a 1% atelocollagen gel carrier. Okafuji, et al. worked on 8 rabbits and assessed the healing using micro-computed tomography (muCT) in vivo. This showed that the bone density increased slightly at the bone marrow side by the seventh day, and kept expanding gradually during the course of the experiment which lasted for 28

days. The authors could construct 3D images from the muCT scans enabling them to visualize bone formation in vivo more accurately. They concluded that the muCT and 3D image reconstruction were useful for the follow-up of reconstructed critical-size mandibular bone defects and that the atelocollagen gel is effective as a carrier of rhBMP-2. Kimura, et al. used 12 rabbits and covered the BMP/atelocollagen graft with PLGA membrane. Histopathological examination of the graft sites at 1, 2 and 3 weeks showed many spindle cells had proliferated and invaded blood clots, and a small amount of immature trabecular bone had formed, this kept proliferating gradually during the second and third weeks. There was however, only a slight difference (not significant) between the experimental group and the control group as regards to the amount of bone formation during the 3 week experimental period. Nonetheless the authors, possibly erroneously, concluded that atelocollagen gel as a carrier of rhBMP-2 and PLGA as a covering membrane were effective for the treatment of critical-size defects in the rabbit mandible. The reason for the lack of a significant difference between the groups was probably due to the short follow-up period.

Chen, et al. in 2007 reported on the use of BMP-2 in the repair of critical-size bone defects (12mm x 5mm x 4mm) in sixteen rabbit mandibles using a collagen-based targeting bone repair system. This was achieved by adding a collagen-binding domain (CBD) to the N-terminal of native BMP-2 to allow it bind to collagen specifically. They showed in-vitro that the collagen-binding bone morphogenetic protein-2 (BMP2-h) had maintained the full biological activity as compared to rhBMP2 lacking the CBD. Demineralised bone matrix

(DBM) was used as a carrier for the BMP2-h. Histological and radiographic examination of the surgical sites at 12 weeks showed the quantities of newly formed bone to be  $18.7\pm 4.6\%$  for the group that received PBS/DBM,  $29.4\pm 4.6\%$  in the group that received rhBMP-2/DBM and  $45.1\pm 6.7\%$  in the group that received rhBMP2-h/DBM, with the difference between each group being statistically significant. The authors therefore concluded that the collagen-based BMP-2 targeting bone repair system induced better bone formation not only in quantity but also in quality.

#### 2.1.5.5 Bone Morphogenetic Protein 7

In 2004 Wang, et al. reported on the repair of unilateral 5cm mandibular continuity defects in five Göttingen mini-pigs. Four animals were treated with the rhOP-1 in carboxymethylcellulose (CMC) and collagen ( $3000\mu\text{g}$  rhOP-1, 2g collagen, 1g CMC), and one animal was treated with CMC and collagen alone. After 12 weeks bony continuity was reestablished in the rhOP-1-treated hemimandibles. The bony regenerates were of good anatomical shape, volume, and showed functional remodeling. There was insufficient bony regenerate in the control and this was of lower volume (volume in 3D-CT scan  $29.81\text{ cm}^3$  vs.  $8.85\text{ cm}^3$ ). To produce 1mm of bending, 1972N were needed for the rhOP-1-treated hemimandibles, 2617N for the untreated contralateral sides, and 642N for the control. The authors concluded that CMC stabilization of collagen carrier biomaterials for rhOP-1 provided good plasticity as well as excellent space-keeping properties and may not interfere with osteoinduction. But a small number of cases were treated and no comparison was made with cases treated



with rhOP-1 with the collagen carrier alone to see if the CMC actually did not delay the healing process.

In 2004 and in 2005 Abu-Serriah, et al. reported on the effect of rhBMP-7 in a type I collagen carrier on the repair of unilateral critical-size continuity mandibular defects in six adult sheep. A 35mm osteoperiosteal defect was created at the parasymphyseal region of the mandible, with the continuity of the mandible being maintained using a bony plate. Bone labels were injected at selected time intervals during the follow-up period. The animals were killed after 3 months and bone samples were examined histologically, histomorphometrically, and by fluorescence microscopy. A mixture of woven and lamellar bone that contained many cells with large nuclei was seen. This had not reorganised to form cortical bone and the rhBMP-7-induced bone was more porous than the native bone. The newly-formed bone restored both endosteal and periosteal layers. The rhBMP-7-induced bone was biocompatible and induced no ossification of soft tissue or abnormal growth of nearby vital structures. The mineral apposition rate was  $1.98\mu\text{m}/\text{day}$  (range  $0.62\text{-}5.63\mu\text{m}/\text{day}$ ), a value close to that reported in humans. This suggested that the rhBMP-7 had a limited effect in accelerating the rate of mineralisation, but promoted the pre-mineralisation processes, and perhaps the formation of woven bone. The mechanical properties of the regenerated bone were very variable. The new bone in three samples contained fibrous tissue and was weaker and less stiff than the untreated contra-lateral side (strength, 10-20%; stiffness, 6-15%). The other half had better-quality bone and was significantly stiffer and stronger ( $p < 0.05$ ), with strength 45-63% and stiffness 35-46% of the contra-lateral side.

The authors concluded that the rhBMP-7 resulted in effective bone regeneration within a critical-size defect in the sheep model but that the wide mechanical variations of the regenerated bone suggested that further basic bone biology research is needed to provide better understanding of the cellular and molecular events which take place during the process of osteoinduction.

### 3 Scaffoldings used for bone regeneration in critical-size bone defects.

#### 3.1 Discussion

Scaffold biomaterials are necessary for critical-size bone defect reconstruction as they provide two main functions; firstly restoring the shape of the critical-sized defect and secondly acting as a biological conductive structure for the cells and/or growth factors to promote bone formation (*osteoconduction*).

A review of the literature showed that there is an overwhelming variety of substances used as scaffolding in the repair of craniofacial skeletal defects. All scaffolds can be divided into two main broad groups; the natural and the synthetic types. These groups are then further subdivided into various subgroups as shown in Table 3.1.

##### 3.1.1 Natural scaffolds

###### 3.1.1.1 Collagen

Saadeh, et al. (2001) evaluated the efficacy of type I collagen implants in repairing critical-sized mandibular defects in twelve male Sprague-Dawley rats. Full thickness, round, 4mm diameter defects were created in the ramus of the right mandible of all the rats. In six rats the defect was filled with a precisely fitted disk of allogenic collagen type I gel, in the remaining six rabbits the defect was left empty. The animals were killed 6 weeks postoperatively and healing of the bone defects was assessed in a blinded fashion using radiological, histological and densitometric analysis. All control mandibles had clearly

NATURAL	SYNTHETIC
<p>Collagen</p> <ul style="list-style-type: none"> <li>▪ Gels, nanofibers, porous scaffolds, films</li> </ul> <p>Fibrin</p> <ul style="list-style-type: none"> <li>▪ Injectable adhesive gel</li> </ul> <p>Alginate</p> <ul style="list-style-type: none"> <li>▪ Hydrogel</li> </ul> <p>Silk</p> <ul style="list-style-type: none"> <li>▪ Nanofibers, films</li> </ul> <p>Hyaluronan</p> <ul style="list-style-type: none"> <li>▪ Gels, sponges, pads</li> </ul> <p>Chitosan</p> <ul style="list-style-type: none"> <li>▪ Sponge, porous scaffold, nanofibers</li> </ul> <p>Agarose</p> <ul style="list-style-type: none"> <li>▪ Hydrogel</li> </ul>	<p>Ceramics</p> <ul style="list-style-type: none"> <li>▪ Calcium phosphate cements <ul style="list-style-type: none"> <li>○ Low-temperature calcium orthophosphate cements</li> </ul> </li> <li>▪ Bioactive glasses</li> <li>▪ Hydroxyapatite</li> <li>▪ <math>\beta</math>-tricalcium phosphate</li> </ul> <p>Titanium</p> <p>Polymeric materials</p> <ul style="list-style-type: none"> <li>▪ Poly(<math>\alpha</math>-hydroxy esters) <ul style="list-style-type: none"> <li>○ Poly(L-lactic acid)</li> <li>○ poly(glycolic acid)</li> <li>○ Poly(lactic-co-glycolic acid)</li> <li>○ Poly(propylene fumarate)</li> <li>○ poly(anhydride)</li> <li>○ poly(phosphazene)</li> <li>○ polyethylene glycol</li> </ul> </li> </ul> <p>Ceramic reinforced polymers</p>

Table 3.1 Types of scaffolding materials used in the repair of bone defects.

demarcated bony edges at the defect border with connective tissue spanning the defect, while all the implanted mandibles were found to have indistinct bony edges at the defect border with a thin layer of osteoblasts and viable bone spanning the defects. There was a statistically significant difference in the bone density between the two groups ( $p = 0.01$ ).

In 2004 Abu-Serriah, et al. investigated the repair of osteoperiosteal critical-size mandibular defects in six sheep using rhBMP-7 on a type I collagen carrier. The animals were killed after 3 months and bone samples were examined histologically, histomorphometrically, and by fluorescence microscopy. There was complete bony union and full integration of the newly formed bone, which showed a mixture of woven and lamellar bone that contained many cells with large nuclei. This had not reorganised to form cortical bone and the rhBMP-7-induced bone was more porous than the native bone. The newly-formed bone restored both endosteal and periosteal layers.

#### 3.1.1.2 Fibrin

Gröger, et al. reported in 2003 on the use of fibrin for the repair of critical-size mandibular bone defects in minipigs. Periosteal cells were isolated from four minipigs, expanded in vitro and seeded with fibrin glue into Ethisorb 510 fleeces. Tissue constructs were used to repair critical-size mandibular defects and compared with two minipigs with untreated bone defects. Bone healing was evaluated after 90 and 180 days radiographically and using a histological scoring system. The radiographs showed increased radiodensity of defects filled with the cell-fibrin-fleece-constructs compared with the untreated control group

after 90 and 180 days. The defects repaired by the cell-fibrin-scaffolds obtained the highest histological mean score 2.9 (range 2-3) at 180 days and 2.1 (range 2-3) at 90 days while the control group scored 2 and 1 at the respective time intervals. So the scaffold seems to have sped up the healing process initially but the difference between the experimental group and the control group does not seem to have been significant after 180 days. The defect was therefore not of a critical-size as the authors suggested.

#### 3.1.1.3 Alginate

In 2008, He, et al. assessed the biological effect of novel calcium alginate film (CAF) on bone tissue regeneration in bilateral critical-size mandibular defects in 45 adult rabbits. The defects were covered either with CAF or conventional collagen membrane (CCM) or left empty as the controls. The animals were killed after 1, 2, 4, 6 and 8 weeks. Morphological and histomorphometric studies were performed to evaluate the bone regeneration pattern. This showed that the regeneration pattern was centripetal in-growth from the defect rim. The quantitative histomorphometric analysis revealed a significantly greater percentage of newly generated bone in the CAF defects than that in both the CCM and empty defects from 2 to 6 weeks post-operatively ( $p < 0.01$ ). After 6 and 8 weeks, significantly more mature lamellar bone had formed with CAF than with CCM. Empty control defects showed bone formation starting from the defect margins and incomplete healing even after 8 weeks. The CAF guided early bone growth and appeared more effective as a bioabsorbable GTR membrane than CCM. The authors concluded that the results suggest that bone defects augmented with CAF may offer most promising results from a

histological and histomorphometric perspective compared to conventional collagen membranes.

#### 3.1.1.4 Silk, Hyaluronan, Chitosan and Agarose

At present there are no reports on silk, hyaluronan, chitosan or agarose being used for the repair of critical-size defects in the mandible. They have however been used for the repair of critical-size defects in other bones.

Fini, et al. in 2005 reported on the use of an injectable silk fibroin (SF) hydrogel in the repair of critical-size defects in fourteen adult New Zealand White rabbit distal femurs. A synthetic poly(D,L lactide-glycolide) copolymer was used as control material. The rabbits were sacrificed at 4 and 12 weeks and the femurs were assessed histologically, histomorphometrically and with high-resolution radiographic investigations. Bone defect healing rate and quality of the newly formed bone inside the defects were determined by measuring trabecular bone volume (BV/TV), trabecular thickness (Tb.Th), trabecular number (Tb.N), trabecular separation (Tb.Sp), mineral apposition rate (MAR) and bone formation rate (BFR/B.Pm). Both materials promoted bone healing when used to fill critical size defects in rabbit femurs. The new-formed bone of the SF hydrogel treated defects showed significantly higher BV/TV, Tb.Th, MAR and BFR/B.Pm and lower Tb.Sp values in comparison with the control gel ( $p < 0.05$ ). The authors therefore concluded that SF hydrogel accelerated the bone remodeling processes.

Zanchetta, et al. (2003) evaluated the effectiveness of a hyaluronic acid-like bacterial exopolysaccharide (HE 800) in the repair of critical-size defects in parietal bone of male rats. The right hole was filled with either HE 800 or with collagen used as a negative control, while the left hole was left empty. After 15 days, the holes and surrounding tissues were examined by direct examination, radiographically and histologically. In the surgical sites repaired with HE 800, bone healing was almost complete ( $95.9\% \pm 6.2$ ). Neovascularisation was also observed along with organized trabecular bone. The control group that received collagen in the defect did not demonstrate significant healing ( $17.8\% \pm 18.1$ ).

Chitosan glutamate (obtained by the deacetylation of chitin, which is the structural element in the exoskeleton of crustaceans) mixed with hydroxyapatite was used by Mukherjee, et al. (2003) for the repair of critical-size defects in the calvaria of 100 rats (8mm diameter). The rats were divided into five treatment groups (20 per group): (1) empty defect as control, (2) defect filled with chitosan/hydroxyapatite only, (3) defect filled with the chitosan/hydroxyapatite containing bone-marrow aspirate, (4) defect filled with chitosan/hydroxyapatite containing 40 $\mu$ g rhBMP-2, and (5) defect filled with chitosan/hydroxyapatite containing osteoblasts cultured from bone-marrow aspirate. The animals were sacrificed at 9 weeks (10 per group) and 18 weeks (10 per group). The calvaria containing the defect were harvested, and the bone mineral density (BMD) was determined by dual energy X-ray absorptiometry. Push-out strength measurements were also performed. The BMD values of empty controls were significantly lower than those of other groups at both 9 and 18 weeks. The mechanical properties, however, were not significantly different between the



samples. Mineralized bone spicules were more prominent in the defect areas that were filled with chitosan/hydroxyapatite and osteoblasts cultured from bone-marrow aspirate. The authors concluded that the chitosan/hydroxyapatite paste could be used effectively to deliver osteoinductive factors for the repair of critical-size bone defects. The reason no statistically significant differences were seen between the different groups is that there was very wide variation in the mechanical properties as well as the bone mineral density measurements for the cases within each of the groups. It might have helped if the authors limited the number of groups and as a result increased the numbers of cases within each group.

Cuevas, et al. in 1997 used human recombinant acidic fibroblast growth factor (hraFGF) loaded in agarose for the repair of critical-size defects in the parietal bones of rats (Agarose is a polysaccharide which is mixed heterogeneously with agaropectin, another polysaccharide, to form Agar). Control animals received agarose alone in the defect. The animals were sacrificed 3 weeks post-operatively and the bone healing was evaluated histologically. HraFGF-treated animals showed a continuous bridge of regenerated bone extending from one edge of the defect to the other. None of the parietal defects that had been treated with agarose alone contained new bone in the central portion of the defect. The authors thus concluded that hraFGF promoted bone regeneration in critical-size defects.

### 3.1.2 Synthetic Scaffolds

#### 3.1.2.1 Ceramics

##### 3.1.2.1.1 Calcium Phosphate Cements

In 2002 Wikesjö, et al. assessed rhBMP-2 in a calcium-phosphate cement carrier (alphaBSM) for vertical alveolar ridge augmentation in six adult Hound Labrador mongrels. Three animals received rhBMP-2/alphaBSM (rhBMP-2 at 0.40 and 0.75mg/mL) in contralateral jaw quadrants (total implant volume/defect approximately 1.5mL). Three animals received alphaBSM without rhBMP-2 (control group). The animals were sacrificed 16 weeks post-operatively, and block biopsies were processed for histological and histometric analysis. RhBMP-2/alphaBSM induced substantial augmentation of the alveolar ridge. Control sites exhibited limited new bone formation. Vertical bone augmentation averaged ( $\pm$  SD)  $4.9 \pm 1.0$ mm (rhBMP-2 at 0.40mg/mL),  $5.3 \pm 0.3$ mm (rhBMP-2 at 0.75mg/mL), and  $0.4 \pm 0.4$ mm (control); new bone area  $8.5 \pm 4.2$ mm<sup>2</sup>,  $9.0 \pm 1.9$ mm<sup>2</sup>, and  $0.5 \pm 0.4$ mm<sup>2</sup>; new bone density  $55.1 \pm 6.4\%$ ,  $61.1 \pm 6.0\%$ , and  $67.7 \pm 9.5\%$ . Residual alphaBSM comprised  $< 1\%$  of the new bone. Bone density for the contiguous untreated bone ranged from 65 to 71%. The authors concluded that surgical implantation of rhBMP-2/alphaBSM appears an effective protocol for vertical alveolar ridge augmentation procedures. But this may not be applicable to critical-size bone defects.

### 3.1.2.1.2 Bioactive Glasses

Bioactive glasses have as yet not been used in the repair of critical-size mandibular defects but there have been reports of their use in the repair of critical-size defects in other bones.

Wheeler, et al. (2000) was the first to report on the use of bioactive glasses in the treatment of critical-size defects in bone. They histologically and biomechanically evaluated, in a rabbit model, bone formed within critical-sized distal femoral cancellous bone defects filled with 45S5 Bioglass particulates, 77S sol-gel Bioglass, or 58S sol-gel Bioglass and compared the bone in these defects with normal, intact, untreated cancellous bone and with unfilled defects at 4, 8, and 12 weeks. All grafted defects had more bone within the surgical area than did unfilled controls ( $p < 0.05$ ). The percentage of bone within the defect was significantly greater for the 45S5 material than for the 58S or 77S material at 4 and 8 weeks ( $p < 0.05$ ), yet by 12 weeks equivalent amounts of bone were observed for all materials. By 12 weeks, all grafted defects were equivalent to the normal untreated bone. The resorption of 77S and 58S particles was significantly greater than that of 45S5 particles ( $p < 0.05$ ). Mechanically, the grafted defects had compressive stiffness equivalent to that of normal bone at 4 and 8 weeks. At 12 weeks, 45S5-grafted defects had significantly greater stiffness ( $p < 0.05$ ). At 8 and 12 weeks, all grafted defects had significantly greater stiffness than unfilled control defects ( $p < 0.05$ ). In general, the 45S5-filled defects exhibited greater early bone ingrowth than did those filled with 58S or 77S. However, by 12 weeks, the bone ingrowth in each defect was equivalent to each other and to normal bone. The 58S and 77S materials

resorbed faster than the 45S5 materials. Mechanically, the compressive characteristics of all grafted defects were equivalent or greater than those of normal bone at all time points.

#### 3.1.2.1.3 Hydroxyapatite

In 1998 Lemperle, et al. compared bone regeneration in bilateral 15mm x 20mm critical-size calvarial and 30mm unilateral critical-size mandibular defects in eighteen adult mongrel dogs. The defects were either left empty, implanted with coralline hydroxyapatite (HA) blocks, or autografted with iliac cancellous bone. All defects were protected with a macroporous titanium mesh and the segmental mandibular defects were additionally stabilized by internal plate fixation. Specimens were retrieved after 2 and 4 months and three undecalcified longitudinal central sections including the osteotomy interfaces were prepared from each specimen for histometry and histology. Sections were analyzed for volume fractions of bone, soft tissue, and implant using scanning electron microscopy, backscatter electron imaging and histometric computer software. Interestingly, in the mandibular model, the empty defects exhibited the greatest amount of bone formation after 4 months (47.3 percent), which was greater than the amount of bone in the autografted group (34.8 percent) and significantly greater than the amount of bone within the hydroxyapatite implants (19.0 percent,  $p < 0.05$ ). In the cranial defects, the autografted specimens demonstrated the greatest volume fraction of bone after 4 months (27.3 percent), which was significantly greater than within both the empty defects (18.2 percent,  $p < 0.05$ ) and the hydroxyapatite implants (18.2 percent,  $p < 0.05$ ). New bone formation in the mandibular defects united the cut ends at 4 months regardless of treatment

and originated predominantly from the periosteum which remained present only along the alveolar border after surgical closure. In the calvarial defects, periosteum was not preserved and bone regenerated centripetally, originating from the diploë without any evidence of dural osteogenesis. Bone bridging was incomplete in the empty cranial defects at 4 months. In both the mandibular and cranial specimens, new bone at 2 months was a mixture of woven and parallel fibered bone. At 4 months, the new bone had remodeled almost entirely into mature Haversian bone. The authors concluded that they demonstrated a remarkable ability of defect protection with a macroporous protective sheet to facilitate bone regeneration in critical size mandibular and cranial bone defects. When active osteogenic periosteum was present, as in the mandibular model, they concluded that defect protection alone was sufficient to allow for healing even of critical size defects. When periosteum was absent as in the cranial defects, the limited spontaneous bone formation benefited from the added contributions of cancellous grafting and osteoconductive implants, both of which promoted bone bridging across the defects.

Mao T, et al. (1998) reported on the use of rhBMP-2 in the repair of critical-size defects in the rabbit mandible and calvarium using four carriers, namely chitin, coral, coral-based porous HA (CHA), and xenogenic cancellous bone. The repaired defects were examined radiographically, histologically (under light microscope and scanning electron microscope), by immunohistochemistry, and biomechanically 2, 4, 8, and 12 weeks post-operatively. In all composite graft groups, except in the CHA group, by 12 weeks the graft had been replaced completely by bone. Only fibrous tissue and a little peripheral new bone formed

in the defects in the control groups that had received only the carrier materials. The authors concluded that all the carriers used in this study would be effective for the use of BMP-2 in the repair of critical-size bone defects in the rabbit.

In 2003 Arosarena, et al. investigated the repair of critical-size defects created in the left mandibular bodies of thirty-seven male Fischer rats. The defects were filled with a bone marrow cell suspension (group 1), a synthetic bone matrix consisting of bovine collagen and calcium hydroxyapatite cement (group 2), the matrix and marrow cells (group 3), the matrix with 100 $\mu$ g of bone growth factor mixture (group 4), or the matrix with bone growth factor mixture and marrow cells (group 5). The animals were sacrificed after 8 weeks, and the nondemineralized specimens were processed histologically. The bone growth factor mixture consisted mostly of BMP-3 and TGF- $\beta$ . Stereologic techniques were used to determine and compare the volume fractions and volume estimates of mature bone, new bone, osteoid, marrow, remaining cement, and fibrous tissue in each defect. Volumes of mature bone, new bone, and remaining cement did not differ significantly among the groups ( $p = 0.30$  for mature bone,  $p = 0.17$  for new bone, and  $p = 0.34$  for cement). However, group 4 and 5 specimens contained significantly more osteoid and larger marrow spaces than did the group 2 and 3 specimens ( $P < 0.001$  for both). The specimens in groups 2 and 3 contained significantly more fibrous tissue ingrowth than did those in groups 4 and 5 ( $P < 0.001$ ). The authors thus concluded that the synthetic bone substitute containing bone growth factor mixture (groups 4 & 5) was effective in stimulating new bone and osteoid development in the rat mandibular model.

The bone inducing capabilities of PGE1 and BMP-5 were compared by Arosarena and Collins (2003). Critical-size mandibular defects were created in 29 Sprague-Dawley rats and were filled in one of seven ways; with collagen/PLA (group 1), PLA with BMP-5 (group 2), PLA with PGE1 (group 3), collagen/calcium hydroxyapatite cement (HAC) (group 4), HAC with BMP-5 (group 5), or HAC with PGE1 (group 6). The control group (group 7) had unfilled defects. The animals were sacrificed after 12 weeks, and the surgical sites were analysed histologically using stereologic techniques that provided quantitative estimates of the three-dimensional composition of the defects. The HAC/BMP-5 group contained significantly more new bone and less fibrous tissue than all the other groups ( $P \leq 0.02$  and  $P < 0.01$ , respectively). The groups containing PGE1 (groups 3 & 6) demonstrated significantly more osteoid development than the other experimental groups ( $P < 0.001$ ) suggesting a property of bone healing *delay*.

Henkel, et al. (2004) assessed a new composite calcium ceramic of HA and TCP fabricated by a sol-gel process at 120°C. Critical-size mandibular defects were created in eighteen 1y old Göttingen minipigs which were divided into three groups depending on how the defects were filled; group 1, 40%  $\beta$ -TCP plus 60% HA (the new product), group 2, HA alone and group 3 served as a control with only gelatinous material being placed in the defect. The animals were sacrificed after eight months and the surgical sites were examined macroscopically and microscopically. In groups 1 and 2 biodegradation of more than 93% of the new calcium phosphate formula was found 8 months postoperatively. No difference was observed between pure HA (group 2) and the combination of HA and beta-

TCP (group 1). In both groups complete bone formation was seen macroscopically. In the control group incomplete bone formation was noted (48.4%). This was significantly less than groups 1 and 2 ( $p < 0.001$ ). The authors concluded that the new calcium phosphate seemed to be suitable for filling critical-size bone defects. But it was not superior to the HA alone.

Henkel, et al. again in 2005 assessed the repair of critical-size mandibular defects in the anterior mandible of 16 adult mini-pigs. The defects were filled with the HA and TCP composite ceramic mentioned previously in one group, in another group the composite ceramic was used in combination with cultured autologous osteoblasts, and in the control group the defects were left empty. Five weeks postoperatively, the animals were sacrificed and the defects analysed macroscopically, histologically and radiographically. The highest rate of new bone formation was in the composite ceramic group without osteoblasts (73% of the defect). The composite ceramic was degraded at the same speed as new bone was laid down. In the control group, bone formation of 'only' 59% was observed. Additional transplantation of autologous osteoblasts in combination with the composite ceramic group did not result in more bone production than in the control group. The authors concluded that this new bioactive calcium phosphate matrix composite seemed to be a promising bone replacement material. But it seems that its properties were adversely affected by the addition of osteoblasts. The fact that 59% bone regeneration was seen in the control group means that the defect created was probably not of a critical size.



Again in 2006, Henkel, et al. assessed a HA and TCP composite ceramic this time sintered at 700°C. Bilateral critical-size defects (>5 cm) in the mandible of 15 adult Göttingen minipigs were filled in 5 different ways; group I, biphasic CaP matrix (HA:β-TCP, 60%:40%), group II, monophasic CaP matrix (HA:100%), group III, conventionally sintered pure hydroxyapatite (HA), group IV, conventionally sintered β-tricalcium phosphate (β-TCP), and group V, gelatin sponge. The animals were sacrificed 8 months post-operatively and the defects were assessed macroscopically, histologically, and morphometrically. In the groups that received the composite ceramics (groups I & II), complete bone formation was observed in the defect area, and the foreign material was resorbed almost completely. Incomplete bone formation and a lesser resorption rate of the scaffolding were noted in groups III & IV. There was a statistically significant difference in bone formation rate between the composite ceramics (93%) and the classical types of ceramics 58% ( $p < 0.01$ ). The authors concluded that the biological behaviour of the new CaP biomaterials (composite ceramics) was better than that of the old-type sintered ceramic bone-grafting materials.

#### 3.1.2.1.4 β-tricalcium phosphate

The articles discussing the use of β-TCP in the repair of mandibular critical-size defects have been discussed in the previous section on hydroxyapatite.

β-TCP has also been used in other bones for the repair of critical size defects. Li, et al. (2005) looked at the repair of critical-size defects in the left metatarses of 20 sheep using β-TCP. The defects were treated in one of three ways; in group 1 (n=8) β-TCP loaded with mesenchymal stem cells (MSCs) obtained

from bone marrow aspirates from the sheep was used, in group 2 (n=8)  $\beta$ -TCP was used alone and in group 3 (n=4) the defect was left empty. The sheep were sacrificed on the 6th, 12th, and 24th week postoperatively and the surgical sites were examined radiographically, histologically, and tested biomechanically. The sheep in group 3 were sacrificed on the 24th week postoperatively. The results showed that new bone growth was observed radiographically and histologically at the surgical sites of the experimental group as early as the 6th week postoperatively, but not in the control group, and osteoid tissue, woven bone and lamellar bone occurred earlier than in the control. At the 24th week, radiographs and biomechanical test revealed an almost complete repair of the defect of group 1, and only partly in group 2. The bone defects in group 3 had not healed. The authors concluded that porous  $\beta$ -TCP together with autologous MSCs were capable of repairing segmental bone defects in sheep metatarses.

In 2006, Jung, et al. evaluated the effect of using  $\beta$ -TCP with different particle sizes on the ability of rhBMP-4 to enhance bone formation in the rat calvarial defect model. 8mm diameter, calvarial critical-size defects were created in 100 male Sprague-Dawley rats. Five groups of 20 animals each received either rhBMP-4 (2.5 $\mu$ g) using  $\beta$ -TCP with a particle size of 50 to 150 $\mu$ m, rhBMP-4 (2.5 $\mu$ g) using  $\beta$ -TCP with a particle size of 150 to 500 $\mu$ m, a  $\beta$ -TCP control with a particle size of 50 to 150 $\mu$ m, a  $\beta$ -TCP control with a particle size of 150 to 500 $\mu$ m, or a sham-surgery control, respectively, and were evaluated by measuring their histological and histometric parameters following a 2 and 8 week healing interval. There were no significant differences in the defect closure, new bone area, or augmented area between either the two rhBMP-4/  $\beta$ -

TCP groups or between the two  $\beta$ -TCP control groups at 2 and 8 weeks. The authors thus concluded that rhBMP-4 combined with either small- or large-particle  $\beta$ -TCP had a significant effect on the induction of bone formation compared to either a small- or large-particle  $\beta$ -TCP control or a sham-surgery control. Within the parameters of this study, varying the particle size of beta-TCP did not seem to have a significant effect on bone formation.

### 3.1.2.2 Titanium

Lemperle, et al. (1998) compared bone regeneration in bilateral 15mm x 20mm critical-size calvarial and 30mm unilateral critical-size mandibular defects in eighteen adult mongrel dogs. The defects were either left empty, implanted with coralline hydroxyapatite (HA) blocks, or autografted with iliac cancellous bone. All defects were protected with a macroporous titanium mesh and the segmental mandibular defects were additionally stabilized by internal plate fixation. The paper is discussed in more detail previously in the section on hydroxyapatite. The authors concluded that they demonstrated a remarkable ability for defect protection with the macroporous protective sheet which facilitated bone regeneration in the critical size mandibular and cranial bone defects. When active osteogenic periosteum was present, as in the mandibular model, they concluded that defect protection alone was sufficient to allow for healing even of critical size defects.

Herford and Boyne (2008) reported on 14 patients who were selected from a larger group having received BMP-2 in different categories of mandibular defects. The rhBMP-2 in all the cases reported was used alone with a collagen

carrier without concomitant bone materials. The cases involved lesions of the body and angle of the mandible in 2 categories: 1) defects resulting from neoplastic diseases; and 2) defects secondary to osteomyelitis (related to bisphosphonates or irradiation). A total dose of 4 to 8 mg of rhBMP-2 was delivered to the surgical site in concentrations of 1.5 mg per cc (depending on the size of lesion). Cases were followed over a period from 6 to 18 months. Occlusal function was restored with implant-borne or conventional prosthesis. All of the cases reported had successful osseous restoration of the edentulous area followed by prosthetic treatment. Bone formation in the surgical area could be palpated at the end of 3 to 4 months and identified radiographically at the end of 5 to 6 months. The maintenance of a periosteal envelope was achieved by the use of a superiorly placed titanium minibar in the upper portion of the defect, or with the use of titanium mesh superiorly. This metallic tenting up to the mucosa was thought to be necessary to maintain the space for osseous regeneration. The authors concluded that the use of rhBMP-2 without concomitant bone grafting materials in large critical sized mandibular defects produced excellent regeneration of the area establishing the basis for the return to prosthodontic function.

### 3.1.2.3 Polymeric materials

#### 3.1.2.3.1 Poly( $\alpha$ -hydroxy esters)

##### 3.1.2.3.1.1 Poly(L-lactic acid)

Schliephake, et al. (1998) reported on the use of polylactic acid (PLA) tubes and pyrolyzed bovine bone for the repair of bilateral bone defects in the mandibles of 15 Göttingen minipigs. In five animals, group 1, 2cm defects on one side were bridged by a system of PLA tubes and pyrolyzed bovine bone alone (alloplastic scaffold), and on the other side with alloplastic scaffolds loaded with 115µg recombinant human basic fibroblast growth factor (rhbFGF). In five other animals, group 2, defects of 4cm were also similarly bridged by the alloplastic scaffold alone on one side and on the other side with the scaffolds loaded with 230µg rhbFGF. In five control animals, group 3, bilateral 2-cm defects were created that were left empty on one side and bridged with an empty PLA tube on the other. Mitogenic efficacy of the growth factor was assessed on fibroblast cultures by di-methyl-thiazol-2-tetrazolium-bromide assay before implantation. After 5 months, there was negligible bone regeneration in the control defects (group 3), regardless of whether they had been left completely empty or bridged by empty PLA tubes. The 2cm defects (group 1) showed bridging in 8 of 10 tubes, with complete consolidation by bone ingrowth in four defects. The 4-cm defects (group 2) showed bony union in six cases, with complete bone fill in two tubes, and four defects incompletely filled. The bFGF had no appreciable effect with regard to velocity, quantity, and three-dimensional structure of bone formation, neither in the short nor in the long defects despite clear in vitro efficacy. The authors concluded that the repair of segmental defects using polylactic acid membranes appears to be possible. However, a single-dose application of bFGF is apparently ineffective, possibly because of rapid dilution.

The use of PLA together with growth factors in the repair of critical-size mandibular defects was again reported in 1999 by Xu, et al. They looked at the effect of basic fibroblast growth factor (bFGF) on bone formation induced by recombinant human bone morphogenetic protein-2(rhBMP-2) in the repair of mandibular defects in rabbits. PLA was used as a carrier and healing was assessed radiographically and histologically. The group that received a composite graft of bFGF and rhBMP-2 on the PLA carrier had the best bone growth at 4 weeks post-operatively ( $p < 0.05$ ), when compared to PLA with rhBMP-2, PLA with bFGF, PLA alone, and a no graft control. The authors concluded that PLA has good biocompatibility, absorbability and osteoconductibility, rhBMP-2 and bFGF cooperated in the bone healing process, and PLA/rhBMP-2/bFGF might be a promising bone substitute.

Arosarena and Collins (2003) discussed the bone inducing effects of PGE1 and BMP-5 in critical-size mandibular defects created in 29 Sprague-Dawley rats that were filled with collagen/PLA or collagen/calcium hydroxyapatite cement (HAC). The article is discussed previously in the section on hydroxyapatite.

Schliephake, et al. (2008) again discussed the use of PLA in the repair of critical-size bone defects in the mandibles of 45 Wistar rats. Fifteen rats received p-DL-lactic acid discs loaded with 96 $\mu$ g rhBMP-2 (Group 2), 48 $\mu$ g rhBMP-2 (Group 1) and unloaded discs without BMP (Group 0) each on one side of the mandible. Unfilled defects of the same size on the contralateral sides of the mandibles served as empty controls. After 6, 13 and 26 weeks, implants of each group were retrieved from five animals each and submitted to flat panel

detector computed tomography. Bone formation and thickness of augmentation was assessed by computer-assisted histomorphometry. In Group 2 significantly more bone was produced than in Group 1. Implants of Group 1 induced significantly more bone than the blank controls only after 6 weeks, whereas the difference was not significant after 13 and 26 weeks. Differences between Group 2 and Group 1 were clearly significant after 26 weeks. The thickness of bone tissue was maintained in Group 2 whereas it decreased in Group 1 and was negligible in Group 0. The authors concluded that the PLA implants with 96µg rhBMP-2 were able to bridge a non-healing defect in the rat mandible and maintained the thickness of an augmented volume. However, a continuous supply of osteogenic signals appears to be required (thus the better result with the higher rhBMP-2 concentration) to compensate for adverse effects during polymer degradation, further supporting the conclusions they had made in their earlier article (Schliephake, et al. 1998). The biocompatibility of the PLA therefore remains a significant problem when it comes to clinical application.

#### 3.1.2.3.1.2 Poly(glycolic acid)

Poly(glycolic acid) has not yet been used in the repair of critical-size defects in the mandible but had been used in other sites. Breitbart, et al. (1998, 1999) reported on the use of poly(glycolic acid) in the repair of critical-size defects in calvarium of rabbits. In the 1998 article they isolated periosteum from 30 New Zealand White rabbits, grew it in cell culture, labelled it with the thymidine analog bromodeoxyuridine for later localization, and seeded it into resorbable polyglycolic acid scaffold matrices. In group I (n=10), the calvarial defects were repaired using the resorbable polyglycolic acid implants seeded with

periosteal cells. In group II (n=10), the defects were repaired using untreated polyglycolic acid implants. In group III (n=10), the defects were left unrepaired. The rabbits were killed at 4 and 12 weeks postoperatively. The defect sites were then studied histologically, biochemically, and radiographically. At 4 weeks islands of bone were found in the defects repaired with polyglycolic acid implants with periosteal cells (group I), whereas the defects repaired with untreated polyglycolic acid implants (group II) were filled with fibrous tissue. Collagen content was significantly increased in group I compared with group II ( $2.90 \pm 0.80 \mu\text{g}/\text{mg}$  dry weight versus  $0.08 \pm 0.11 \mu\text{g}/\text{mg}$  dry weight,  $p < 0.006$ ). At 12 weeks there were large amounts of bone in group I, whereas there were scattered islands of bone in groups II and III. Radiodensitometry demonstrated significantly increased radiodensity of the defect sites in group I, compared with groups II and III ( $0.740 \pm 0.250 \text{ OD}/\text{mm}^2$  versus  $0.404 \pm 0.100 \text{ OD}/\text{mm}^2$  and  $0.266 \pm 0.150 \text{ OD}/\text{mm}^2$ , respectively,  $p < 0.05$ ). Bromodeoxyuridine label, as detected by immunofluorescence, was identified in the newly formed bone in group I at both 4 and 12 weeks, confirming the contribution of the cultured periosteal cells to this bone formation. It might have been useful to have another group where the periosteal cells were placed in the defect without the polyglycolic acid implants to check for the contribution the scaffold itself was making on the regeneration.

In their 1999 article Breitbart et al again repaired critical-size cranial vault defects in rabbits using periosteal cells. This time the periosteal cells were transduced retrovirally with the bone morphogenetic protein 7 (BMP-7). Human BMP-7 complementary deoxyribonucleic acid was generated from a cell



line using reverse transcription polymerase chain reaction and cloned into a retroviral vector plasmid. Retroviral vector particles were then used to transduce the rabbit periosteal cells. The transduced periosteal cells demonstrated substantial production of both BMP-7 messenger ribonucleic acid by Northern blot analysis and BMP-7 protein by enzyme-linked immunosorbent assay. These cells were then seeded into polyglycolic acid (PGA) matrices and used to repair the critical-size defects. At 12 weeks, defect sites repaired with BMP-7-transduced periosteal cells/PGA had significantly increased radiographic and histological evidence of bone repair compared with those defect sites repaired with negative control-transduced cells/PGA, nontransduced cells/PGA, PGA alone, or unrepaired defects. Again a group with just transduced cells and no PGA might have been useful, as the effect of the scaffold itself on the healing was not being directly assessed.

#### 3.1.2.3.1.3 Poly(lactic-co-glycolic acid)

In 1999, Higuchi, et al. looked at the repair of bilateral round through-and-through bone defects (5 mm in diameter) in the angle of the mandible in eight Long-Evans rats, using, rhBMP-2 in a PLGA/gelatin sponge (PGS) carrier. The control side received only the PGS carrier. The rats were sacrificed after 4 weeks and the surgical sites analysed histologically and histomorphometrically. In the control group, bone formation was present only along the border of the surgical site. In all cases in the BMP-2 group, a significantly larger quantity of newly formed bone was observed, with the bone defect being completely filled with new bone in 4 of 8 rats ( $p < 0.0001$ ). The authors thus concluded that

rhBMP-2/PGS induced effective bone regeneration on mandibular defects in rats. However, these defects were not continuity defects.

Critical-size defect repair in the canine mandible was assessed by Nagao, et al. (2002). RhBMP-2 in a PGS carrier was used to repair bilateral rectangular bone defects (10 x 8 x 7 mm) in the premolar region of twelve adult beagle dogs. On examining the surgical sites with soft x-rays, three-dimensional computed tomography, histologically and peripheral quantitative computed tomography, the control group that received only PGS showed no bone regeneration. In contrast, in the group that received the BMP-2, newly formed bone was found in all defects from 4 weeks onward and was marked at 12 weeks, and the density of the newly formed bone was similar to that of the surrounding cortical bone at 12 weeks.

In 2001 and 2002 Marukawa, et al. reported on the repair of critical-size mandibular defects in the rhesus monkey (*Macaca mulatta*) with BMP-2 using PGS as a carrier. 20mm and 30mm size defects were created in the respective studies and in all cases there was excellent bone regeneration both radiographically and histologically compared to controls. The article is discussed further in the section on BMP-2.

Abukawa, et al. (2004) treated critical-size defects in *one* porcine mandible with PLGA loaded with mesenchymal stem cells (MSCs) isolated from the ilium. Four full-thickness bony defects (2 x 2 cm) were created in the pig's mandible. The loaded PLGA scaffolds (n = 2) were placed into two of the defects. One

unseeded scaffold and 1 empty defect served as controls. At 6 weeks postimplantation, the pig was sacrificed, the mandible harvested, and the grafted sites were evaluated clinically, radiographically, and histologically. The construct-implanted defects appeared to be filled with hard tissue resembling bone, whereas controls were filled with fibrous tissue. Radiographically, the tissue-engineered constructs were uniformly radiodense with bone distributed throughout. The interface between native bone and constructs was indistinct. Complete bone ingrowth was not observed in control defects. Osteoblasts, osteocytes, bone trabeculae, and blood vessels were identified throughout the defects implanted with constructs.

Critical-size mandibular defect repair in rabbits using PLGA was also assessed by Ren, et al. (2005). The defects were filled with; PLGA loaded with MSCs, PLGA scaffold alone, and nothing in the control group. The animals were sacrificed after 3 months and the surgical sites were assessed histologically. The surgical defects had healed completely in the group treated with PLGA loaded with MSCs but did not heal in the other two groups.

#### 3.1.2.3.1.4 Poly(propylene fumarate)

Trantolo, et al. (2003) assessed the osteoinductive capacity of a bioresorbable bone graft substitute made from the unsaturated polyester poly(propylene glycol-co-fumaric acid) (PPF) for mandibular reconstruction in twenty adult Sprague-Dawley rats. Animals in group A (n=10) were treated with implantation of the PPF-based bone graft substitute. In group B animals with similar defects (n=10), the drill holes were left to heal unaided. The amount of

new bone formation and the presence of an inflammatory infiltrate were evaluated at 7 weeks postoperatively. Histological analysis of the healing process revealed enhanced in vivo new bone formation with the PPF bone graft substitute. These findings were corroborated by the histomorphometric analysis of new bone formation. The authors concluded that the results of this study demonstrated biocompatibility of the porous PPF-based scaffold in a mandibular defect. However, the defects were just 3mm diameter *outer-cortical defects* of the mandibular ramus, so not critical-size defects.

#### 3.1.2.3.1.5 Poly(anhydride)

In 1998, Ibim, et al. tested the osteocompatibility of poly(anhydride-co-imides) polymers based on poly[trimellitylimidoglycine-co-1,6-bis(carboxyphenoxy)hexane] (TMA-Gly:CPH) and poly[pyromellitylimidoalanine-co-1,6-bis(carboxyphenoxy)hexane] (PMA-Ala:CPH), in the healing of bone defects in rat tibias. 3mm diameter defects were filled with the poly(anhydride-co-imide) matrices and compared to the control PLGA. The animals were sacrificed at 3, 6, 9, 12, 20, and 30 days and tissue histology was examined for bone formation, polymer-tissue interaction, and local tissue response by light microscopy. The studies revealed that matrices of TMA-Gly:CPH and PMA-Ala:CPH produced responses similar to the control PLGA with tissue compatibility characterized by a mild response involving neutrophils, macrophages, and giant cells throughout the experiment for all matrices studied. Matrices of PLGA were nearly completely degraded by 21 days in contrast to matrices of TMA-Gly:CPH and PMA-Ala:CPH that displayed slow erosion characteristics and maintenance of shape. Defects in

control rats without polymer healed by day 12, defects containing PLGA healed after 20 days, and defects containing poly(anhydride-co-imide) matrices produced endosteal bone growth as early as day 3 and formed bridges of cortical bone around the matrices by 30 days. In addition, there was marrow reconstitution at the defect site for all matrices studied along with matured bone-forming cells. The authors concluded that their study suggested that the novel poly(anhydride-co-imides) were promising polymers that may be suitable for use as implants in bone surgery, especially in weight-bearing areas due to their slow erosion characteristics. But, the fact that the polymers delayed healing when compared to the empty defects puts the utility of these products for the repair of critical-size bone defects into question.

#### 3.1.2.3.1.6 Poly(phosphazene)

There is only one report on the assessment of the repair of bone defects with the use of poly(phosphazene) and it was not used in critical-size defects. Veronese, et al. (1999) assessed membranes or microcapsules made from polyphosphazenes for the treatment of four rabbit tibial bone defects. The authors stated that polyphosphazene membranes prepared with alanine ethyl ester and imidazole had a degradation rate that corresponded to the healing rate of natural bone. They concluded that these membranes were much more successful in promoting healing of rabbit tibia defects than polytetrafluoroethylene membranes. However, the material was used more as a barrier membrane for guided tissue regeneration rather than as a scaffold.

#### 3.1.2.3.1.7 Polyethylene glycol

Polyethylene glycol, also known as poly(ethylene oxide), has been used in copolymer constructs for the repair of critical-size defects in the mandible in two main forms; poloxamer gel, which is a nonionic triblock copolymer composed of a central hydrophobic chain of poly(propylene oxide) flanked by two hydrophilic chains of poly(ethylene oxide), and Polyactive<sup>®</sup>, which is poly(ethylene oxide)-p-bromotoluene a hydrogel copolymer (PEO/PBT).

Meijer, et al. (1996) reported on the repair of bone defects with PEO/PBT hydrogel copolymers in beagle dogs. The defects were filled with either precalcified or nonprecalcified porous cylindrical PEO/PBT 80/20 implants, or hydroxyapatite granules held together with PEO/PBT 70/30, or were left unfilled. A significantly higher percentage of mineralization was present in the cavities filled with the precalcified PEO/PBT 80/20 copolymer than in the control defects. As a result of swelling by fluid-uptake, the press-fit inserted copolymer implants showed a significant reduction in pore size, thus preventing optimal bone ingrowth. The authors concluded that both precalcification of the copolymer and underfilling of the defect, to create space for the copolymer to increase in diameter, stimulate postoperative calcification and bone ingrowth in PEO/PBT 80/20 copolymers.

In 2008, Issa, et al. evaluated the poloxamer gel as a potential carrier of rhBMP-2 for the repair of critical-size mandibular defects in fifty-six male Wistar rats. They also checked if collagen sponge can further improve the healing process. The rats were divided into two main groups (for sacrifice at 2 and 4 weeks), which were further subdivided into four groups with seven animals in each group the defects were then filled as follows; in one group the defect was filled

with 4µg rhBMP-2 in aqueous solution, in another group with 4µg rhBMP-2 in aqueous solution with collagen sponge, in another with 4µg rhBMP-2 combined with the poloxamer gel, and in the remaining group with 4µg rhBMP-2 combined with poloxamer gel with collagen sponge. After 2 and 4 weeks the animals were sacrificed and the hemi-mandibles removed for histological analysis. There was a statistically significant difference in bone regeneration between all the analysed groups ( $p < 0.01$ ), and between the periods of time ( $p = 0.0118$ ). There was no association between the treatment used and time of sacrifice ( $p = 0.642$ ). Results showed that the rhBMP-2 used in this study was able to induce bone regeneration and that its action was optimized significantly when it was combined with the poloxamer gel was and covered with collagen sponge.

**Aim**



#### 4.1 Aim of the study

The aim of this investigation was to assess the histological, radiographic and mechanical properties of the tissue regenerate following the application of tricalcium phosphate (TCP) scaffolding and recombinant human bone morphogenetic protein 7 (rhBMP-7) for the reconstruction of a critical-size osteoperiosteal mandibular continuity defect in the rabbit model.

#### Hypothesis

The addition of rhBMP-7 to TCP will increase the quality and quantity of bone regeneration.

## **Materials and Methods**

## 5.1 Preclinical investigations

### 5.1.1 Rabbit mandible anatomy

Assessment of the veterinary anatomy text books and of dry mandibular specimens showed that the bone of the ramus of the rabbit mandible was too thin to be used for the creation of the critical-size defect (Figures 5.1 & 5.2). Furthermore, several muscles of mastication are attached in this region (Table 5.1), and reflection of these muscles may interfere with the animal welfare.

The rabbit dentition consists of (per quadrant):

- Maxilla; incisors 2, canines 0, premolars 3, molars 2-3
- Mandible; incisors 1, canines 0, premolars 2, molars 3 (Figures 5.3, 5.4)

Radiographic evaluation of the mandible showed that the premolar and molar teeth took up most of the posterior body of the mandible (Figure 5.3); the risk of damaging the teeth therefore also precluded this site for creation of a critical-size defect. The anterior half of the body of the mandible was noted to contain only the mental foramen and an incisor tooth on each side (Figures 5.1, 5.3 & 5.4). This site was therefore selected for the creation of a critical-size mandibular defect (just over one quarter of the body of the mandible on one side) without compromising the rehabilitation of the animal.

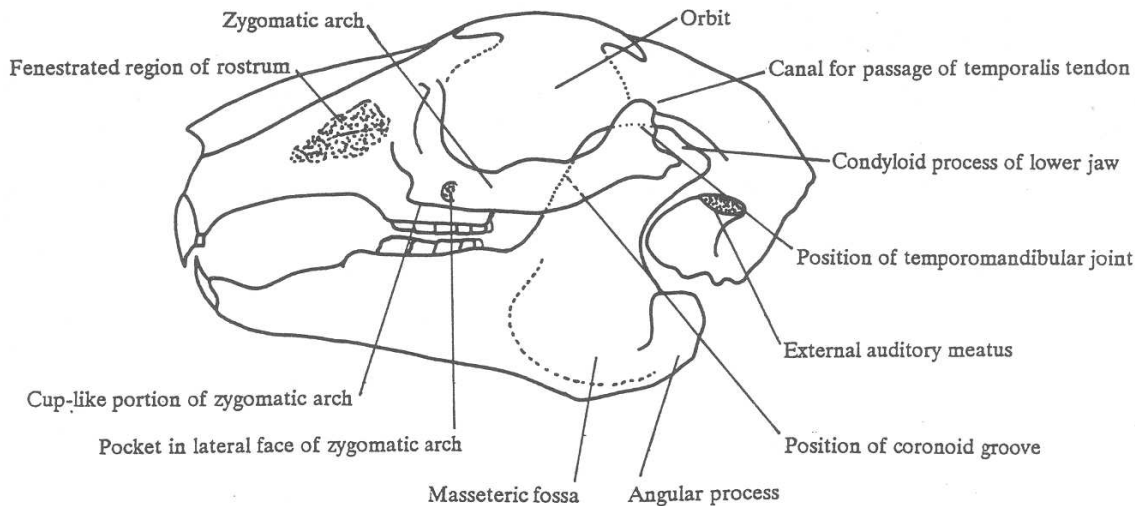


Figure 5.1 Lateral view of the anatomy of the skull and mandible of the rabbit.

(Russell AP. The mammalian masticatory apparatus: an introductory comparative exercise. Karcher SJ. 1998:271-286).

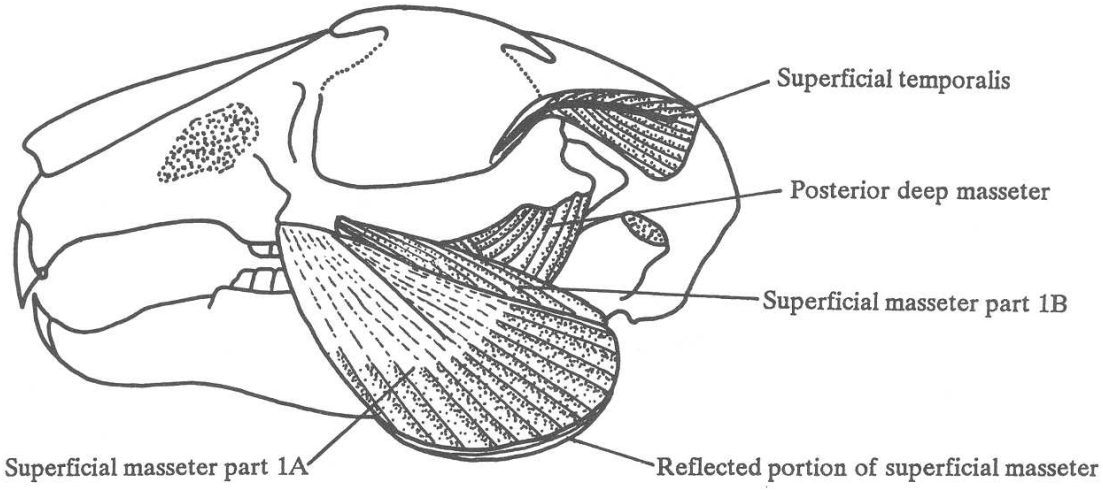


Figure 5.2 Lateral view of skull and mandible with muscles of mastication still attached.

(Russell AP. The mammalian masticatory apparatus: an introductory comparative exercise. Karcher SJ. 1998:271-286).

Muscle Mass	Major Components	Subdivisions
Temporalis	<ul style="list-style-type: none"> <li>Superficial</li> <li>Deep</li> </ul>	<ul style="list-style-type: none"> <li>Lateral</li> <li>Medial</li> </ul>
Masseter	<ul style="list-style-type: none"> <li>Superficial</li> <li>Deep (Zygomaticomandibularis)</li> </ul>	<ul style="list-style-type: none"> <li>Reflected Portion</li> <li>Part 1A</li> <li>Part 1B</li> <li>Part 2</li> <li>Anterior</li> <li>Posterior</li> </ul>
Pterygoideus	<ul style="list-style-type: none"> <li>Medial</li> <li>Lateral</li> </ul>	<ul style="list-style-type: none"> <li>Superior</li> <li>Inferior</li> </ul>

Table 5.1 Rabbit muscles of mastication.

(Russell AP. The mammalian masticatory apparatus: an introductory comparative exercise. Karcher SJ. 1998:271-286).

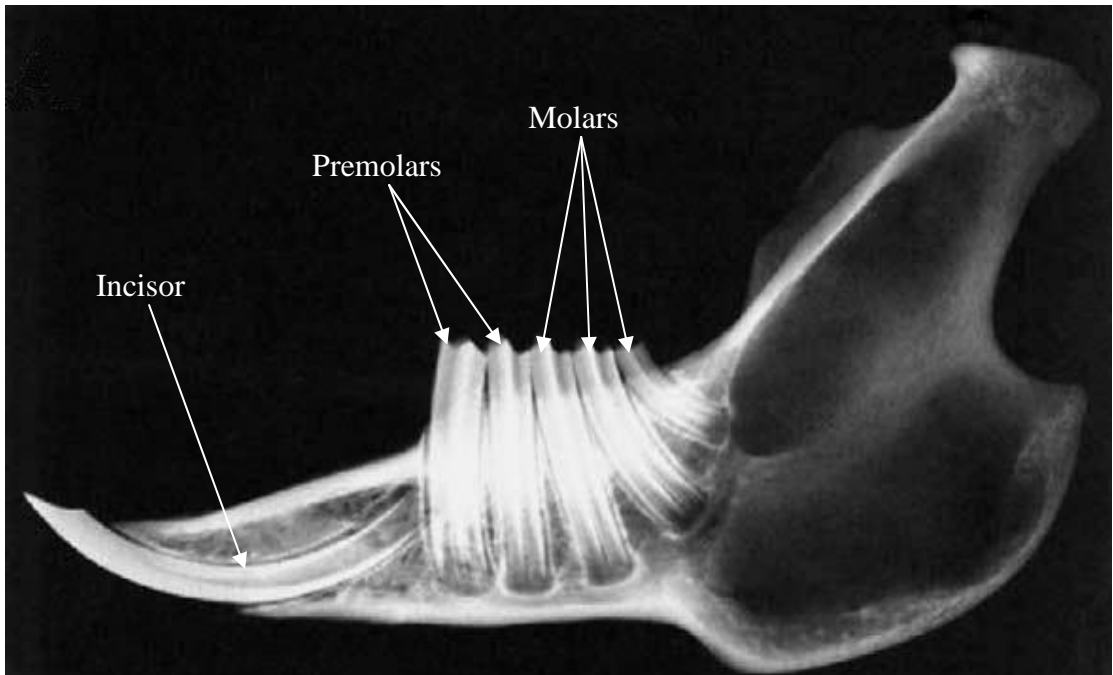


Figure 5.3 Lateral plain radiographic film of an explanted rabbit mandible showing the long roots of the incisor, premolar and molar teeth.

### 5.1.2 Dry mandible specimens

Creation of the critical-size defect was performed in four dry rabbit mandible specimens to test the most effective method for maintaining the integrity of the mandible after mandibular resection (Figures 5.4 & 5.5).

#### 5.1.2.1 Surgical site creation

A surgical tungsten carbide fissure bur was found to be the most effective and easily available tool for the creation of the surgical site defect. This was used on a surgical handpiece rotating at 40,000 revolutions per minute. Water irrigation would be used intra-operatively on the live cases so as to avoid overheating of the surgical site.

#### 5.1.2.2 Surgical site support

Two different methods for post-operative support of the mandible were tested. The first method (Figure 5.6) involved the creation of two through-and-through bur holes, in line with each other, with a 1mm diameter fissure bur; one on each side of the mandible just posterior to the last molar tooth and above the inferior border of the mandible. A 1.1mm diameter Kirshner surgical wire was then placed across these holes and cut so that 5mm of wire was left protruding from each side of the mandible. Two 2mm diameter 8mm long titanium screws (Synthes cortex screw, Synthes GmbH) were then placed into the outer cortex in pre-prepared holes 5mm anterior to the Kirshner wires.

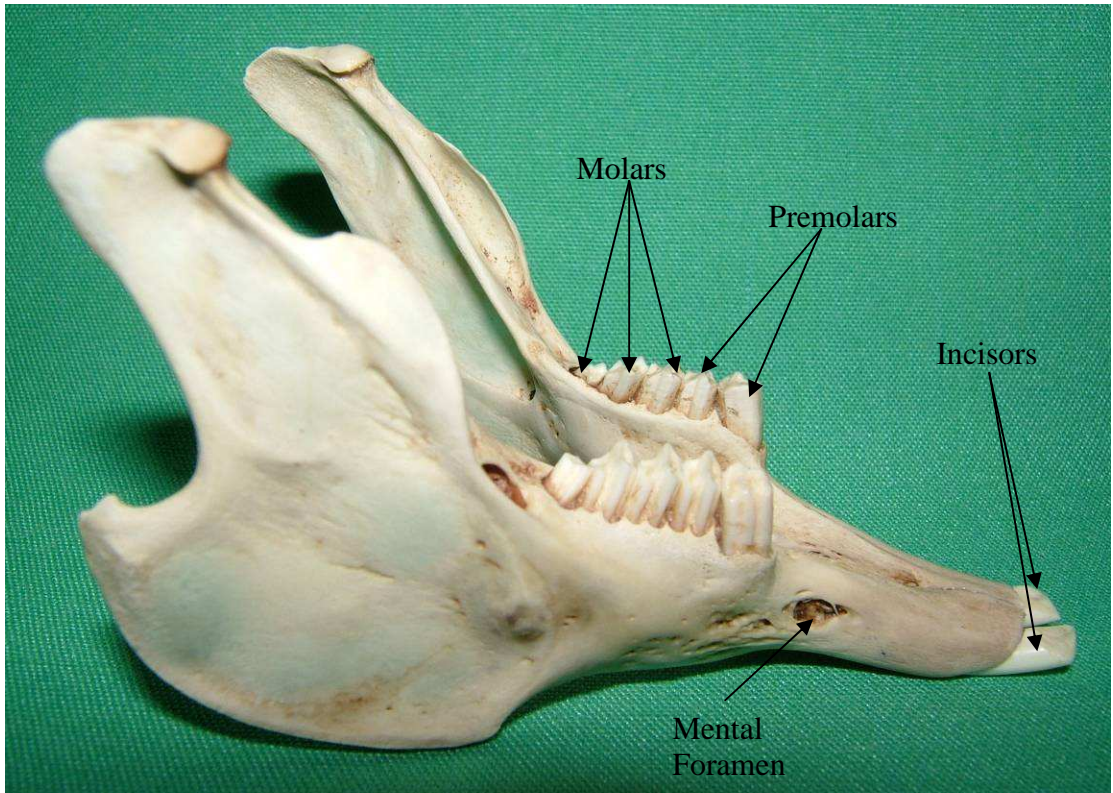


Figure 5.4 Lateral view of dry explanted rabbit mandible.

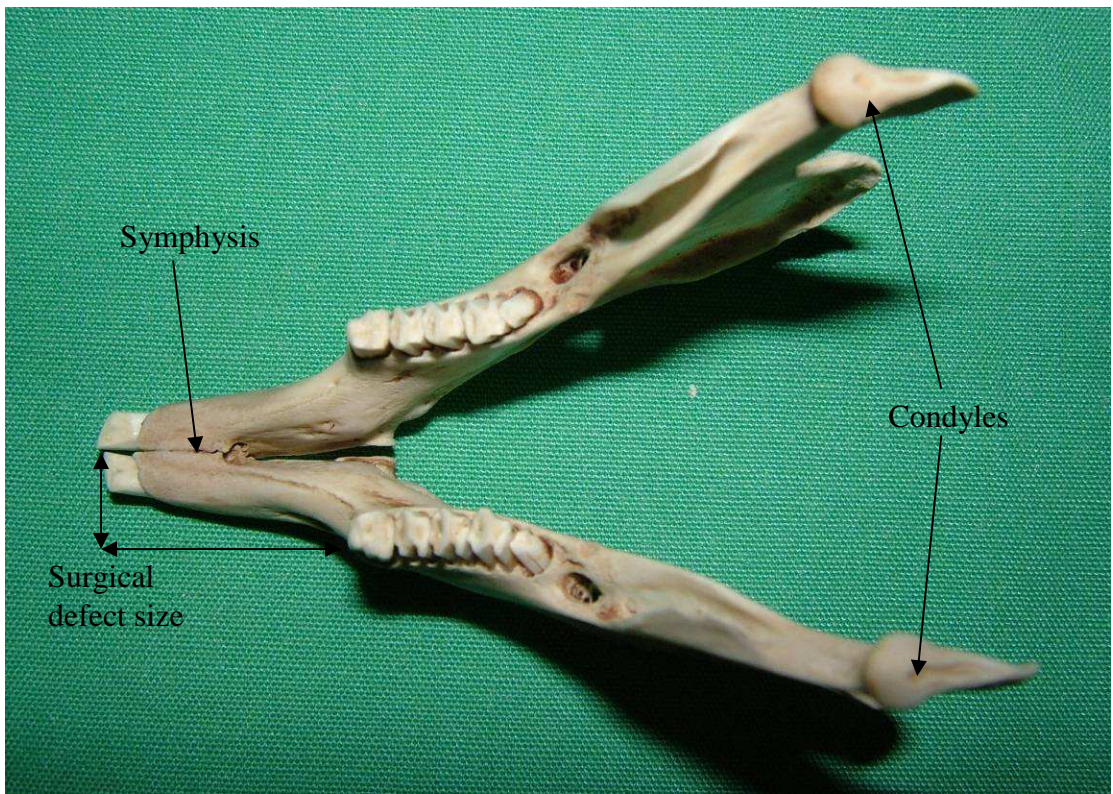


Figure 5.5 Superior sagittal view of dry explanted rabbit mandible.



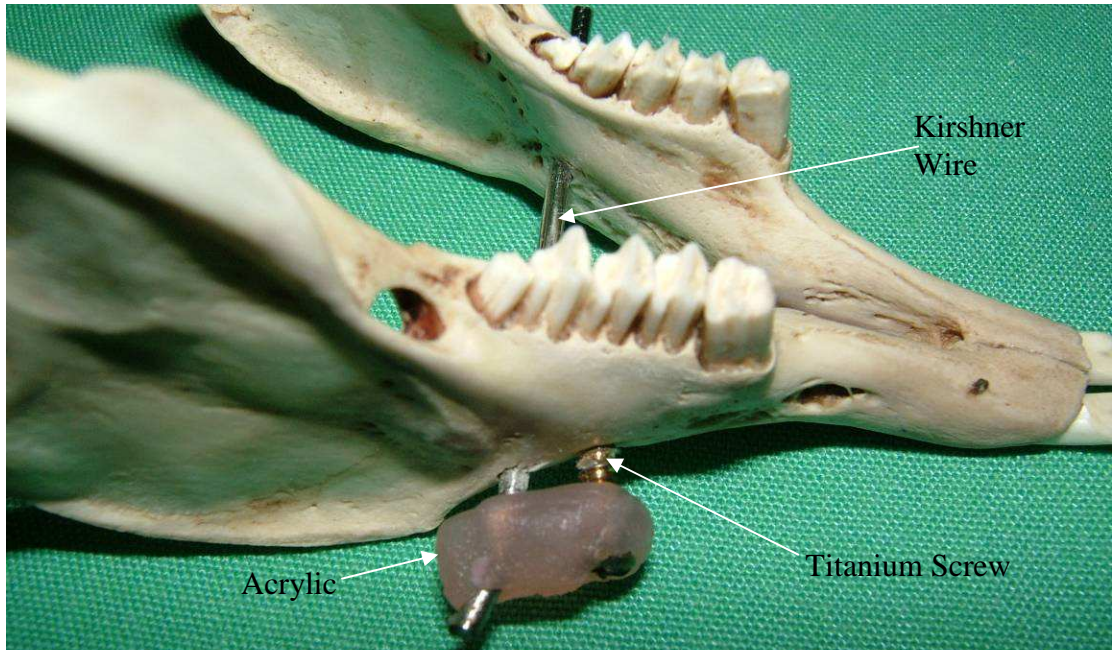


Figure 5.6 Close up view of first tested method for mandibular support using Kirshner Wire and titanium screws.

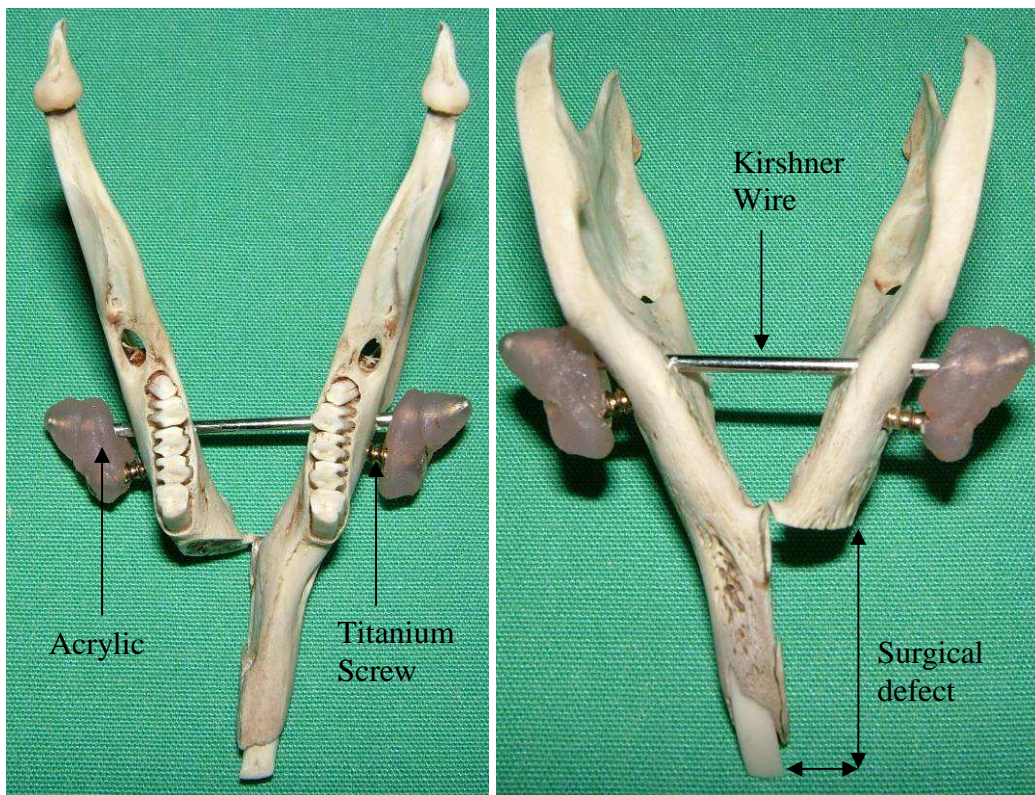


Figure 5.7 Superior view of surgical defect. Figure 5.8 Inferior view of surgical defect.

The screws and Kirshner wire were then joined together on each side with fast setting, cold curing pink acrylic. This produced effective support for the surgical site allowing creation of the surgical defect (Figures 5.7 & 5.8), but would have required the rabbits to have external fixators attached to the mandible which might have increased the risk of injury to the animal and the possible spread of infection within the surgical site.

A second method was therefore tested. Before the creation of the surgical defect, a horizontal bur hole was created with a 1.5mm diameter surgical fissure bur just in front of the roots of the first premolar tooth and 1mm above the inferior border of the mandible. This hole was made to a depth of at least 14mm to ensure perforation of the contralateral mandibular body. A 2mm diameter, 12mm or 14mm long (depending of width of mandible) titanium screw (Synthes cortex screw, Synthes GmbH) was then inserted to engage the cortex of the contralateral mandible (Figures 5.9 to 5.12). This provided the necessary support required after the creation of the surgical defect. The screw head was placed flush with the cortical bone of the mandible (Figure 5.12), to facilitate complete closure of the surgical site post-operatively and avoid the risk of infection.

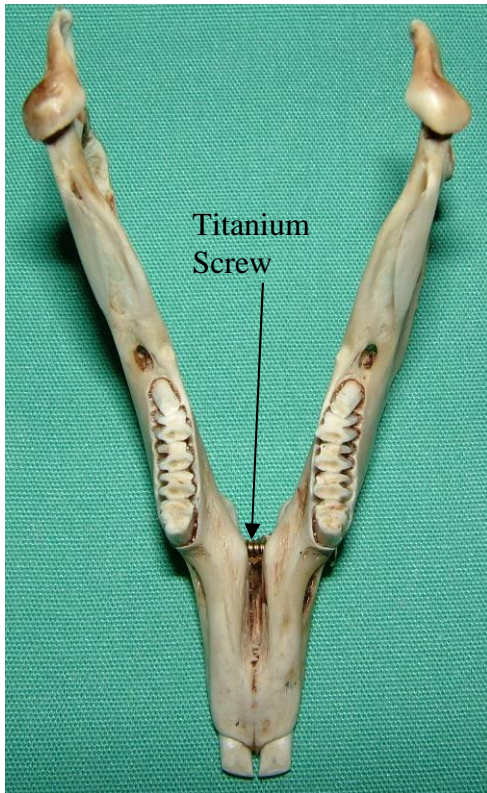


Figure 5.9 Superior view of titanium screw in place.

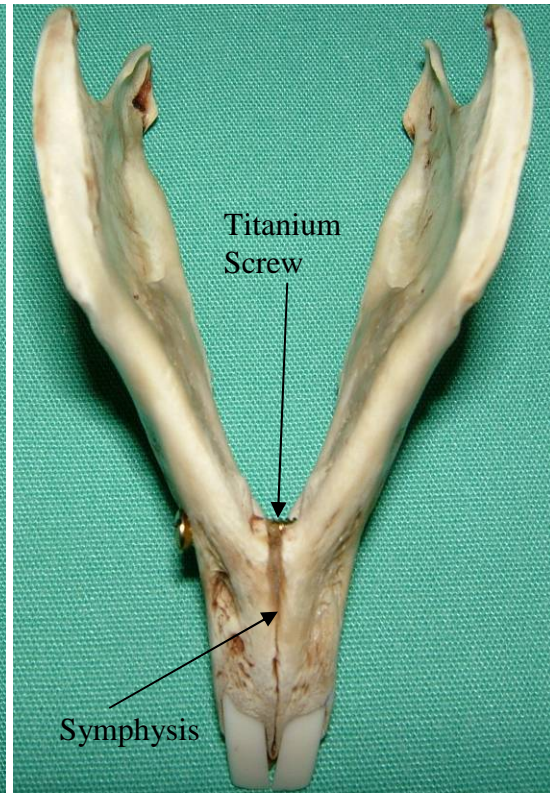


Figure 5.10 Inferior view of titanium screw in place.

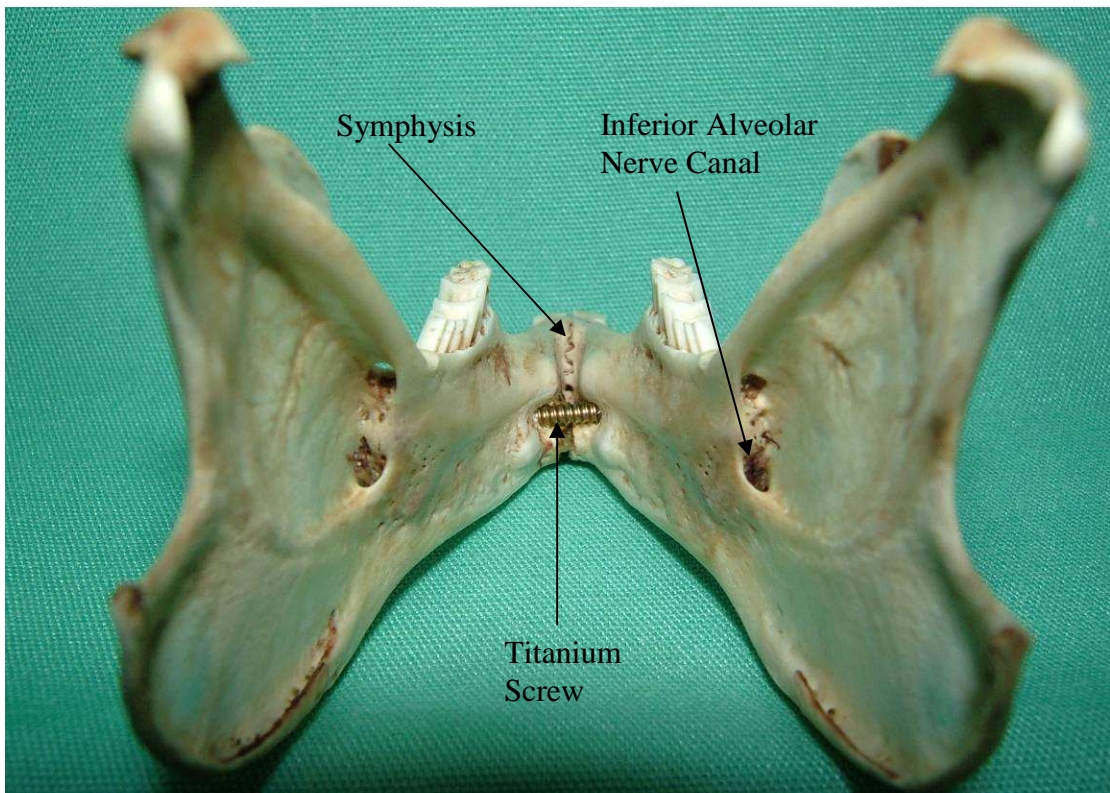


Figure 5.11 Posterior view of titanium screw in place in the dry mandible.

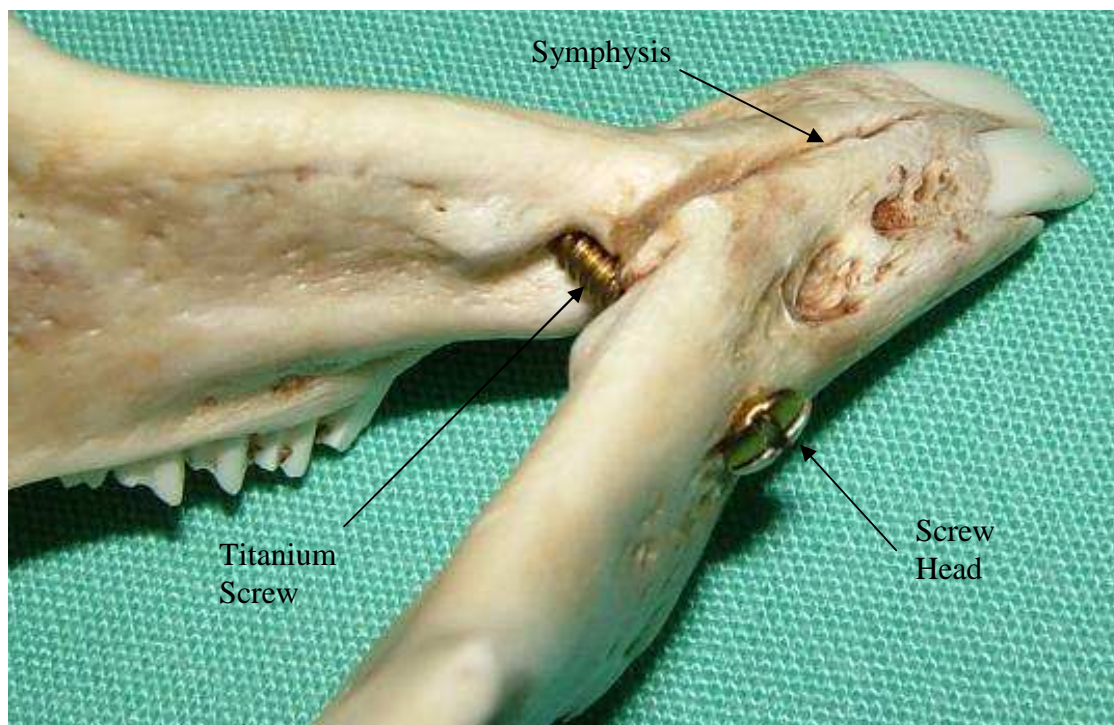


Figure 5.12 Inferior close-up view of the titanium screw in place in the dry explanted rabbit mandible.

### 5.1.3 Cadaveric work

The effectiveness of the previously described surgical defect creation method as well as the surgical site support technique was then tested on two cadaveric rabbits. Two New Zealand white rabbits weighing 3.5kg were killed using an overdose of pentobarbitone sodium (140mg/kg). An incision was made along the inferior border of the mandibular body on the right side. The platysma was reflected and by supra-periosteal dissection elevating the buccinator, the mental nerve and foramen were identified, just anterior to the first premolar tooth (Figure 5.13). The medial surface of the mandibular body was then exposed and the tongue was elevated. The 2.0mm diameter titanium screw was then inserted through the body of the mandible just anterior to the first premolars as described above to reinforce the lower border of the mandible before creating the critical size defect (Figures 5.14 & 5.15). The mental neurovascular bundle was ligated and cut. A straight body osteotomy was then performed on that side with the first cut made 2mm anterior to the first premolar, and the second cut was made across midline in the region of the mandibular symphysis (Figures 5.16 & 5.17). The segment of bone was removed together with the associated periosteum & incisor tooth (Figure 5.17). In both cases the surgical defect was created successfully, with no perforation of the oral mucosa or damage to the contralateral lower incisor tooth.

The anterior intraoral mucosal defect created secondary to the removal of the right incisor was sutured with resorbable braided sutures (4-0 Vicryl Rapide\* [Polyglactin 910] Suture, Ethicon). The prefabricated tricalcium phosphate

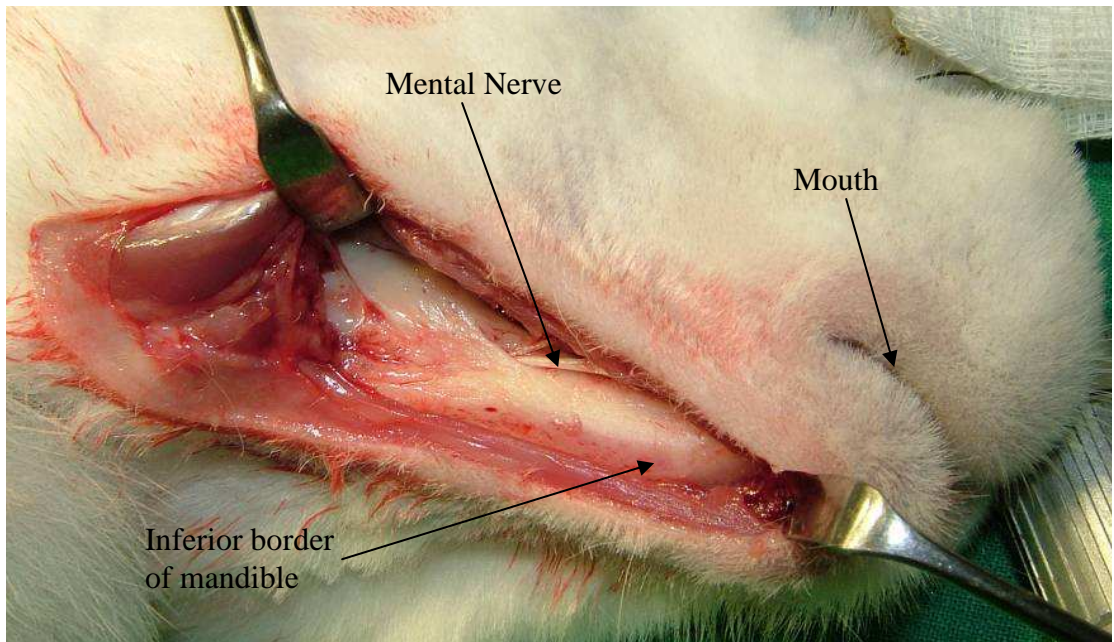


Figure 5.13 Exposure of mandible and mental nerve in cadaveric case.

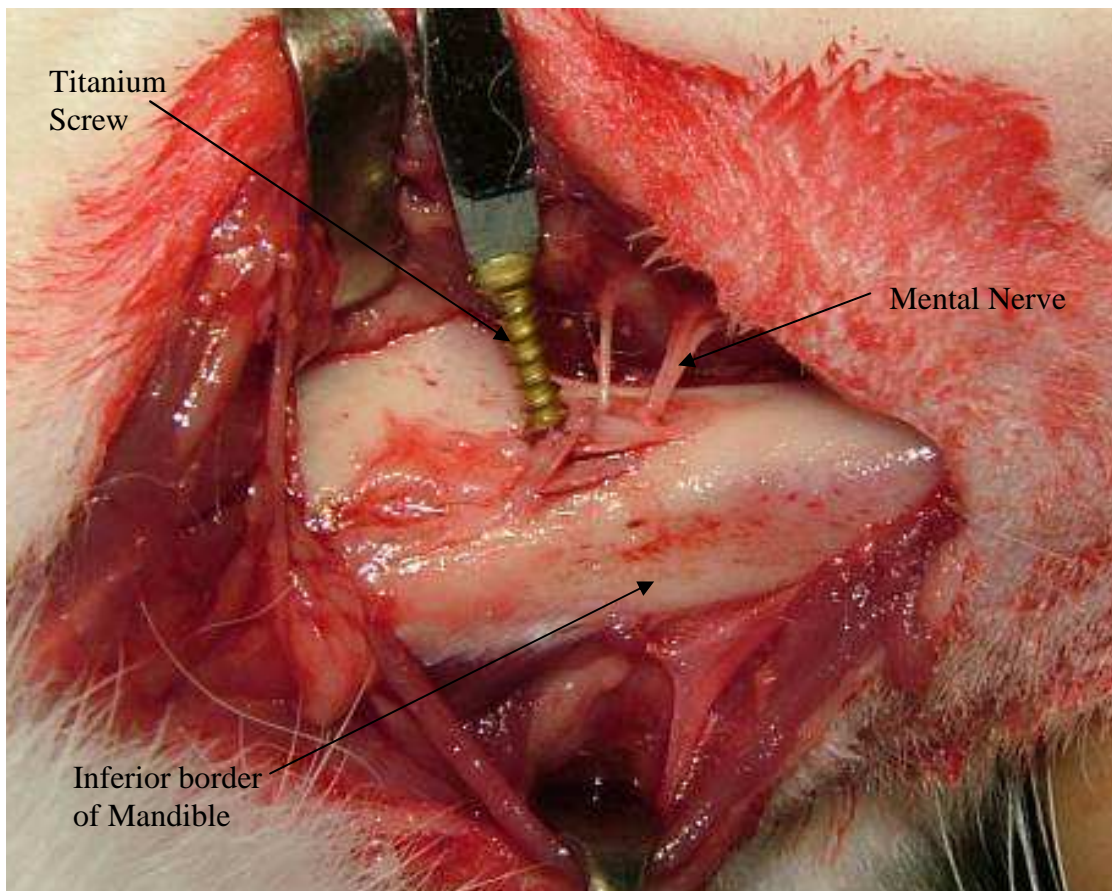


Figure 5.14 Placement of titanium screw for reinforcement of the mandible.

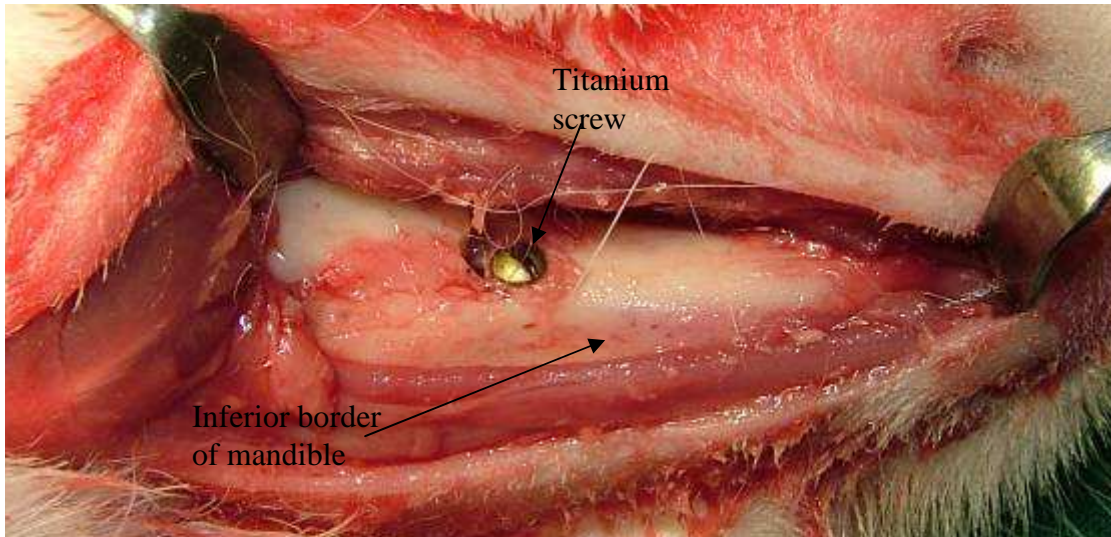


Figure 5.15 Titanium screw in place.

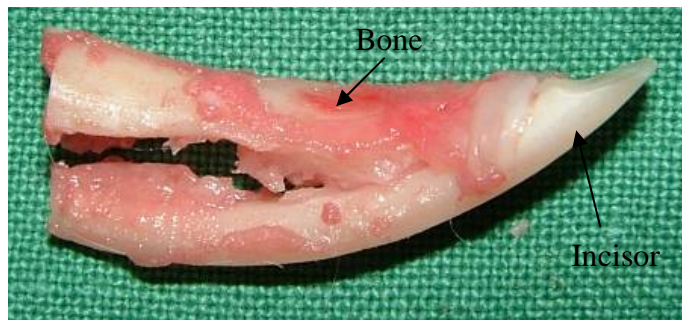


Figure 5.16 Segment of bone removed with incisor.

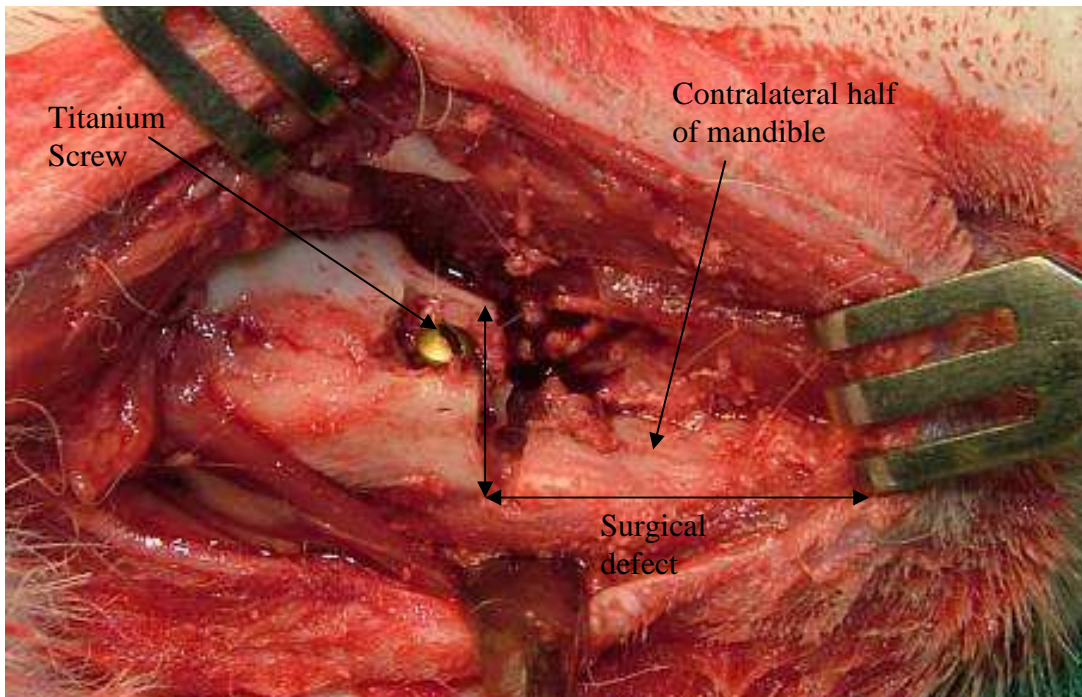


Figure 5.17 Unilateral critical-size surgical defect created.

scaffolding was then adapted to the created defect with a Swann-Morton Surgical Scalpel Blade, No.15. This was then secured in the surgical defect by enclosing it within the surrounding soft tissues with multiple polyglactin sutures. The skin was then closed in layers with a final subcuticular continuous suture done with a 5-0 resorbable monofilament material (Monocryl [poliglecaprone 25] Suture, Ethicon).

#### 5.1.3.1 Plain film radiography

Plain film radiographs were taken with size 1 E/F speed AGFA Dentus M2 radiographic film (Figure 5.18) which was placed intraorally with the x-ray beam directed from beneath the chin at 90° to the film (true mandibular occlusal view). A 50kV, 2mA and 0.32sec setting of the x-ray machine was found to produce the best radiographic appearance. A 30cm distance between the x-ray film and the machine cone was maintained so as to standardise the exposure for all the cases (Figure 5.19). The radiographic assessment showed accurate positioning of the titanium screws as well as the tricalcium phosphate scaffolding in the surgical sites (Figure 5.20).

## 5.2 Clinical cases

### 5.2.1 Cases

Based on the positive results obtained with the dry mandible and cadaveric work described previously, the second fixation method using the single titanium screw was selected for use with the clinical cases. Approval was obtained from the Home Office under the Animals (Scientific Procedures) Act 1986 to carry





Figure 5.18 Size 1 E/F speed AGFA Dentus M2 radiographic film.

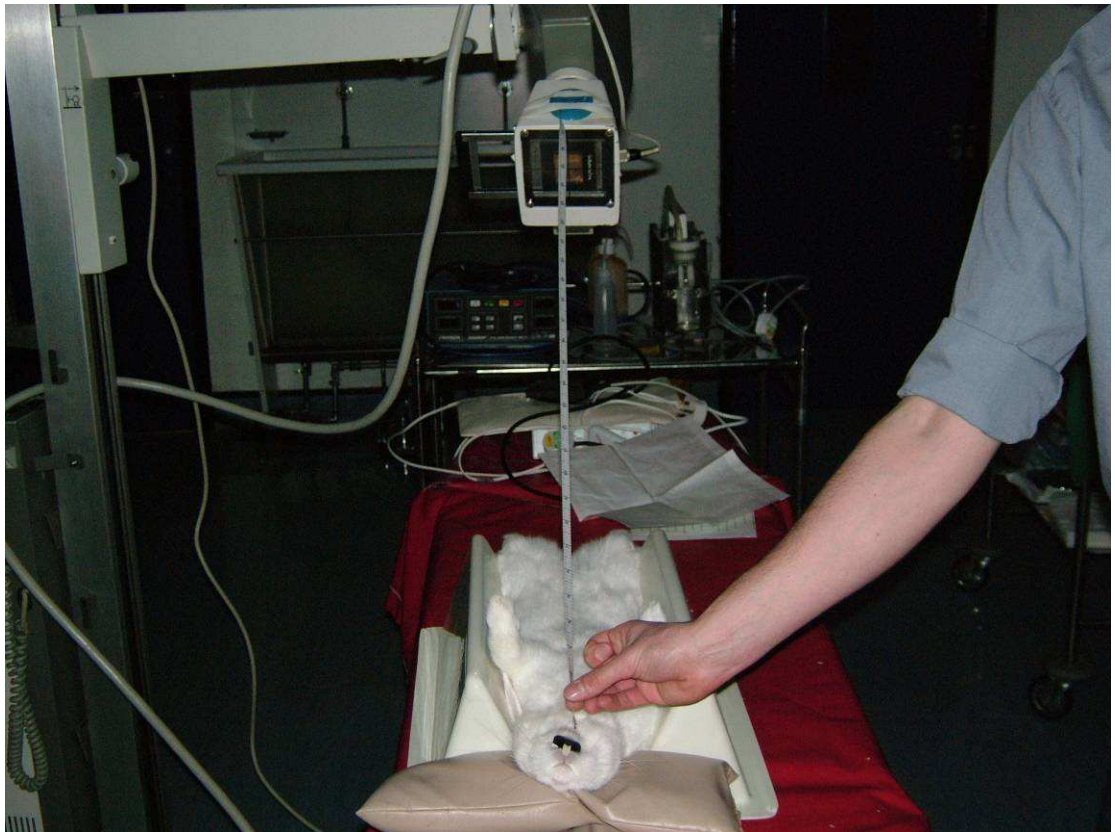


Figure 5.19 X-ray machine with attached objective measuring tool.

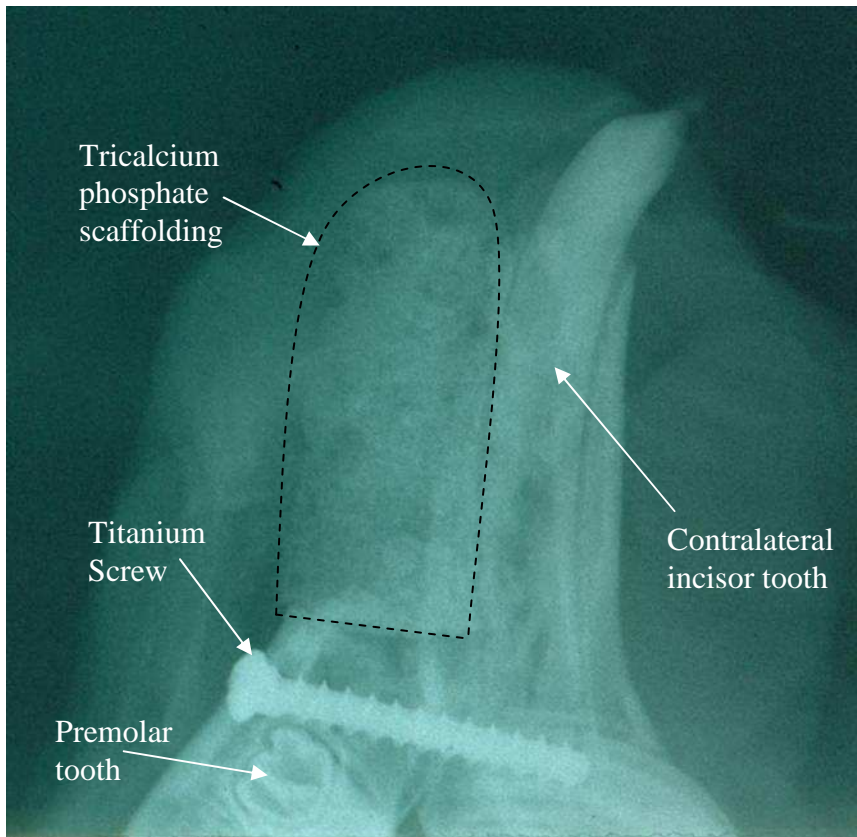


Figure 5.20 Plain film of TCP scaffolding in surgical defect in cadaveric case.

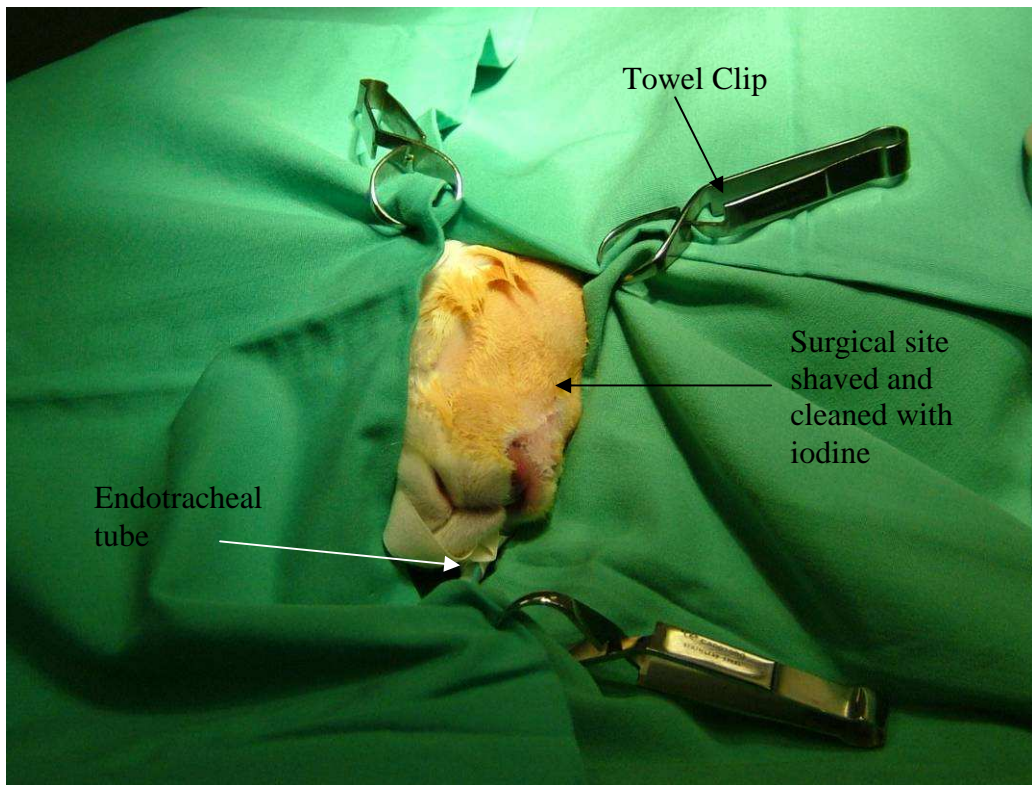


Figure 5.21 Draping method on one of the clinical cases.

out regulated procedures on living animals. Ten adult New Zealand white rabbits (3.0-4.0kg) were used for the planned study. These rabbits were obtained from a supplier in France as the local suppliers were closed for a year for refurbishing. They were therefore given a 2 week period for acclimatization prior to any treatment being performed. The animals were kept in a dedicated animal house under veterinary supervision in the Small Animals Research Teaching Department, Biological Services, Vet School, University of Glasgow. Surgery was carried out on two cases initially on two separate sessions to assess the recovery of the animals post-operatively and refine the surgical technique if deemed necessary. Both animals recovered well and were eating normally by 3 to 4 days post-operatively. The remaining eight cases were treated following the same treatment protocol in a further four sessions. One of these cases died immediately post-operatively due to anaesthetic complications, unrelated to the operative procedure, and had to be excluded from the study.

### 5.2.2 Surgical procedure

Each case was premedicated with 12.5µg fentanyl (opioid analgesic) transdermal patch applied the afternoon prior to the surgery. On the day of the surgery meloxicam (non-steroidal anti-inflammatory drug) at a dose of 0.2mg/kg was administered subcutaneously, one hour pre-operatively. Hypnorm (fentanyl citrate & fluanisone), at a dose of 0.5ml/kg, was given intramuscularly thirty minutes pre-operatively and midazolam (short-acting benzodiazepine), at a dose of 2mg/kg, was administered intravenously at induction. The case was then intubated with 3 or 3.5mm endotracheal intubation tubes and given isoflurane, nitrous oxide and oxygen with the

saturation being constantly monitored. Buprenorphine (opioid analgesic), at a dose of 0.05mg/kg, and oxytetracycline (antibiotic), at a dose of 30mg/kg, were both administered subcutaneously prior to commencing treatment. Ointment was placed in both eyes and these were taped shut (Figure 5.21). Full theatre surgical conditions were adhered to with clinicians scrubbing and wearing surgical gowns and gloves and the surgical site disinfected with povidone-iodine followed by the case being draped leaving only the surgical site visible (Figure 5.21). Bupivacaine 0.25% (long acting local anesthetic) at a dose of 1mg/kg was given locally in the surgical site for post-operative analgesia. As described in the cadaveric specimen cases earlier, an incision was made along the inferior border of the mandibular body on the left side. The platysma was reflected and by supra-periosteal dissection elevating the buccinator, the mental nerve and foramen were identified, just anterior to the first premolar tooth. The medial surface of the mandibular body was then exposed and the tongue was elevated. The 2.0mm diameter titanium screw was then inserted through the body of the mandible just anterior to the first premolars (Figure 5.22) as described in the dry mandible specimens.

The mental neurovascular bundle was ligated and cut. A straight body ostectomy was then performed on that side with the first cut made 2mm anterior to the first premolar, and the second cut across the midline in the region of the mandibular symphysis. The segment of bone was removed together with the associated periosteum & incisor tooth (Figure 5.23).

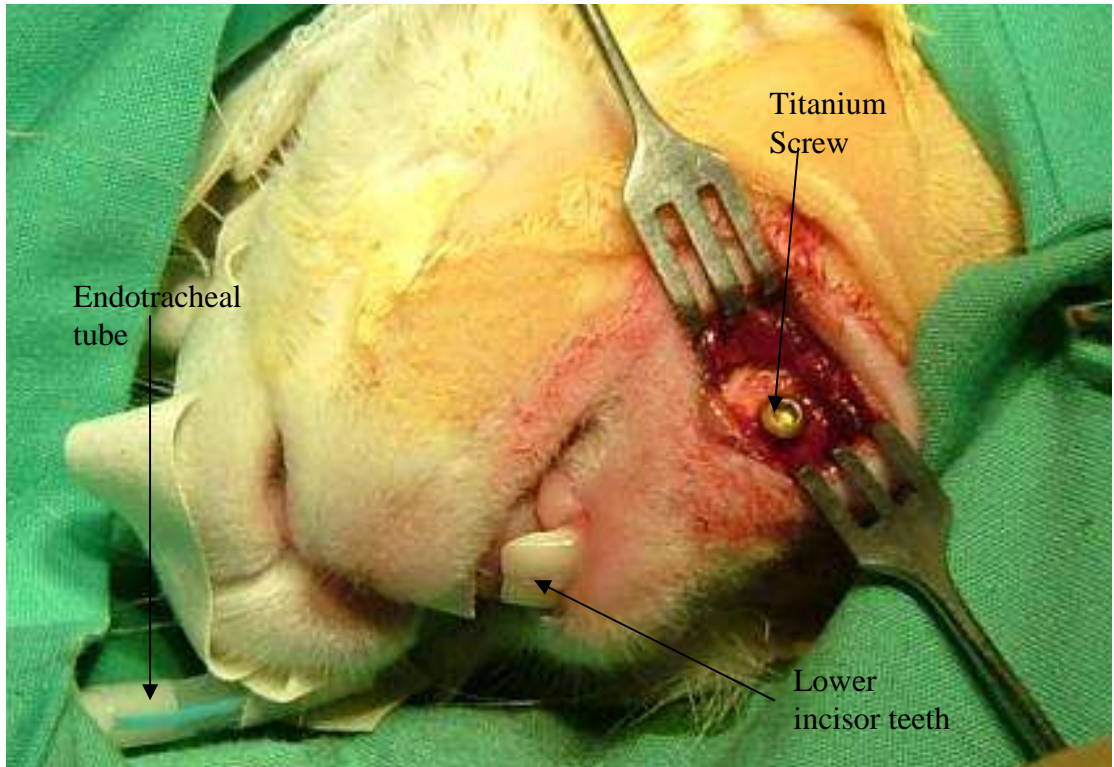


Figure 5.22 Titanium screw in place in one of the clinical cases.

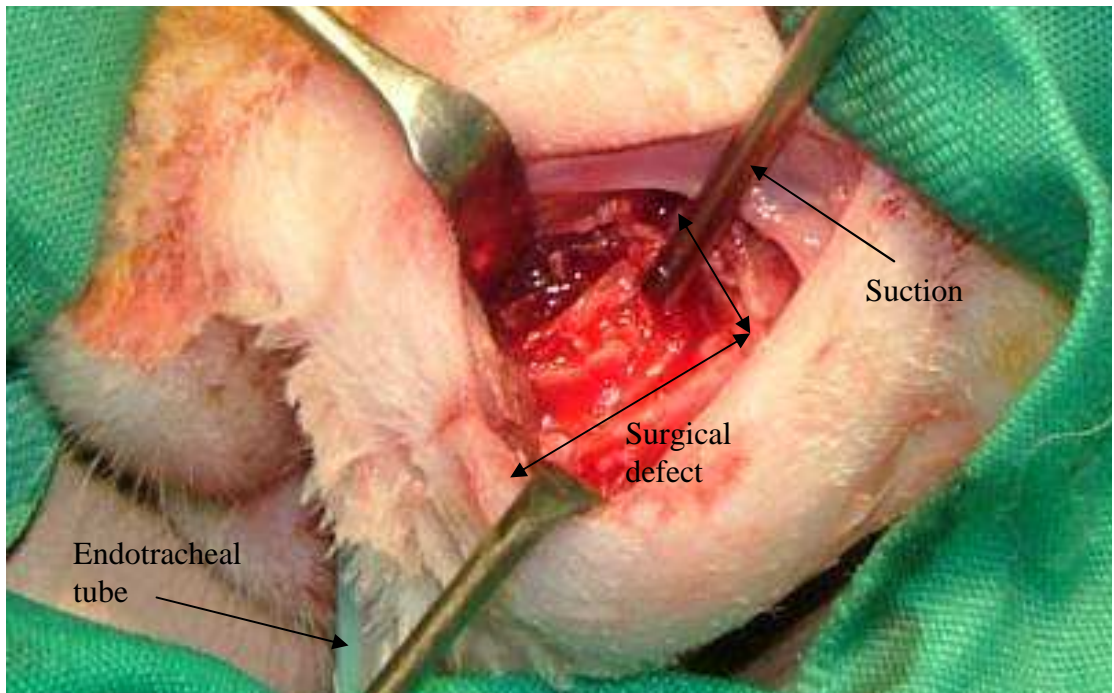


Figure 5.23 Unilateral critical-size surgical defect in one of the clinical cases.

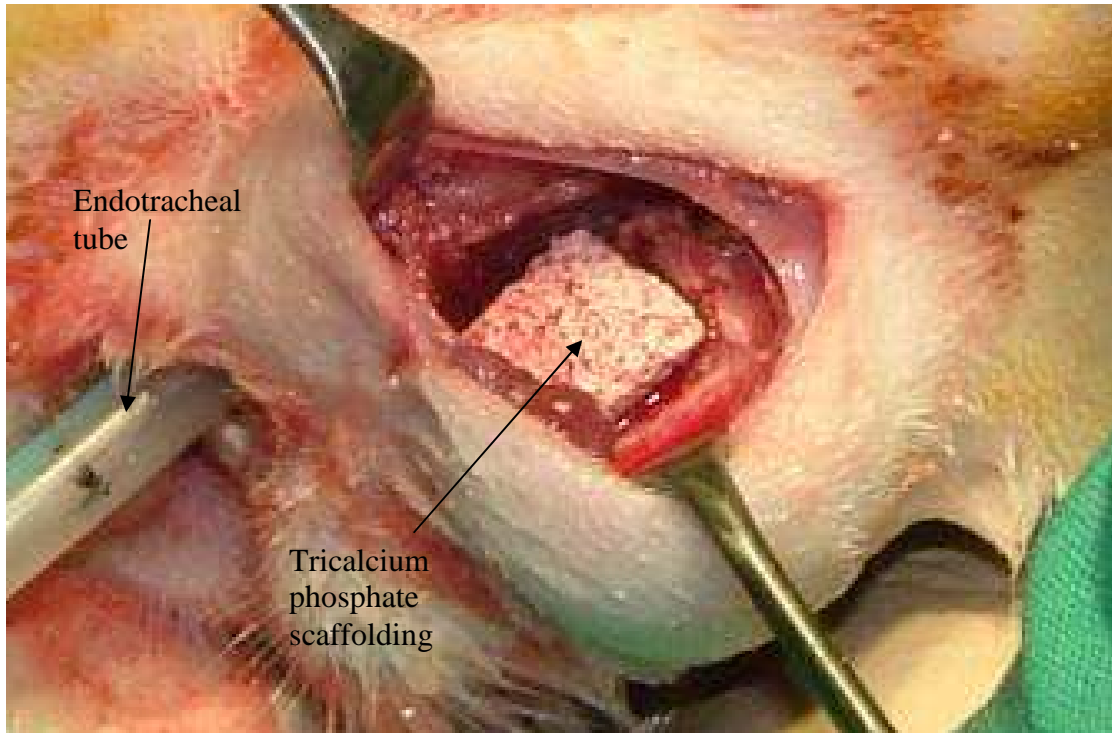


Figure 5.24 Placement of TCP scaffolding into surgical site in the clinical case.

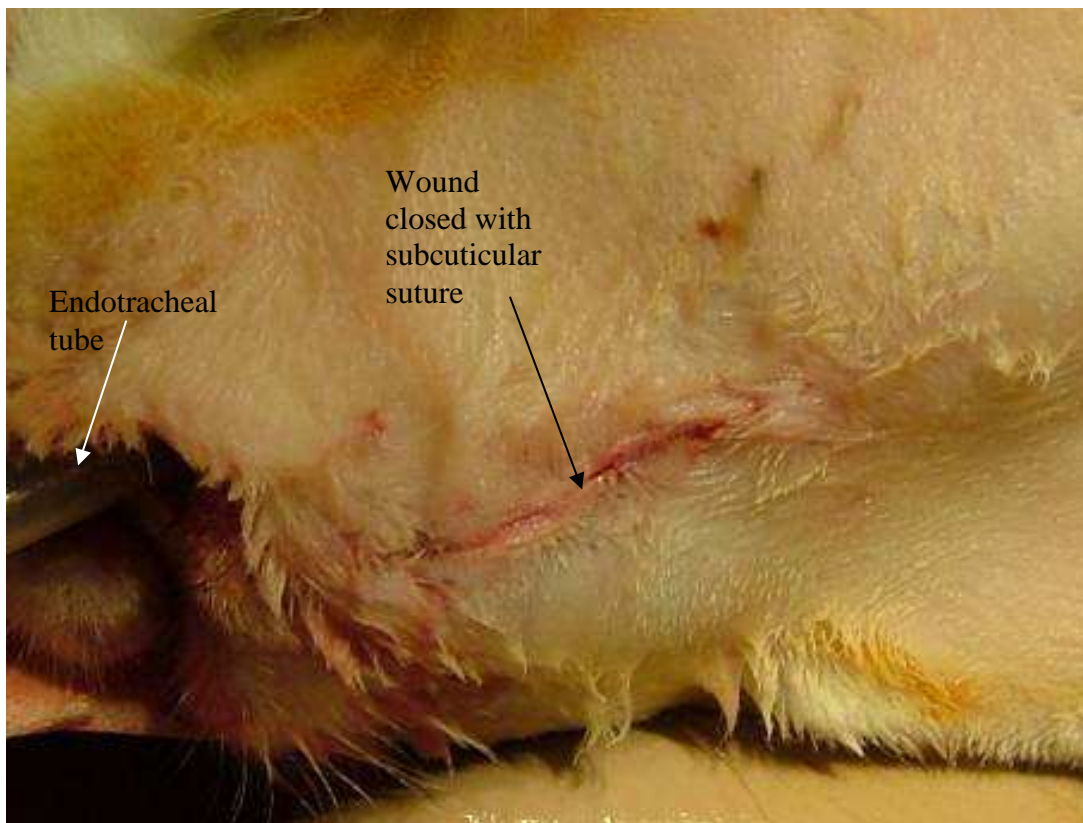


Figure 5.25 Closure of the surgical site with resorbable sutures.

The anterior intraoral mucosal defect created by removing the left incisor was sutured with resorbable braided sutures. The prefabricated TCP scaffoldings were then adapted and contoured to the created defect (Figure 5.24) using a fresh no.15 scalpel and secured in the surgical defect by enclosing it within the surrounding soft tissues with multiple polyglactin sutures. The skin was then closed in layers with a final subcuticular continuous suture done with a 5-0 resorbable monofilament suture (Figure 5.25).

Plain film radiographs were taken as described above for each case immediately post-operatively. All animals were observed carefully until they regained full consciousness. Meloxicam at a dose of 0.2mg/kg was administered subcutaneously for two days post-operatively and the rabbits were closely monitored for any possible loss of appetite or weight. Further plain film radiographs were taken at four, eight, and twelve weeks of the follow-up period. For these follow-up radiographic assessments the rabbits were sedated with Hypnorm (fentanyl citrate & fluanisone), at a dose of 0.5ml/kg, this was given intramuscularly thirty minutes prior to the procedure. The animals were then observed until recovery a few hours later.

Three months post-operatively the cases were sacrificed with an overdose of pentobarbitone sodium (140mg/kg), the mandibles were surgically removed (Figures 5.26, 5.27 & 5.28), and the soft tissue carefully dissected off (Figure 5.29 & 5.30). The specimens were labelled and stored on ice in 10% neutral buffered formalin for twenty four hours (Figure 5.31). They were then removed

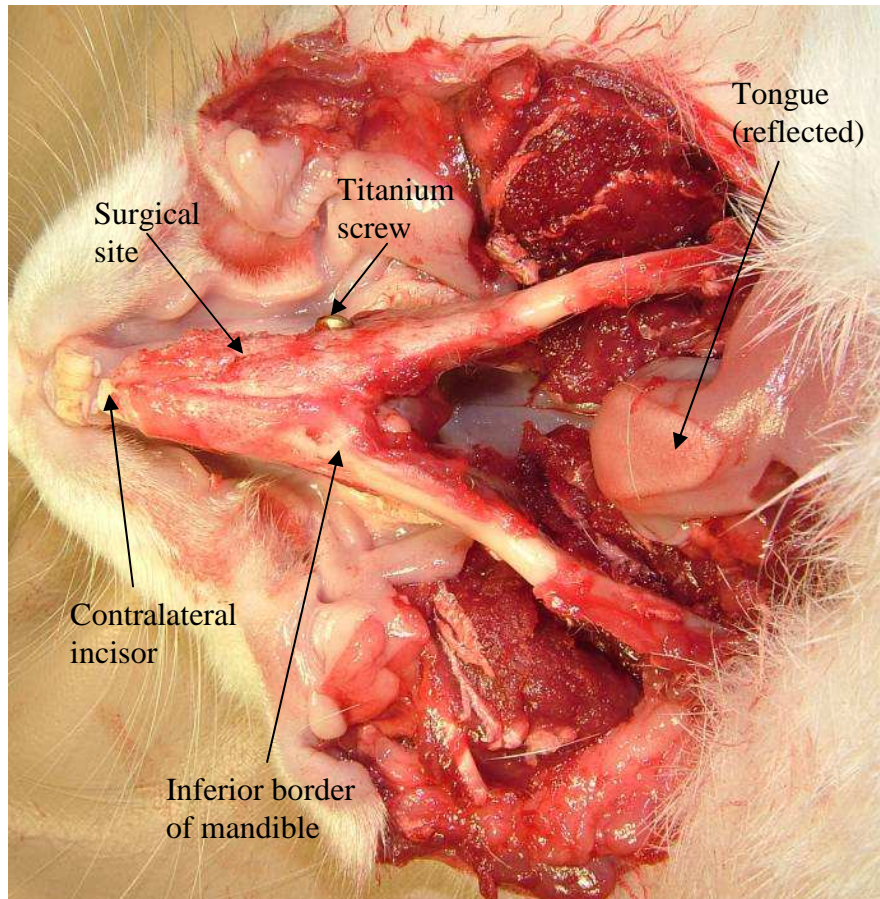


Figure 5.26 Dissection of a case, 3 months after placement of graft.



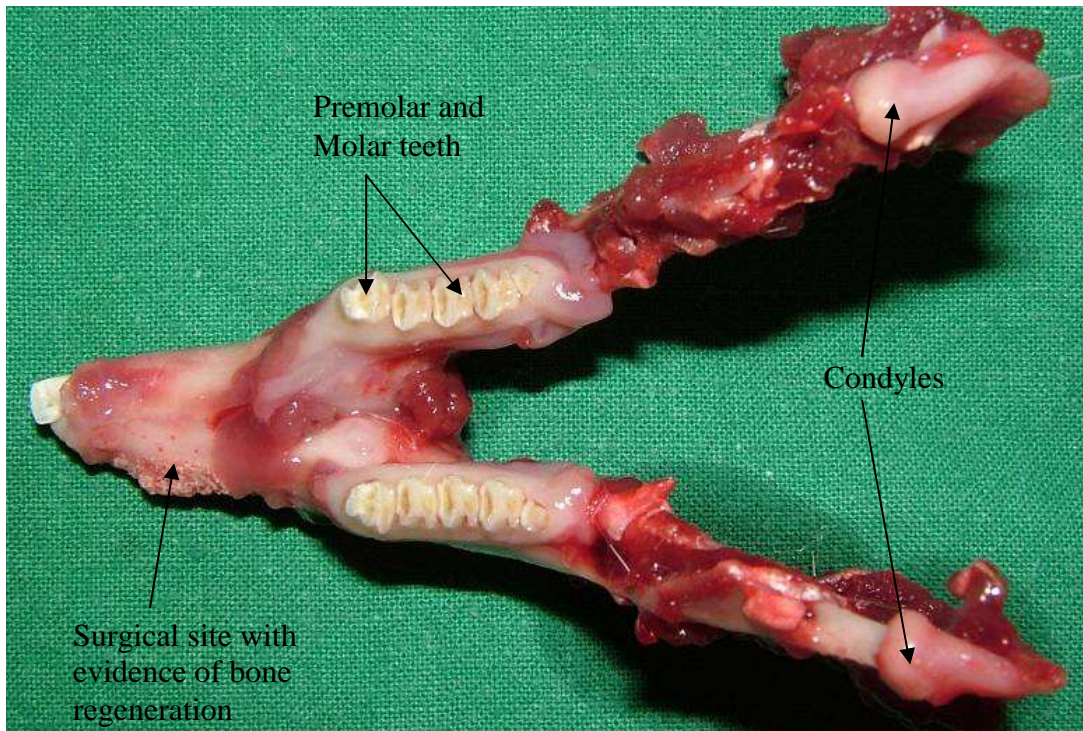


Figure 5.27 Explanted mandible of case 10 before removal of attached soft tissue, superior view.

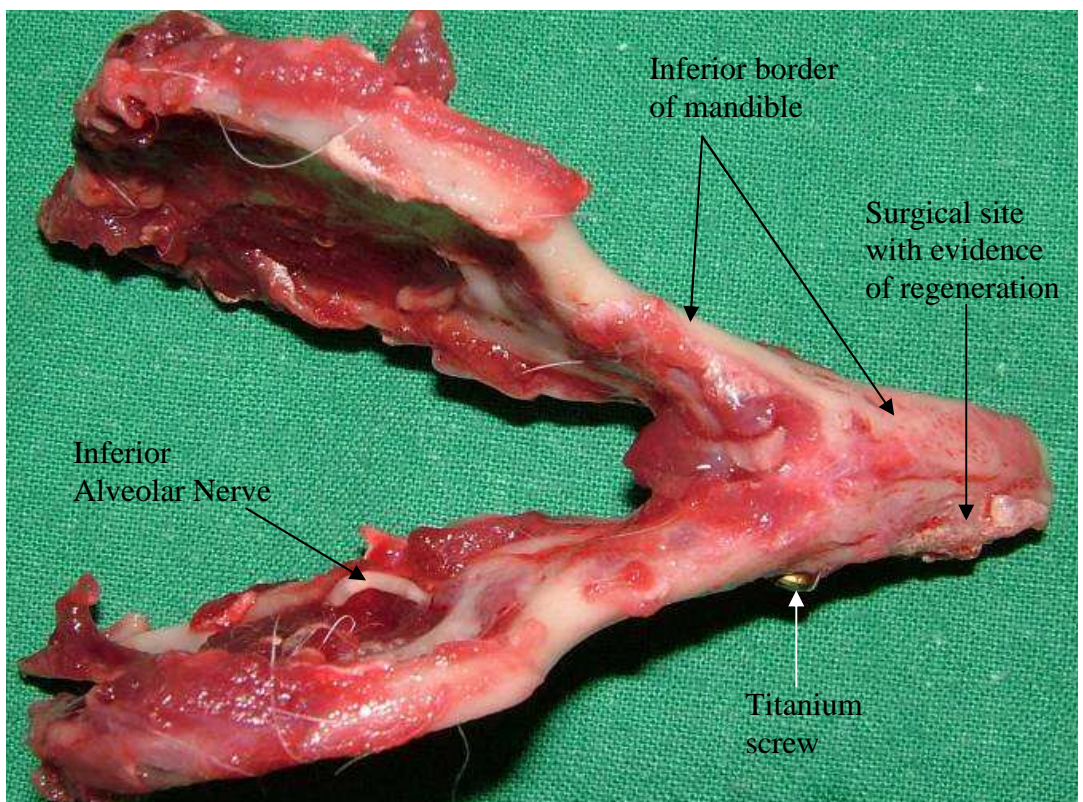


Figure 5.28 Explanted mandible of case 10 before removal of attached soft tissue, inferior view.

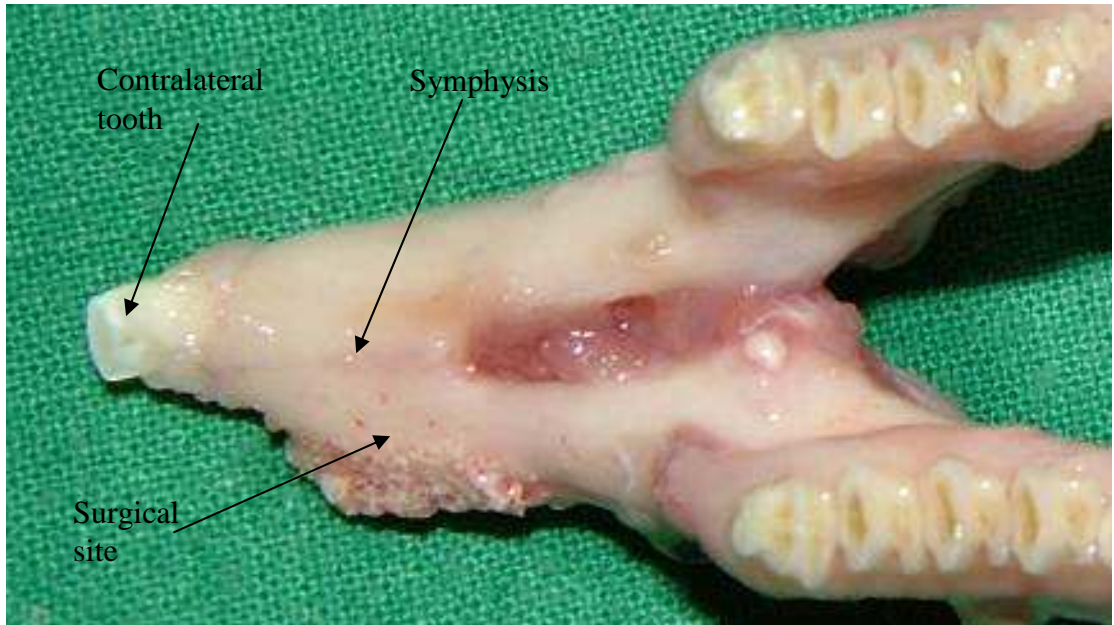


Figure 5.29 Close-up of the superior view of the surgical site of case 10 after removal of most of the soft tissue.

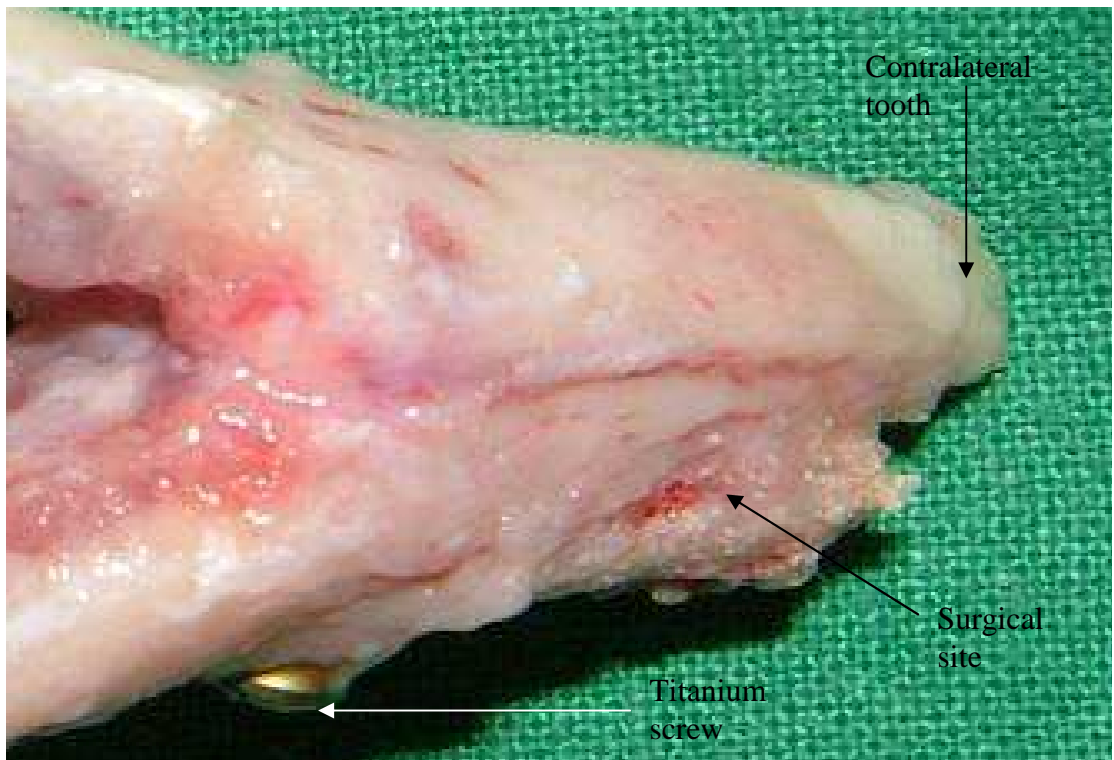


Figure 5.30 Close-up of the inferior view of the surgical site of case 10 after removal of most of the soft tissue.



Figure 5.31 Labeled, explanted mandibles of cases 6, 7 and 8 in formalin on ice.



Figure 5.32 Explanted mandibles of all cases in freezer at -80°C.

from the formalin scanned in the i-CAT<sup>®</sup> and frozen at -80° Celsius (Figure 5.32).

### 5.2.3 Cone beam computed tomography

Cone beam CT is a versatile radiographic method that is particularly valuable for the radiographic assessment of the bones of the face and jaws. This radiographic assessment method was chosen due to its ease of use, high image resolution and capability to construct three dimensional radiographic images of the specimens.

Each of the specimens was removed from the formalin solution, placed on an acrylic platform which was placed on an inverted plastic container which itself was placed on a purpose built metal framework (Figures 5.33 & 5.34) for use with the i-CAT<sup>®</sup> (Imaging Sciences International) cone beam CT scanner. The specimens were then scanned in the i-CAT<sup>®</sup> using a setting of 6 centimetres, 0.25 voxel, and 40 seconds at high resolution.

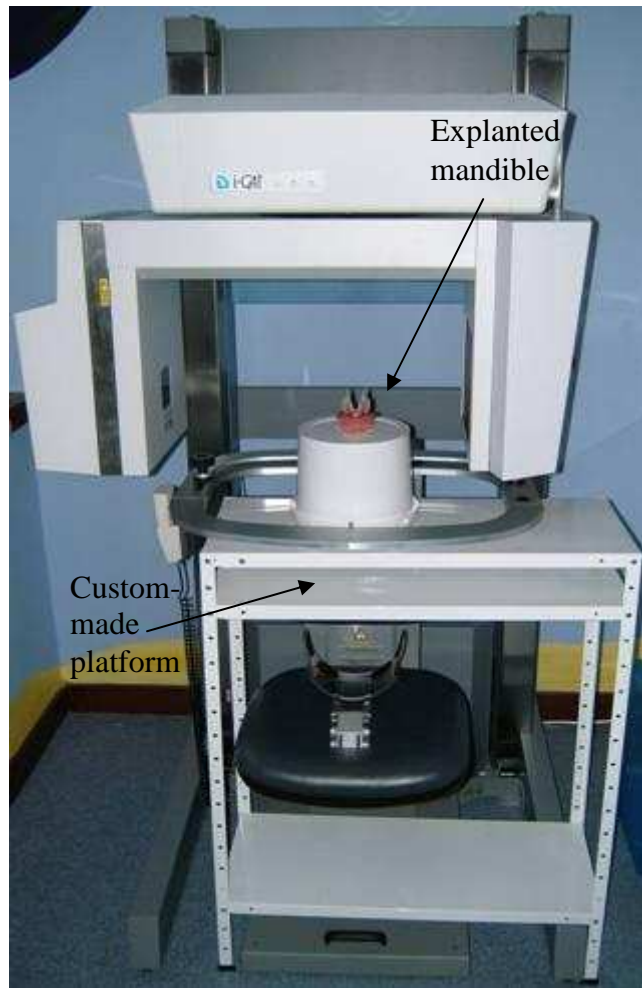


Figure 5.33 i-CAT<sup>®</sup> scanner, with the explanted mandible on the custom made platform.

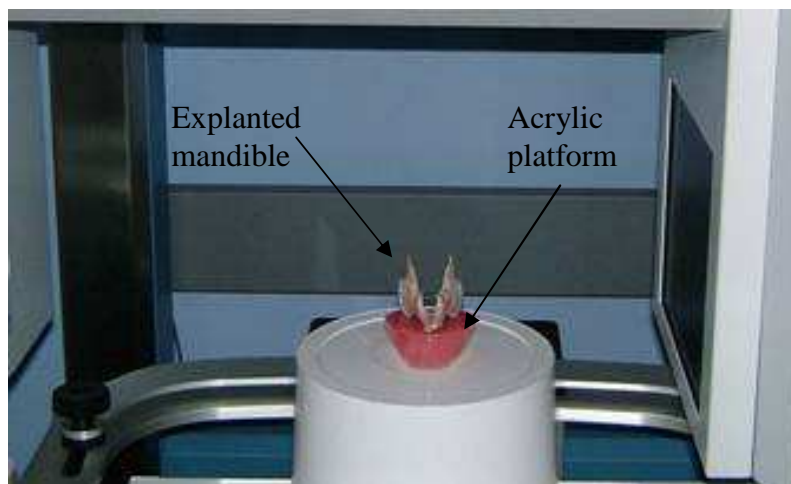


Figure 5.34 Close-up of the explanted mandible on the acrylic platform in the i-CAT<sup>®</sup> scanner.

## 5.2.4 Mechanical testing

### 5.2.4.1 Preliminary investigations

#### 5.2.4.1.1 Selection of testing method

The principles used for the mechanical testing of the surgical specimens were based on the previous work of Kontaxis, et al. (2004). The mechanical properties of the regenerated bone in the surgical sites were therefore tested by applying the principle of cantilevers. This method was used as it allowed histological analysis of the specimens afterwards. Prior to mechanically testing the surgical specimens, six dry rabbit hemi-mandible specimens were tested to assess the effectiveness and reliability of the testing method.

Two different patterns of fracture of the test hemimandibles were noted. In some cases the fracture occurred through the socket of the first premolar tooth (Figure 5.35), where there was less bone than in the non-tooth bearing part of the anterior body. This was also noted in previous studies. To avoid this, the hemi-mandibles were embedded in dental stone and gripped within an aluminium box frame (Figures 5.36 & 5.37) up to 2mm anterior to the first premolar socket. In the other cases, fracture occurred through the long rooted incisor rather than through the anterior body. To try and eliminate this effect the loading was applied 14mm anterior to the first premolar socket.

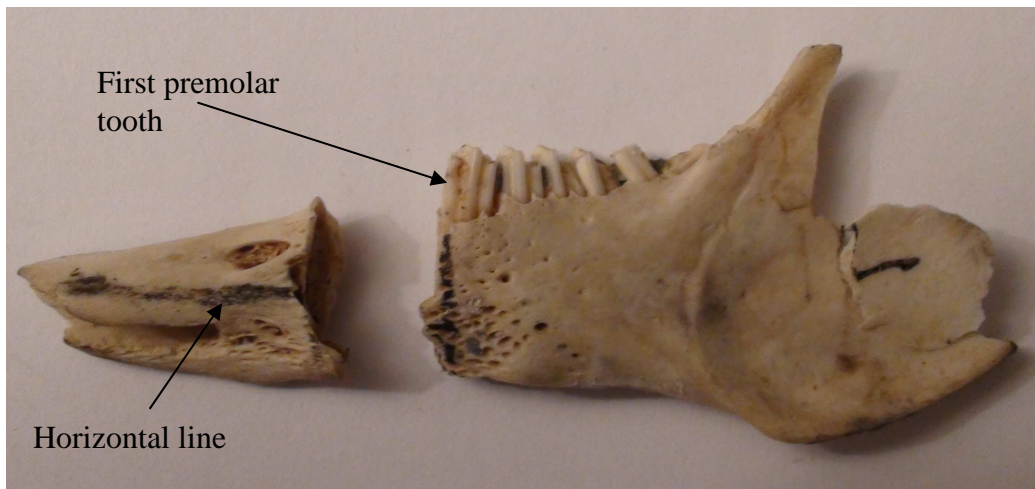


Figure 5.35 Dry rabbit mandible specimen showing failure along the first premolar tooth socket.

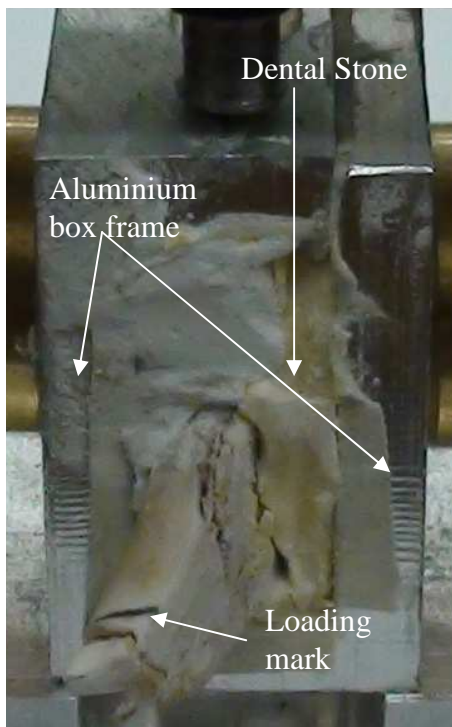


Figure 5.36 Specimen in the aluminium box frame.

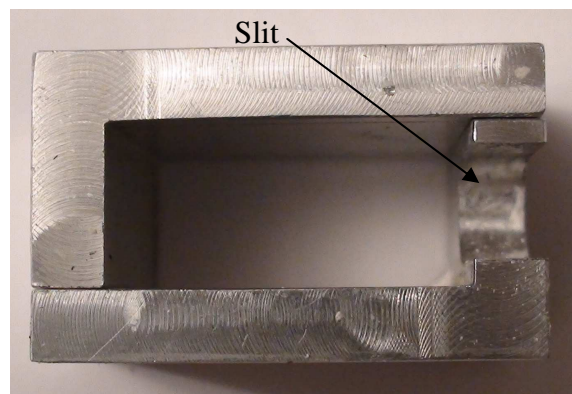


Figure 5.37 Aluminium box frame

#### 5.2.4.2 Clinical case testing

##### 5.2.4.2.1 Specimen preparation

The mandibles were divided into left and right hemi-mandibles at the symphysis with a surgical grade rotating diamond tipped saw. These hemi-mandibles were then mechanically tested as cantilevers as described previously. On each specimen three lines were marked; a horizontal line on the lateral surface midway between the upper and lower borders of the anterior body of the mandible (Figure 5.35), a posterior line on the dorsal surface at right angles to the first line and 2mm anterior to the first premolar socket, and a second line on the dorsal surface 12mm anterior to the second line (i.e. 14mm anterior to the premolar socket) (Figure 5.36).

##### 5.2.4.2.2 Specimen mounting

The hemi-mandibles were mounted in pairs of “L” shaped sections of extruded aluminium 4.7mm thick (Figures 5.37 & 5.38). The sections were 25mm long, 32mm high and 15mm wide. Half the sections had a slit 13.5 mm long and 7mm wide in the 15mm side. Dental stone was spread on the inner surface of a section without the slit and hemi-mandible placed in the stone, ensuring that the 2mm line was at the edge of the longer side of the section and that the mid-line was horizontal. The specimen was pressed into place to minimize the thickness of the stone and to produce a continuous layer of stone to resist the loading force applied to the mandible. After the stone had set the second section containing the slit, which provided room for the ramus of the mandible, was fixed in place against the first section using dental plaster of Paris. The procedure achieved the



required stability having the hemi-mandible being firmly located within the rectangular space produced by the apposed paired sections (Figures 5.36 & 5.39).

To hold the mounted specimen in the mechanical testing machine a larger rectangular aluminium block, 63.5mm long, 63.5mm high and 30mm deep, with a central cavity 40mm long and 40mm high was used to mount the hemi-mandible in the paired aluminium sections (Figures 5.40 & 5.41). The boxed specimen was placed within the cavity of the larger aluminium box and secured firmly in place by 2 lateral screws and one vertical screw (Figure 5.40). At the ends of these screws were rotatable thrust pads that were used to compensate for any non-parallelism of the aluminium sections (Figure 5.40).

The holder was supported on a rectangular aluminium plate attached to the moveable cross head of the test machine (Figure 5.42). The central slot in the plate allowed the lateral and rotational movement of the holder in order to ensure that the loading point on the mandible was located over the load cell of the test machine.

Mechanical loading of the specimen was carried out using the loading jig (Figure 5.43) which consisted of a stainless steel tube 20.5mm long and 8mm in diameter. The tube was internally threaded to house two rods, one with a right-handed and one with a left-handed thread. The lower end was screwed to the centre of an insert located in the centre of the load cell of the test machine; the upper rod terminated in a loading saddle into which the hemi-mandible fitted.

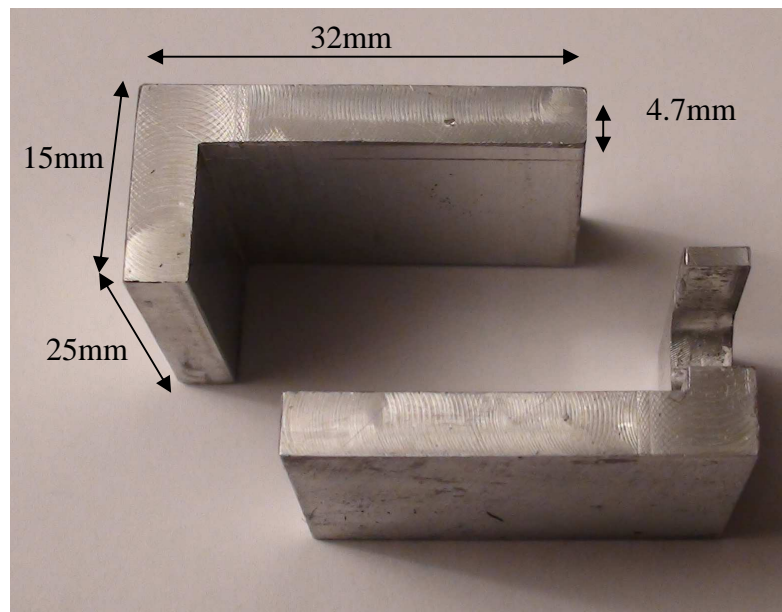


Figure 5.38 “L” shaped sections of extruded aluminium.



Figure 5.39 Specimen in the box frame covered in tape.

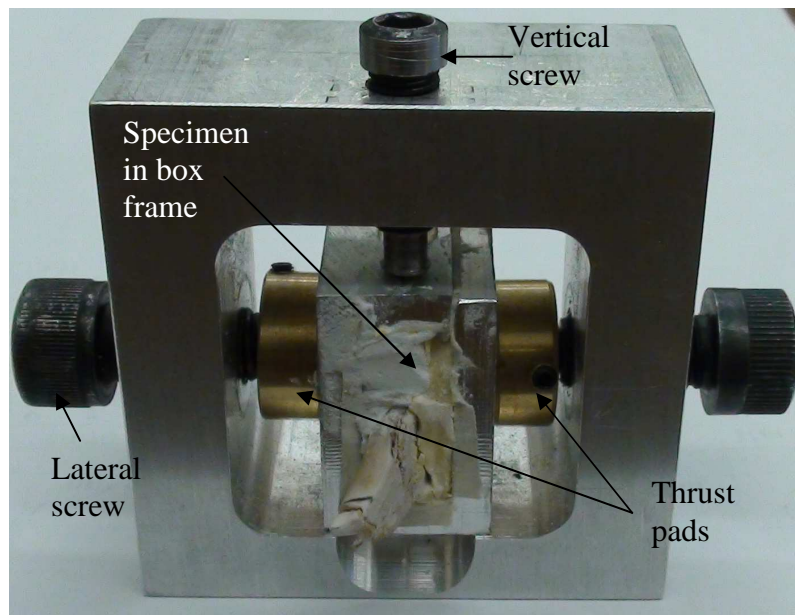


Figure 5.40 Specimen in the larger aluminium frame.

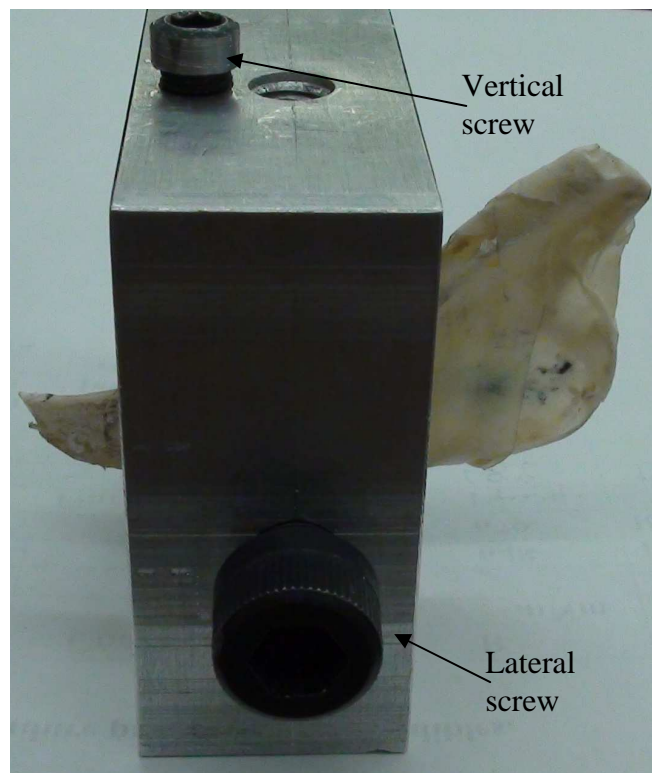


Figure 5.41 Lateral view of the large aluminium frame.

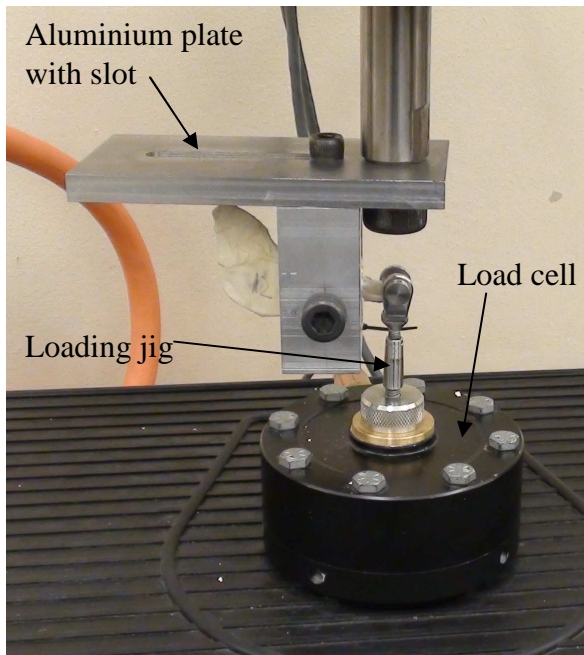


Figure 5.42 Specimen loaded into mechanical testing machine.



Figure 5.43 Loading jig.

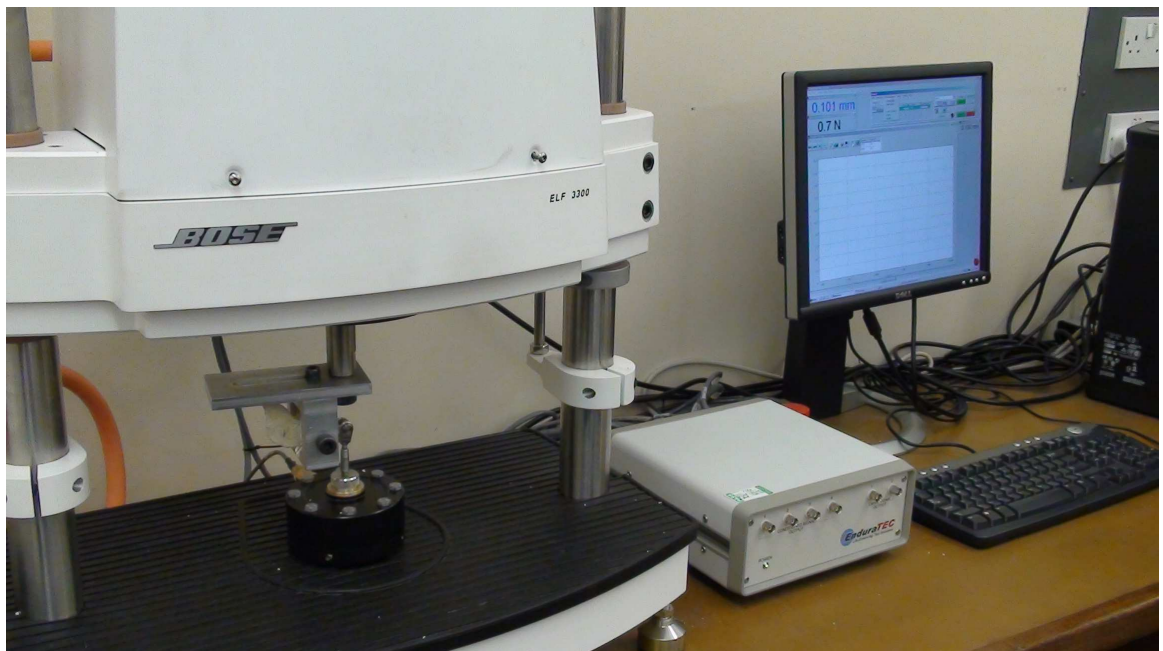


Figure 5.44 BOSE Electroforce® 3300 test instrument with VDU of the control computer which displays the load and displacement.

The horizontal position of the holder was adjusted so that the loading point was over the loading mark (Figure 5.36) on the upper surface of the mandible. Rotation of the counter-threaded tube allowed the loading saddle to be raised without rotating the loading saddle itself.

#### 5.2.4.2.3 Mechanical testing machine

Tests were carried out using the BOSE Electroforce® 3300 test instrument shown in Figure 5.44, which contains a magnetic actuator that can be moved at a specified rate. The specimens were mounted as described above (Figure 5.42), the loading saddle brought into contact with the upper surface of the mandible while monitoring the load, and the actuator was driven upwards at 1mm/s until fracture of the specimen occurred. The displacement and load was recorded at 10 points per second.

After completion of the mechanical testing, the hemi-mandible in the paired aluminium sections was removed from the holder, the “L” sections were separated, the stone and plaster removed and the masking tape stripped from the mandible. The specimens were then analysed histologically as described below.

#### 5.2.5 Quantitative histological assessment

The surgical site with the regenerate was removed from the rest of the hemimandible by sectioning anterior to the first premolar. These mandible sections were then decalcified in 10% formic acid for 1 week before sectioning in the sagittal plane into two halves. These two halves were embedded separately in wax, processed and one section from each block was stained using

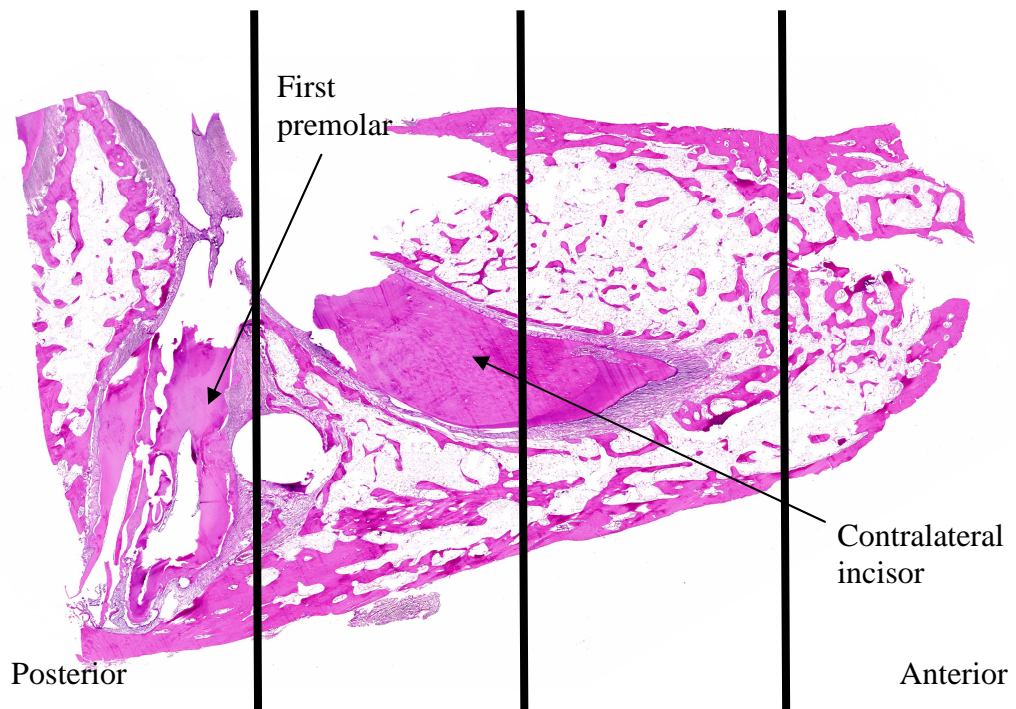


Figure 5.45 H&E stained sagittal section across one of the surgical specimens at x10 magnification. The vertical lines demonstrate the three assessment fields described in the text.

haematoxylin and eosin (H&E) (Figure 5.45).

#### 5.2.5.1 Quantitative analysis of bone content

Two decalcified, H&E stained sections from each mandible (one from each specimen half) were viewed at x20 (Figure 5.46) and x40 magnification. Three fields were selected (Figure 5.45):

- 1) Proximal end of the regenerated tissue, adjacent to the premolar tooth root
- 2) Mid surgical field
- 3) Distal end of the regenerated tissue, towards the symphysis

These were captured digitally on a photo microscope (Olympus UK Ltd, Watford, UK) fitted with a Colourview IIIu camera using CellB software. The digital image was opened in Adobe Photoshop Elements 2.0 and after background correction was converted to greyscale. Using the threshold function, unstained areas were converted to white and then the eosin stained areas rendered black to create a binary (two-colour) image. This was subjected to clean-up by comparing the binary image to the H&E stained image, and any connective tissue elements other than bone were removed (Figures 5.46 & 5.47). The binary image was then imported into ImageTool image analysis software (version 3.00, UTHSCSA, Texas USA). The proportion of black and white pixels was counted and expressed as a percentage of the total image. The average of the six values measured for each mandible gave a quantitative measurement of the total bone volume (adapted from Revell, 1983).

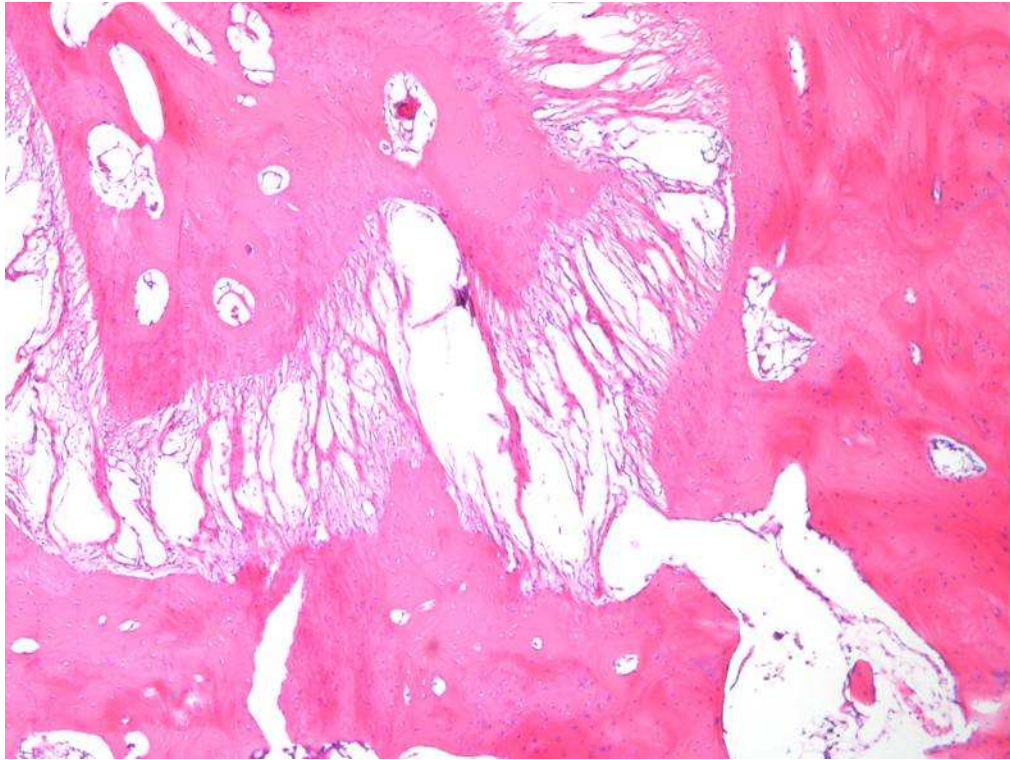


Figure 5.46 H&E stained section of the regenerate under x20 magnification, showing bone and intervening fibrous tissue.



Figure 5.47 The same image converted into binary format after clean up, leaving the bone coloured black (x20).



#### 5.2.5.2 Statistical analysis

The results were expressed as mean bone volume (% of total) and standard error. Statistical analysis of the results was conducted using the Student's t-test.

The value used for the statistical analysis was the mean bone volume of all 6 fields or the mean of the 2 central fields. Differences were considered significant if  $p < 0.05$ .

## **Results**

## 6.1 Clinical Findings

The surgery proceeded uneventfully in all of the experimental cases. All the cases recovered well following surgery and were initially placed on a soft diet. All rabbits started to eat normally and put on weight by four days post-operatively (Figure 6.1). The surgical site was regularly monitored and there was no wound breakdown or development of infection. None of the cases needed any further surgical interventions. Due to the loss of the lower left central incisor, the opposing upper left central incisor had a tendency to overgrow due to the reduced wear. This tooth was trimmed down every 4 weeks when the rabbit was sedated for the radiographic assessment.

## 6.2 Gross appearance of surgical site

Following explantation of the mandibles and removal of the associated soft tissues, general evaluation of the surgical site demonstrated the appearance of new bone formation within the cases that received rhBMP-7 with TCP. This new bone appeared to be fused to the adjacent normal untreated bone (Figure 6.2).

## 6.3 Radiographic assessment

### 6.3.1 Plain Films

The serial radiography (0, 4, 8 & 12 weeks) showed gradual replacement of the tricalcium phosphate (TCP) scaffolding with radio-opaque tissue, and it was noted that the TCP implant was gradually remodeled to the shape of the surgical site (Figures 6.3 & 6.4).

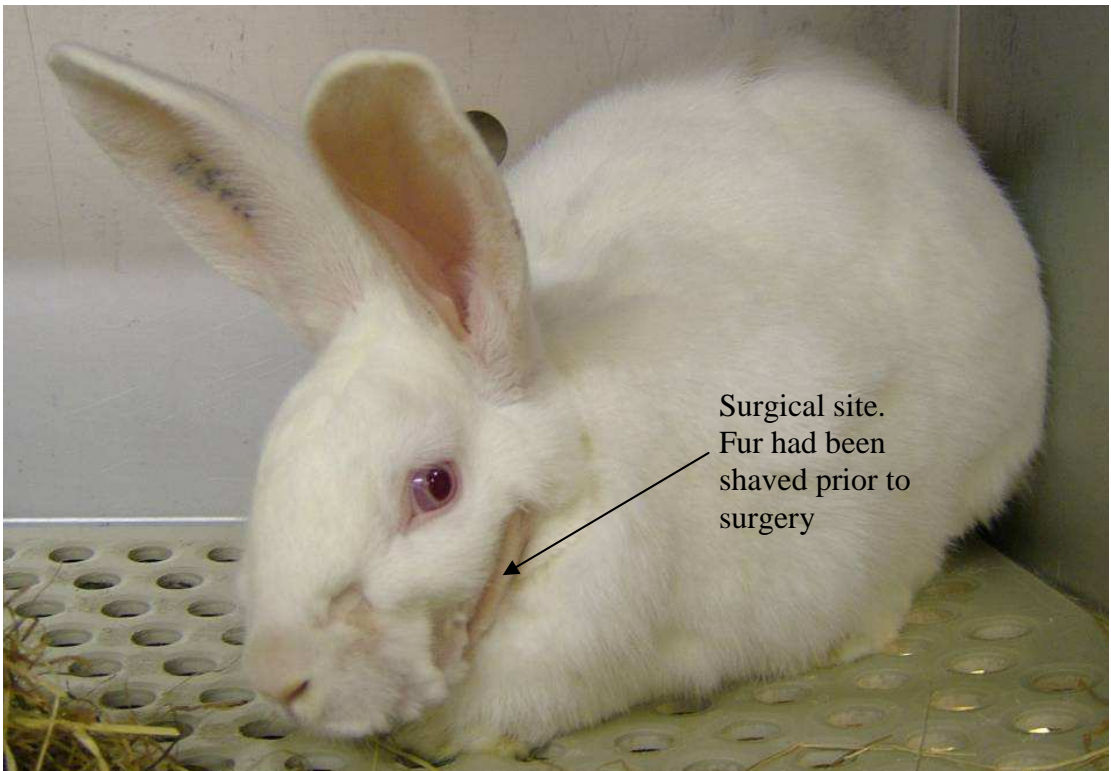


Figure 6.1 Case 10, one week post-operatively.

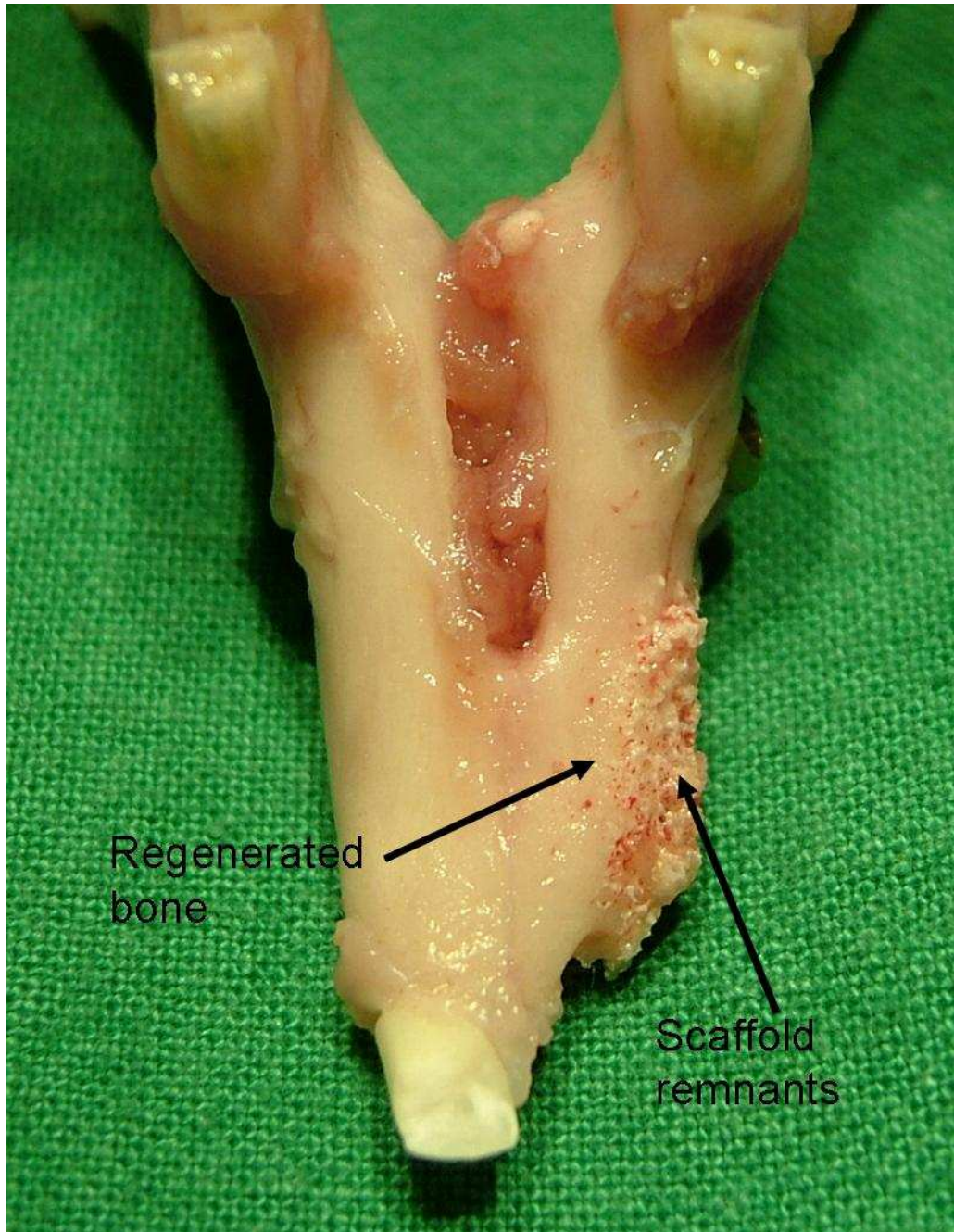


Figure 6.2 Clinical image of explanted mandibular specimen in one of the cases treated with TCP and rhBMP-7.

It was apparent that overall there was more extensive remodeling and dense radio-opacity in the cases that received the TCP loaded with BMP-7 than those that received the TCP alone (Figures 6.5 & 6.6). In the cases that received TCP alone (Figure 6.5), the regenerated tissue did not seem to bridge the original gap between it and the proximal bone and the graft itself maintained the grainy appearance of the TCP with no hints of differentiation into outer and inner cortices. In these cases the regenerated tissue did not show marked remodeling over time to match the width of the contralateral side (Figure 6.3).

In the TCP and BMP-7 cases (Figures 6.4 & 6.6) there was remodeling of the regenerated tissue into what appeared to be complete bridging of the critical defect. There was some possible differentiation of an outer and inner cortex, particularly on the medial surface. The width of the regenerated tissue was also reduced to a size more similar to that of the contralateral side (Figure 6.4).



Figure 6.3 Case 4, TCP scaffolding alone, at 0, 4 and 8 weeks.



Figure 6.4 Case 5, TCP and rhBMP-7, at 0, 4 and 8 weeks.



Figure 6.5 Case 6 TCP alone at 8 wks. Figure 6.6 Case 10 with BMP-7 at 8 wks.



### 6.3.2 Cone beam computed tomography

Once the animals were sacrificed (3 months) and the mandibles surgically removed these were scanned as described previously in the i-CAT<sup>®</sup> scanner.

CT data confirmed the impression obtained from the analysis of the plain radiography that there was more extensive remodeling of the graft in the cases that received the TCP loaded with BMP-7 than those that received the TCP alone (Figures 6.7 to 6.10). In the former, the scans showed reorganization of the regenerated tissue into what looked like an outer cortex and an inner trabecular region (Figure 6.8, images 10.00 & 12.00). There was complete fusion of the regenerated tissue with the proximal bone segment (Figure 6.8, image 1.00) with a radiodensity similar to that of bone. The width of the remodeled graft was similar in size to the contralateral non-operated side but appeared deficient anteriorly (Figure 6.8, images 2.00 & 4.00) probably due to the lack of the presence of an incisor tooth within the graft. In the group that received TCP alone, there was no bridging of the gap between the graft and the proximal bone (Figure 6.10, image 1.00) and the remodeling of the scaffolding was very limited with a clear deficiency of the vertical height in comparison to the contralateral side (Figure 6.10, images 8.00 & 12.00). There was also no development of a visible outer cortical or inner cancellous appearance as seen in the cases which received TCP and rhBMP-7 (Figure 6.10, image 10.00).

There were no radiographic signs of infection in any of the experimental cases. None of the titanium screws appeared displaced or loose, and no mandibular fractures were detected.

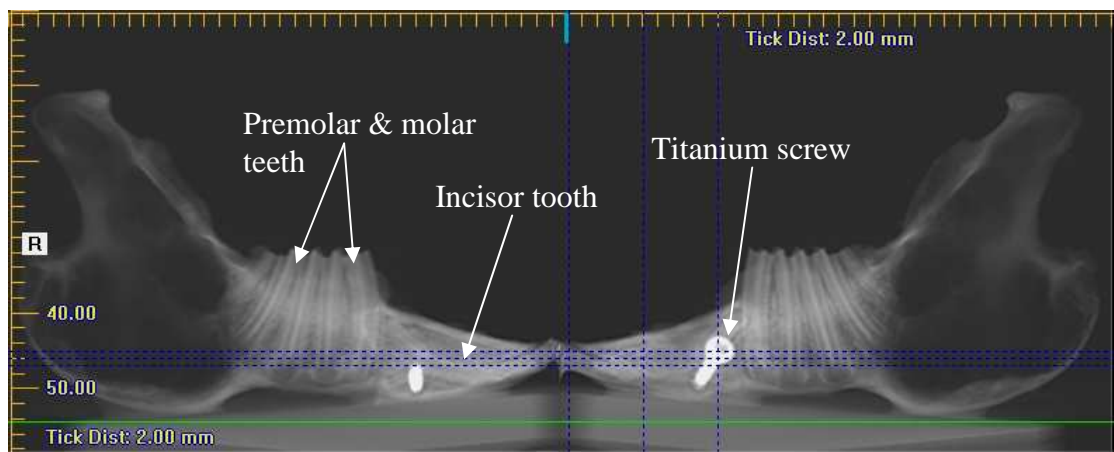


Figure 6.7 Panoramic reconstruction from the i-CAT<sup>®</sup> scan of the mandible in case 10, treated with TCP and BMP-7.

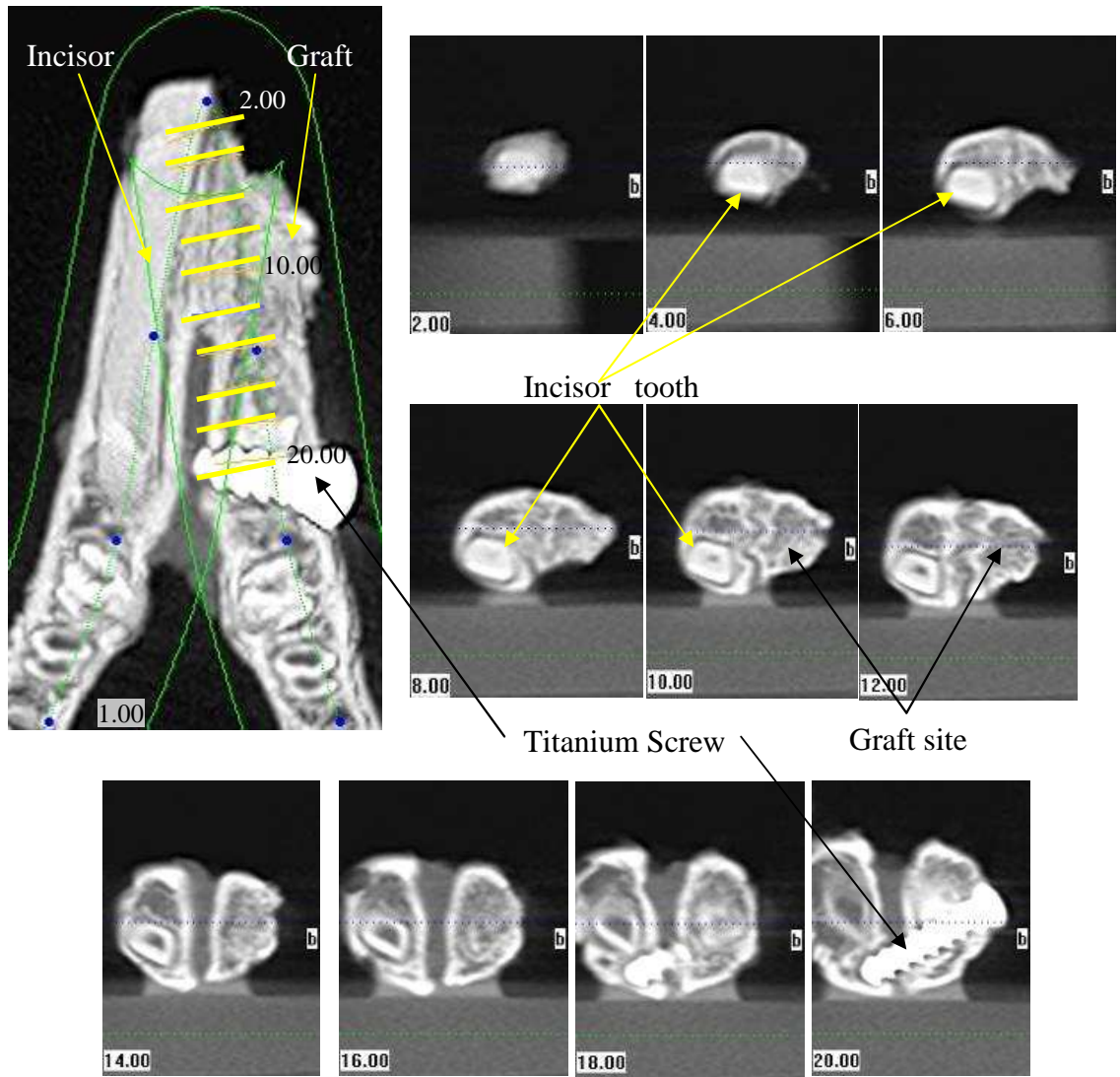


Figure 6.8 Axial (1.00), and coronal sections (2.00 – 20.00) of the surgical site reconstructed from the i-CAT<sup>®</sup> scan of a case treated with TCP and BMP-7. The sites for the various coronal sections are marked on the axial scan in yellow.

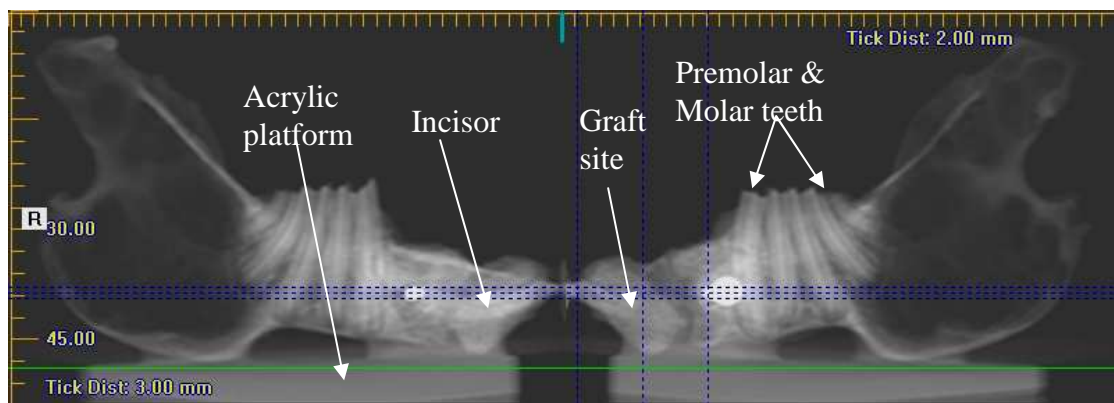


Figure 6.9 Panoramic reconstruction from the i-CAT<sup>®</sup> scan of the mandible in a case treated with TCP alone.

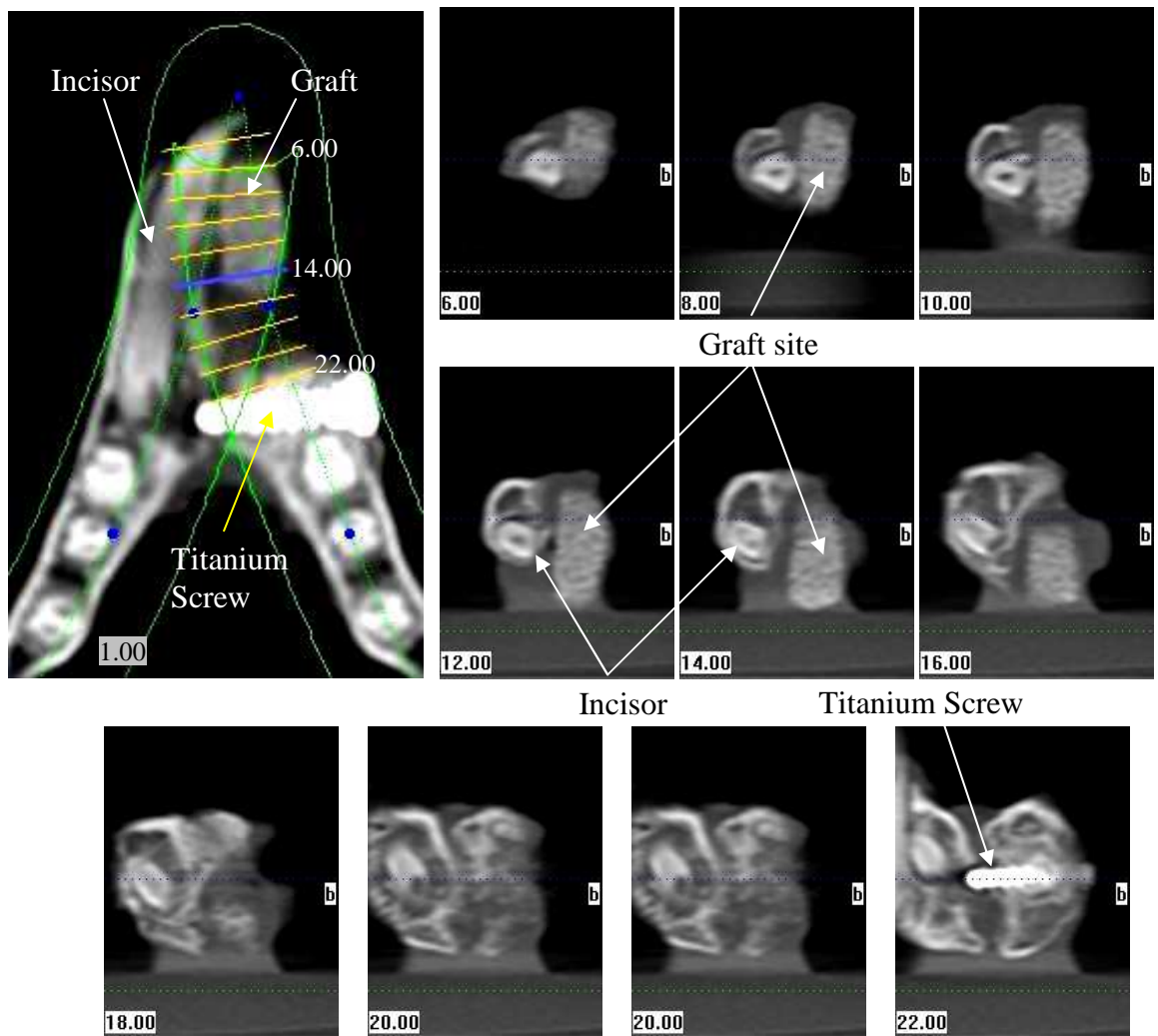


Figure 6.10 Axial (1.00), and coronal sections (6.00 – 22.00) of the surgical site reconstructed from the i-CAT<sup>®</sup> scan of a case treated with TCP alone. The sites for the various coronal sections are marked on the axial scan in yellow.

#### 6.4 Mechanical testing

Fracture in all the specimens occurred by a crack appearing on the dorsal surface of the anterior portion of the body of the mandible; the crack propagated rapidly across the width of the mandible, leading to an abrupt fall in load (Figure 6.11). The maximum load that occurred at fracture was recorded ( $N_{\max}$ ) and the distance between the 12mm loading point (described previously) and the site of failure on the dorsal surface of the specimen was measured (L). The failure moment, which is considered as the most appropriate measure of loading when using cantilever mechanical tests of this type, was then calculated:

$$\text{Failure Moment} = N_{\max} \times L$$

The values of the failure moments for all the treated and untreated sides of the specimens are shown in Table 6.1.

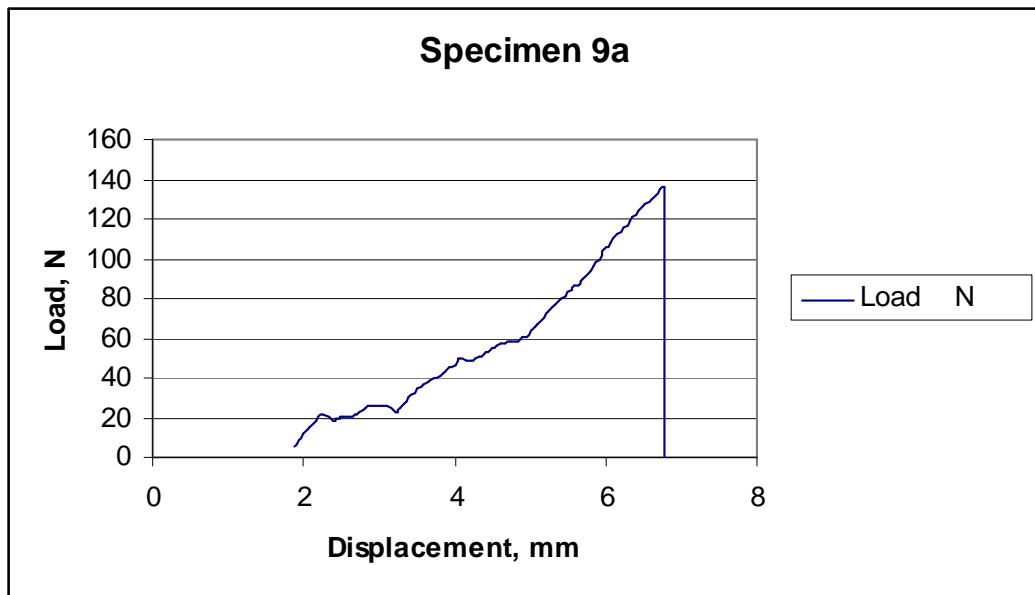


Figure 6.11 A typical mechanical test result showing an abrupt fall in load at the failure point.

Specimen Number	Treated side mNm	Untreated side mNm
2	170	719*
3	54.8	679*
4	48.2	1404
5	383	689*
6	0	588*
7	300	1332
8	20.0	604*
9	2040	2772
10	2115	2652

\* failures involving incisor tooth.

Table 6.1 Magnitude of failure moments for all specimens.

#### 6.4.1 Treatment side

The failure moments of the treated side were clearly different among groups. Specimens 4, 6 and 8 of the TCP only group showed low strengths; no load could be recorded in case 6 and case 8 showed large displacement before eventual fracture. It appears that these specimens had fibrous union which was confirmed histologically (Figure 6.14, pg147).

The histograms in Figure 6.12 show the wide range of mechanical properties of the bone regenerate with a tendency of higher mechanical properties in cases with significant bone formation as shown histologically. Intergroup variations were marked; in two cases that received TCP with rhBMP-7 the mechanical properties of the treated side reached similar levels to that of the normal bone on untreated side.

#### 6.4.2 Untreated side

On the untreated side some specimen fractures involved the incisor teeth despite the standardised loading point, possibly due to minor anatomical variations between the cases. Table 6.1 shows that in the cases where the fracture was affected by the incisor tooth, the failure moment was less than 1 Nm. In those cases not affected by the tooth the failure moment was greater than 1 Nm. No specimens fractured through the premolar socket thanks to the embedding in dental stone and aluminium box frame as described earlier. When the magnitude of the failure moment strengths was ranked and turned into histograms this also separated the specimens into two groups, with those that fractured across the incisor tooth obtaining much lower failure moment values (Figure 6.13).



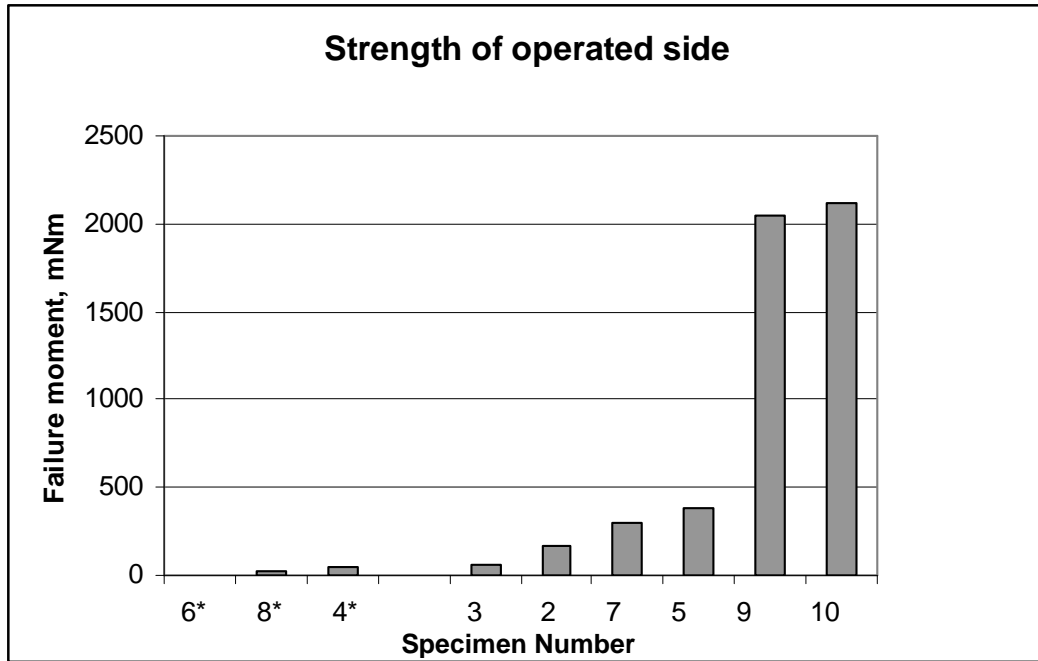


Figure 6.12 Histogram of the failure moments of the TCP only cases (denoted by \*) that were weaker than the specimens treated with TCP and rhBMP-7.

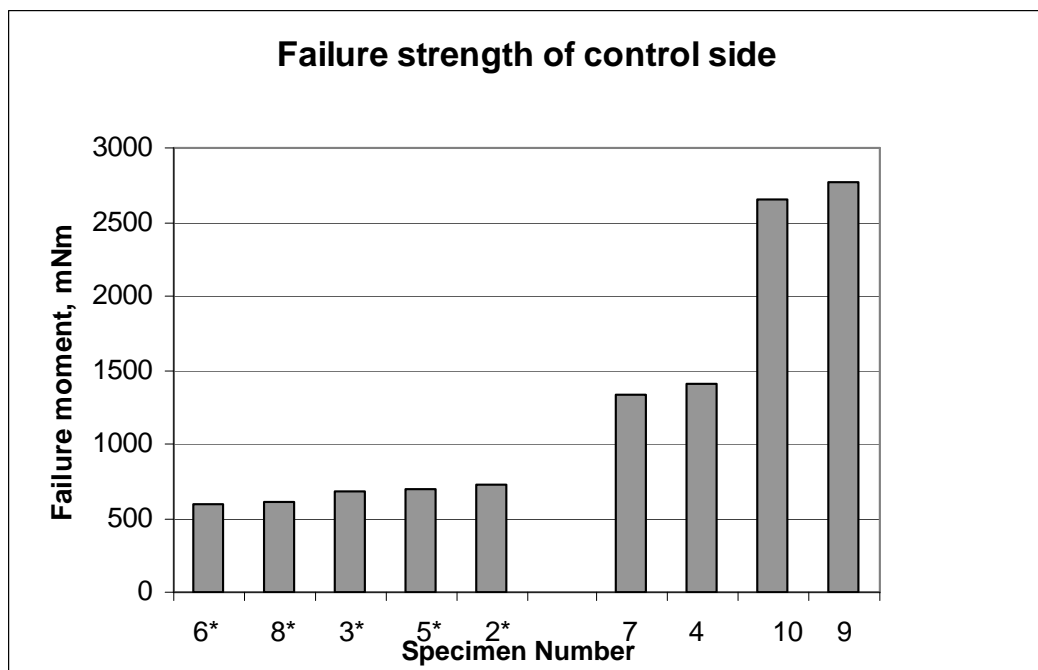


Figure 6.13 Histogram of the failure moments of the untreated sides, showing lower values for the specimens that failed across the incisor tooth (denoted by \*).

## 6.5 Quantitative histological assessment

### 6.5.1 Gross histological appearance

Visual inspection of the H&E stained sections under 40x magnification showed more bone regeneration within the cases that received TCP with rhBMP-7, with evidence of differentiation into woven and lamellar types of bone (Figure 6.15). There was histological union between the regenerated bone and the adjacent untreated bone at the surgical site with no cartilage formation noted. There was no evidence of bone marrow formation and the regenerated bone was confined to area that received the scaffold. No calcification of the surrounding soft tissues was noted. Many osteocytes and osteoblasts were visible but very few osteoclasts. The TCP was also resorbed almost completely in the rhBMP cases (Figures 6.16 & 6.17). The pattern of bone formation varied even in the cases that received TCP and rhBMP-7. In some cases a well formed cortex was identified, whilst in others the new bone formation was primarily cancellous. Very little bone was formed in the cases where the defect was filled with TCP alone (Figure 6.18). In two of the cases with TCP alone there was evidence of a chronic inflammatory response, with macrophages and lymphocytes, in relation to the TCP scaffold (Figure 6.19). This appearance was also seen focally in the rhBMP cases, particularly in relation to the unresorbed TCP scaffold.

A small amount of acellular eosinophilic material was noted in the connective tissue of the regenerate in all the cases. The nature of this material is unclear and it was not included in the assessment of the bone volume.

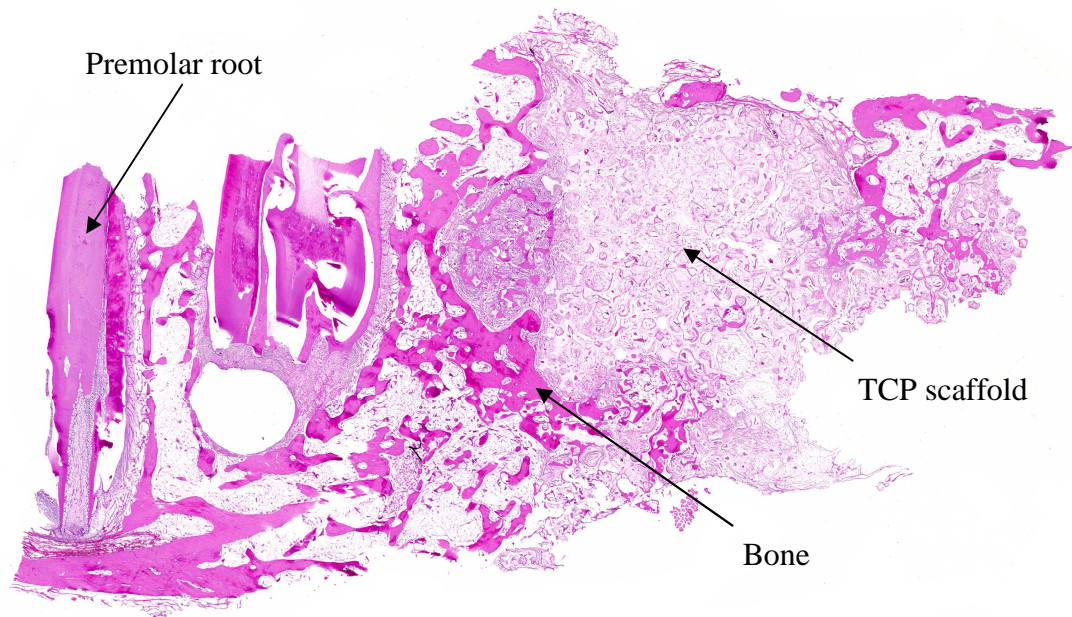


Figure 6.14 H&E stained section of a case that received TCP alone showing minimal bone formation (x10).

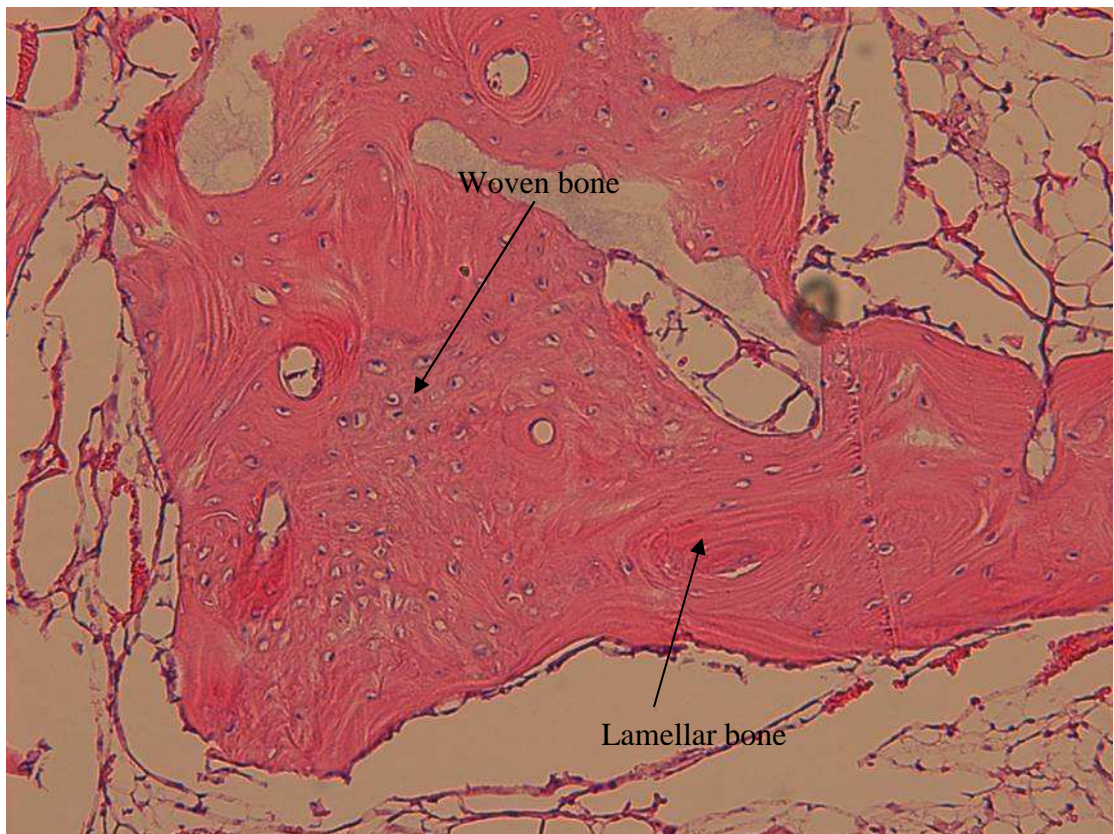


Figure 6.15 H&E stained section of a case that received rhBMP-7 showing woven and lamellar bone formation (x40).

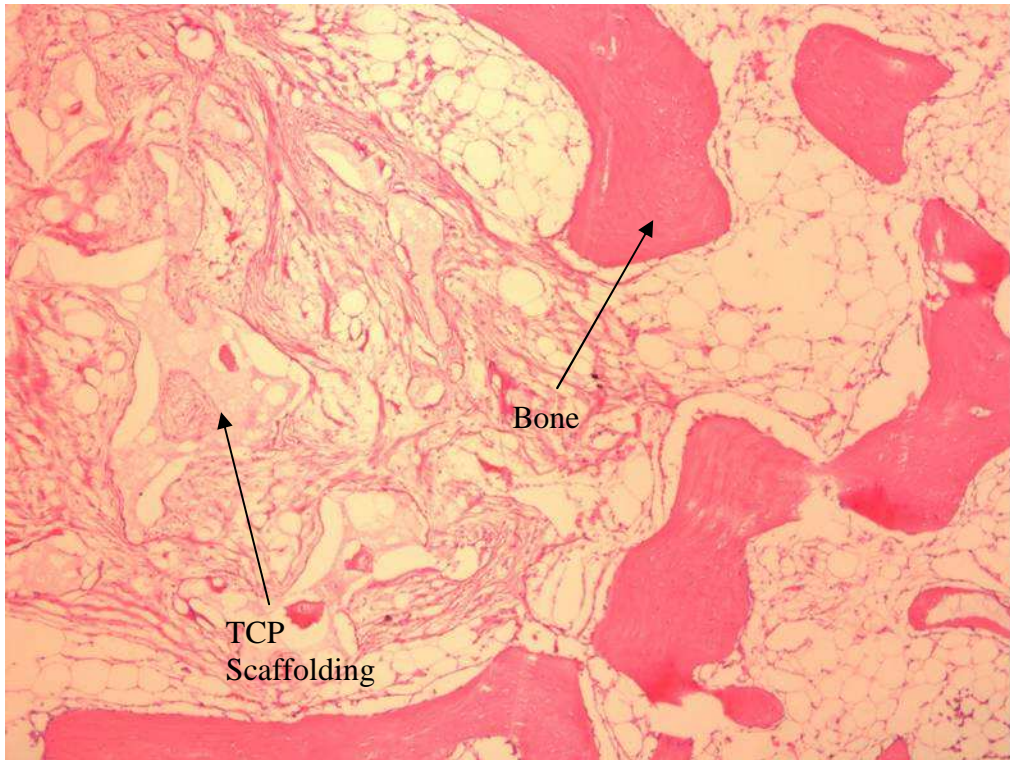


Figure 6.16 H&E stained section of a case that received rhBMP-7 showing minimal amounts of scaffolding (x20).

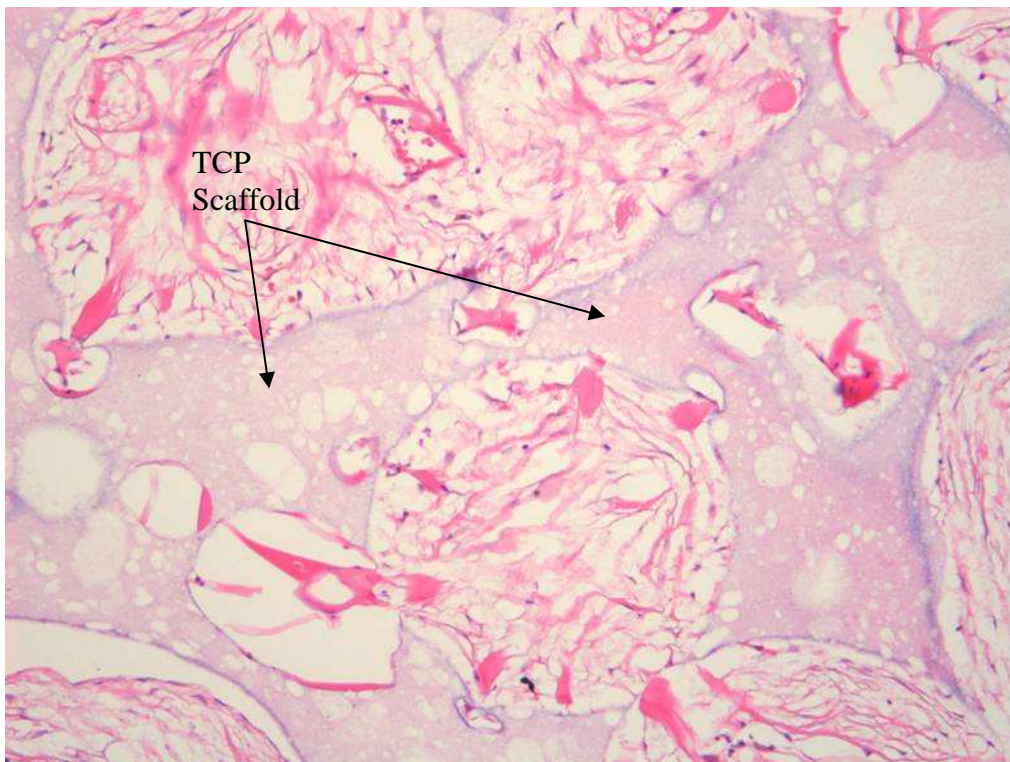


Figure 6.17 H&E stained section of a case that received TCP alone showing no bone and large amounts of retained scaffold (x40).

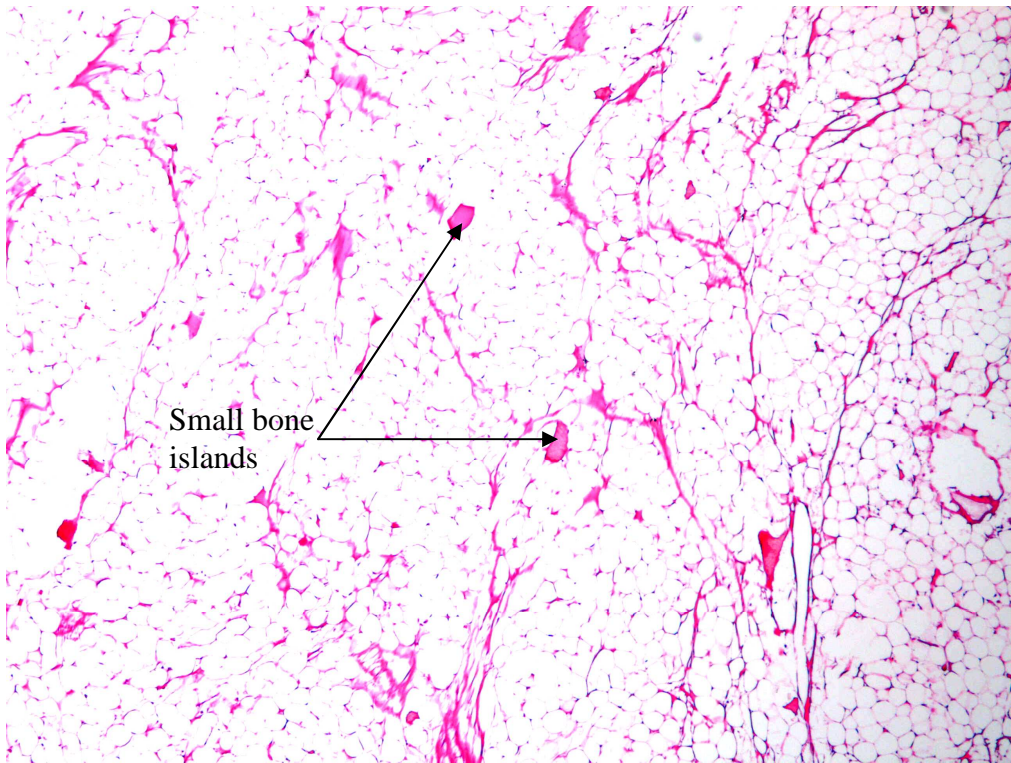


Figure 6.18 H&E stained section of the mid-surgical field of one of the cases treated with TCP alone. Minimal bone formation is evident (x20).

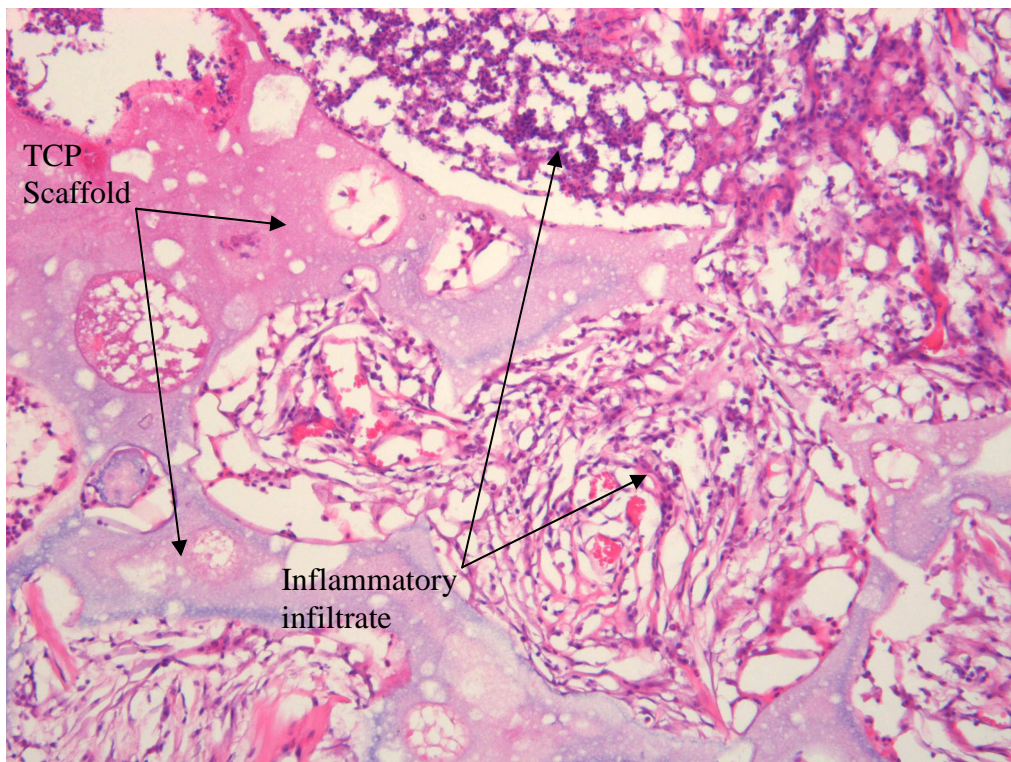


Figure 6.19 Inflammation in relation to the scaffold in a case that received TCP alone (x40).

### 6.5.2 Binary image analysis

The overall mean of the percentage regenerated bone volume, in all the three fields tested, in the rhBMP-7 cases was  $29.41\% \pm 6.25$ , while that for the TCP alone cases was  $6.35\% \pm 3.08$  (Figure 6.20). The difference between the groups was statistically significant,  $p = 0.014$ . If the percentage of regenerated bone volume in the mid surgical field alone was compared between groups, the value for the rhBMP-7 cases was again statistically significantly higher than that of the TCP only cases,  $p = 0.009$  (rhBMP-7 cases,  $22.8\% \pm 5.0$ ; TCP only cases,  $2.9\% \pm 1.8$ ) (Figure 6.21).

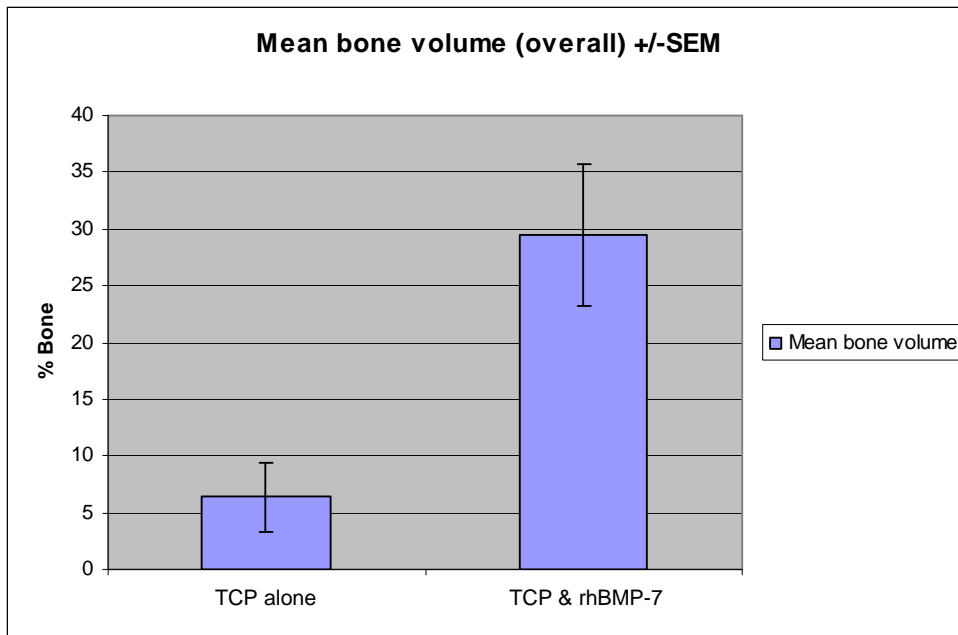


Figure 6.20 The percentage overall mean bone volume in the two groups and the standard error. The difference in mean bone formation was significant ( $p = 0.014$ ).

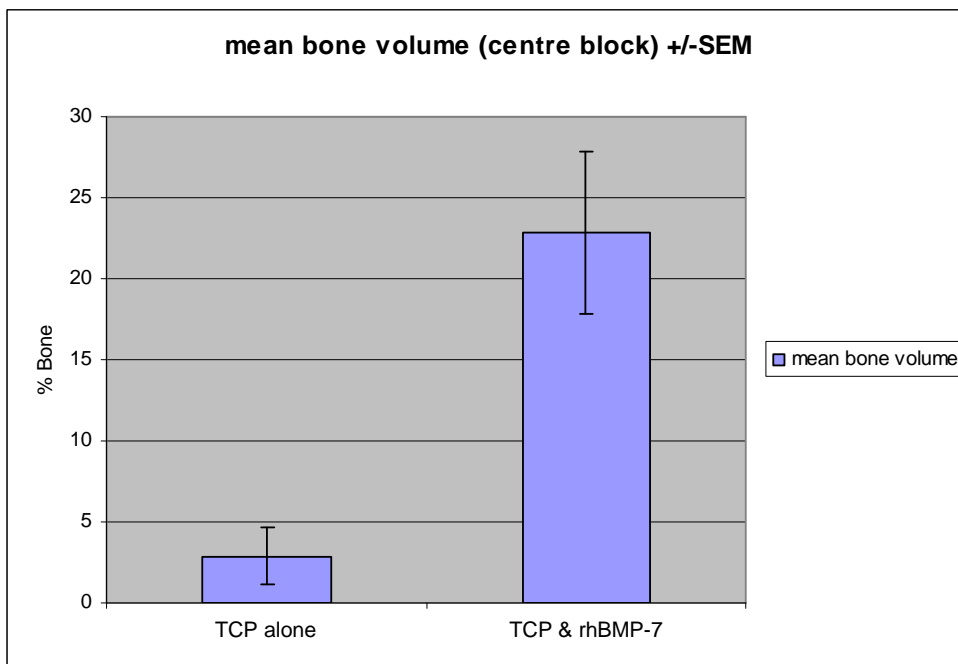


Figure 6.21 The percentage mean bone volume in mid surgical field of the two groups and the standard errors. The difference in mean bone formation was significant ( $p = 0.009$ ).

## **Discussion**



## 7.1 Discussion on the study rationale

The outcomes of this study confirmed the suitability of the rabbit model for the analysis of the healing of a mandibular continuity critical-size defect. All the animals returned to function without adverse effects. The rabbits returned back to normal chewing and mandibular loading within a few days after surgery and this might have had a positive impact on the bone healing and remodelling. The rabbit mandible is large enough to allow the creation of a significantly-sized bone defect in a standardised, reproducible manner. Rabbits are also relatively small mammals and are therefore easily housed and cared for within dedicated veterinary facilities.

The rabbit is also a mammal that is similar biologically to the human and has been recognised as an appropriate model to study bone bioengineering in the craniofacial region (Mao, et al. 1998, Lu and Rabie, 2002).

The periosteum was surgically removed together with the associated incisor tooth and about 20mm of the body of the mandible to create a critical-size defect that simulated the clinical scenario in oral cancer patients where the periosteum would generally be removed along with the bone being removed following tumour invasion.

Three rabbits were allocated to the control group to prove the concept that the created defect was of a critical size and the scaffold on its own would not induce enough bone formation to reconstruct the defect. This was confirmed when statistically significant differences in bone regeneration were found between the

groups even though the number of rabbits used for the project was small (six cases that received rhBMP-7 and 3 the received TCP alone). This finding is in agreement with previous published data regarding the size of a critical defect (Hollinger and Kleinschmidt, 1990).

The use of screw fixation to maintain the mandibular integrity, before creating the critical-size continuity defect, was a novel method. The effectiveness of this technique was tested on dry rabbit mandibles and cadaveric cases, before the live application.

RhBMP-7 had been previously used effectively on its own for the reconstruction of a critical-size mandibular defect in the sheep model by our group (Abu-Serriah, et al. 2004). We reported that bone regeneration was not confined to the boundaries of the defect, and therefore did not satisfactorily restore the shape of the resected mandible. The rationale behind using the TCP scaffolding in this study was to control the shape of bone regeneration in an attempt to restore the normal morphology, 'medio-lateral width' and vertical height of the excised mandibular bone segment. The gross appearance of the regenerated bone confirmed the effectiveness of the TCP and rhBMP-7 in achieving this objective.

A multidisciplinary assessment method was used to evaluate the outcome of the surgical interventions. This involved radiographic assessment with plain films and cone-beam computed tomography, mechanical testing and histological

analysis. This allowed the quality and quantity of tissue regeneration to be assessed and the relationship between the variables to be investigated.

In this study there is a lack of immunohistochemistry analysis that would have allowed a better understanding of the pattern of bone regeneration. All the cases were sacrificed after three months; this did not allow any long term follow-up of the surgical site, which might have shown bony regenerate with even better radiographic, mechanical and histological properties at six and 12 months.

## 7.2 Radiographic assessment

The radiographic assessment of both the plain films and the cone-beam CT was performed in a subjective manner. But, there were obvious differences noted between the cases that received TCP scaffolding and rhBMP-7 and those that received the TCP alone. TCP was more remodeled and integrated with the regenerated tissue in the cases that received the TCP and rhBMP-7.

Lagravère et al (2006) concluded that the cone-beam CT provides an effective option for the determination of material density when expressed as Hounsfield Units (Brooks, 1997). Hounsfield units (HU) are named after Sir Godfrey Hounsfield, born in 1919, an electroengineer who developed the first clinically useful CT machine. HU are considered a standardized and accepted unit for reporting and displaying reconstructed X-ray computed tomography CT values. An objective method of evaluating bone density using the Hounsfield scale was proposed by Norton and Gamble in 2001, who demonstrated a strong correlation between the obtained bone density value and subjective quality score. However,

within our study group, the radio-opacity of the residual TCP scaffolding within the grafted site would have made objective radiographic analysis of the quantity of bone regeneration difficult as the numbers obtained in HU would have been affected by the TCP.

Mulconrey et al (2008) evaluated bone formation and TCP scaffolding degradation when used with BMP-2 for spinal deformity fusions. They suggested that the TCP would degrade at the same rate as that of bone formation. This was not the case in our study. Remodeling may have continued in our cases if the animals were kept for a longer follow-up interval, however this would need a different study to be proven.

It would have been ideal to include X-ray microcomputed tomography (MicroCT) scanning (Laib and Rügsegger, 1999) for the assessment of the microarchitecture and quantity of bone regeneration at the microscopic level. Unfortunately, these were not available to the authors when the research was carried out. One of the main advantages of using scaffolding for the restoration of mandibular defects is the restoration of the shape and continuity of the bone. This objective was achieved in this study and overcame the problems that we reported previously regarding excessive bone formation using BMP-7 for mandibular reconstruction (Abu-Serriah, et al. 2004).

Despite the fact that the scaffolding was not rigidly fixed in the created defect, we could not detect radiographic evidence of dislodgement or displacement of the scaffold. The newly formed tissue followed the contour of the adjacent bone

margins. Cone-beam CT demonstrated that the width and height of the regenerated bone matched the opposite non-operated side. However, we could not detect the formation of a medullary cavity radiographically. This high level of morphological differentiation may have been achieved with a longer follow-up interval.

In all the cases which received TCP and BMP-7 there was no radiographic line of demarcation between the regenerated bone and the proximal and distal edges of the created defect. This is a demonstration of the full integration of the regenerated bone with the surrounding untreated bone.

### 7.3 Mechanical assessment

There was a wide variation in the values of failure moment obtained for the specimens treated with rhBMP-7 (54.8mNm - 2040mNm) (Figure 6.12, pg145). The two high values (2040mNm & 2115 mNm) obtained were comparable to the failure moments of the untreated sides that failed across the anterior body. This would suggest that the potential for acquiring the original pre-operative mechanical properties was possible with the use of rhBMP-7 in TCP for repairing the critical-size defect.

There is considerable variation in the literature regarding the effect of a prolonged healing time on the mechanical properties of bioengineered bone. Depending on the animal model used, the length of postoperative follow-up before animal sacrifice varied from; 5 weeks (Henkel, et al. 2005) to 8 months (Henkel, et al. 2006) in minipigs, 6 weeks (Saadeh, et al. 2001) to 12 weeks

(Arosarena and Collins, 2003) in rats, and 3 weeks (Lu and Rabie, 2002) to 3 months (Pekkarinen, et al. 2006) in rabbits. The longer the follow-up intervals did not always necessarily improve the quality of the mechanical properties of the bioengineered bone.

The mechanical testing performed in previous work (Abu-Serriah, et al. 2005, Kontaxis, et al. 2004) showed the regenerate in critical-size defects reconstructed with BMP-7 and BMP-2 (Toriumi, et al. 2001) had a wide range of mechanical properties which was similar to our findings. In our cases the rhBMP-7-induced bone achieved a mean of 36% of the strength of the bone on the non-operated side. The mechanical properties of the control sides also varied substantially (Figure 6.13, pg145); from 1404mNm to 2772mNm in the cases where the fracture occurred within bone. The presence of an incisor tooth within the control side made the mechanical testing more complex, due to the need to avoid fracture through the tooth socket. A custom-made aluminium frame (Figure 5.37, pg119) was constructed and the load was applied 14mm anterior to the premolar socket to try to minimise this occurrence. The variation in mechanical properties in this study group might also be due to the varying proportions of woven and lamellar bone formation in the bioengineered tissues that were seen histologically. The possible variations in the concentration of rhBMP-7 within the grafts, even though standardised methods were used for the loading of the TCP, may also have influenced the quality of bone formation resulting in changes in the mechanical properties. Histomorphometric analysis demonstrated a large proportion of trabecular spaces in the regenerated bone, when compared to bone on the control side. Some of the cases that received

TCP with rhBMP-7 developed an outer cortex that was visible radiographically (Figure 6.6, pg136). This should have improved the mechanical properties of the bioengineered bone, due to the higher percentage of compact bone present in cortical bone.

This study, along with previous work by our group (Abu-Serriah, et al. 2005, Kontaxis, et al. 2004), has further emphasized the potential bone regenerative properties of rhBMP-7 and has also shown that the use of TCP scaffolding could result in the regeneration of bone with mechanical properties similar to those of natural bone in some cases. There was a close association between the quality of histological bone formation and the mechanical properties achieved, where  $\rho$  was found to be +0.7 using Spearman's rank correlation coefficient.

#### 7.4 Quantitative histological evaluation

Classically, histomorphometric analysis of bone involves the application of probability theory to geometry by the use of estimates, rather than exact measurements. Repeated counting was used in order to make the estimates as accurate as possible. Histomorphometric analysis can be carried out in three ways; simple eye-piece grids, semiautomatic instruments in which a digitising tablet is linked to a desk-top microcomputer, or fully automatic computer-linked image analysis equipment (Revell, 1983). The method used in this report was a modification of these techniques and used decalcified sections in combination with image analysis, conversion into a binary image with a manual clean-up with removal of connective tissue and computerised pixel analysis. Although the measurements were made on two dimensional images, the information

derived may be interpreted on a three dimensional basis. Results are usually expressed in percentages (Revell, 1983). Decalcified sections present many advantages as specimen processing and section generation are considerably easier. The weakness of this method of assessment is that the mineral content of the regenerated bone cannot be assessed, thus the technique does not provide the information on the dynamics of bone formation which may be assessed from calcified sections or x-ray microtomography.

The histological and binary image analysis of the regenerate in the critical-size defects in this study showed that TCP loaded with rhBMP-7 was significantly superior in its capacity for bone regeneration than TCP alone (Section 6, Figures 14-21). It was noted that the regenerated bone was either lamellar or woven in appearance, as seen in previous studies (Abu-Serriah, et al. 2004, Boyne, 1996, Toriumi, et al. 1991), with evidence of some outer cortex formation in some of the cases. Previous studies have shown that longer healing periods, of up to one year, are required for the complete maturation of the regenerated bone with complete formation of an outer cortex and medullary cavity (Boyne, et al. 1999, Kirker-Head, et al. 1995, Toriumi, et al. 1999).

In order to avoid the influence of the innate osteoinductive and osteogenic properties of the bone on the edge of the surgical site, the analysis was also performed on the 2 images from the centre of the surgical site. This provided a more reliable measure of the effect that rhBMP-7 had within the scaffold, with minimal influence from the adjacent bone on bone regeneration. The extent of variation in bone formation across the surgical site demonstrates the influence of



the intact bone boundaries at either end of the surgical defect on osteogenesis. Comparison of the histological nature of the bioengineered bone in the middle of the scaffold with that of the proximal and distal ends adjacent to native bone showed both a reduction in the amount of bone formed overall and an increased proportion of woven bone at the centre. This indicated that much of the new bone formation was initiated at the interface between the scaffolding and the intact mandibular bone. This is likely to be due to the diminished vascularity at the centre of the scaffold. It is well known that vascular proliferation is limited to a few millimetres from the intact bone margins. The low oxygen tension at the centre of the scaffold secondary to the diminished blood supply is an important reason for the reduced quality of the bone formation. The same process will apply with remodelling as the osteoclasts have to access the scaffold before remodelling can occur. In fact limited remodelling was noted at the centre of the scaffolding in comparison to the proximal and distal margins adjacent to the surrounding intact bone.

The inflammatory infiltrate seen in some cases seemed to be a reaction to the TCP scaffolding, but this did not manifest itself with any clinical signs or symptoms as the rabbits completed the study successfully with no signs of infection.

No cartilaginous remnants were found in any of the specimens suggesting that the new bone regenerate was formed by intramembraneous ossification as opposed to endochondral ossification, although a transitional phase involving cartilage formation could not be excluded (Abu-Serriah, et al. 2004).

As described earlier, the TCP  $\pm$  rhBMP-7 was secured in place within the adjacent soft tissues and this did not result in significant foreign body reactions. Rigid fixation of the scaffolding in situ would have been ideal; however, the fragile nature of the TCP prevented any type of internal fixation. This is one of the drawbacks of this type of scaffolding which may limit its application to anatomical areas which may be subjected to direct substantial mechanical forces during the early stages of healing.

This project combined two materials with two particular properties; TCP being osteoconductive and rhBMP-7 being osteoinductive. This leaves out the third and just as important property necessary for bone formation that is, bone osteogenesis. This is a property held by the pluripotent mesenchymal stem cells. It would be useful to study the impact of seeding mesenchymal stem cells in a three dimensional scaffolding to maximise the effect of the cytokines in promoting bone regeneration in critical-size bone defects. This could improve both the quality and rate of bone regeneration.

Comparison of the radiological and histological findings within the two groups appeared to show a positive correlation. With the cases which received rhBMP-7 and the TCP showing both histological and radiographic signs of early bone differentiation into an outer cortex but no evidence of inner medullary cavity formation.

The findings of this investigation should be interpreted with caution before clinical application. Our preclinical findings were in healthy subjects, the tissues surrounding the created surgical defects were intact, and the blood supply was not compromised. This would often not be the case in older patients with limited regenerative ability due to osteoporosis and diminished blood supply due to previous radiotherapy within the surgical site.

The ultimate aim of this preclinical study is to translate the bioengineering technology into a format with a human application to facilitate maxillofacial rehabilitation following resection or following traumatic loss. We believe that as a result of this study we are actively approaching this target.

#### 7.5 Future Study

The next phase of the project would be to look at the regeneration of bone in similar critical-size defects repaired with TCP together with mesenchymal stem cells (MSCs) as well as rhBMP-7. The aim would be to produce histologically and radiographically better quality of bone regeneration, with more consistently higher mechanical failure moments with values close to natural bone for most if not all of the experimental cases.

#### 7.6 Clinical implications of the study

The reconstruction of critical-size bone defects following tumour resection or bone loss due to trauma is very topical due to the complexity of the treatment involved and poor healing outcomes. The results of this study show that

rhBMP-7 together with a TCP scaffolding may potentially be an effective bone bioengineering tool that could be used in such cases.

## **Conclusions**

RhBMP-7 in a prefabricated TCP scaffolding proved to be an effective method for bone regeneration in mandibular critical-size defects in the rabbit model which could have possible future clinical applications.

The rabbit model proved to be an effective model for the creation of a standardised critical-size mandibular defect and radiographic, histological and mechanical assessment of bone formation.

TCP scaffold on its own does not induce enough bone formation to reconstruct critical-size rabbit mandibular defects.

Close correlation was found between the mechanical properties and the histological quality of the regenerated bone.

Within 3 months satisfactory bone regeneration was achieved when the TCP and rhBMP-7 were applied in a critical-size mandibular bone defect. In some cases, the mechanical properties reached the standard of untreated bone on the contralateral side.

#### Hypothesis

The addition of rhBMP-7 to TCP will increase the quality and quantity of bone regeneration.

The hypothesis is accepted.

## **References**

Abukawa H, Shin M, Williams WB, Vacanti JP, Kaban LB, Troulis MJ. Reconstruction of mandibular defects with autologous tissue-engineered bone. *J Oral Maxillofac Surg.* 2004;62(5):601-6.

Abu-Serriah MM, Odell E, Lock C, Gillar A, Ayoub AF, Fleming RH. Histological assessment of bioengineered new bone in repairing osteoperiosteal mandibular defects in sheep using recombinant human bone morphogenetic protein-7. *Br J Oral Maxillofac Surg.* 2004;42(5):410-8.

Abu-Serriah M, Kontaxis A, Ayoub A, Harrison J, Odell E, Barbenel J. Mechanical evaluation of mandibular defects reconstructed using osteogenic protein-1 (rhOP-1) in a sheep model: a critical analysis. *Int J Oral Maxillofac Surg.* 2005;34(3):287-93.

Aithanasiou KA, Zhu C, Lanctot DR, Agrawal CM, Wang X. Fundamentals of biomechanics in tissue engineering of bone. *Tissue Eng.* 2000;6(4):361-81.

Alden TD, Beres EJ, Laurent JS, Engh JA, Das S, London SD, Jane JA Jr, Hudson SB, Helm GA. The use of bone morphogenetic protein gene therapy in craniofacial bone repair. *J Craniofac Surg.* 2000;11(1):24-30.

Arosarena OA, Falk A, Malmgren L, Bookman L, Allen MJ, Schoonmaker J, Tatum S, Kellman R. Defect repair in the rat mandible with bone morphogenic proteins and marrow cells. *Arch Facial Plast Surg.* 2003;5(1):103-8.



Arosarena OA, Collins WL. Defect repair in the rat mandible with bone morphogenic protein 5 and prostaglandin E1. Arch Otolaryngol Head Neck Surg. 2003;129(10):1125-30.

Arosarena O, Collins W. Comparison of BMP-2 and -4 for rat mandibular bone regeneration at various doses. Orthod Craniofac Res. 2005;8(4):267-76.

Barboza EP, Duarte ME, Geolas L, Sorensen RG, Riedel GE, Wikesjo UM. Ridge augmentation following implantation of recombinant human bone morphogenetic protein-2 in the dog. J Periodontol. 2000;71(3):488-96.

Boyne PJ. Animal studies of application of rhBMP-2 in maxillofacial reconstruction. Bone. 1996;19(1 Suppl):83S-92S.

Boyne PJ, Nakamura A, Shabahang S. Evaluation of the long-term effect of function on rhBMP-2 regenerated hemimandibulectomy defects. Br J Oral Maxillofac Surg. 1999;37(5):344-52.

Boyne PJ. Application of bone morphogenetic proteins in the treatment of clinical oral and maxillofacial osseous defects. J Bone Joint Surg Am. 2001;83-A Suppl 1(Pt 2):S146-50.

Boyne PJ, Shabahang S. An evaluation of bone induction delivery materials in conjunction with root-form implant placement. Int J Periodontics Restorative Dent. 2001;21(4):333-43.

Boyne PJ, Salina S, Nakamura A, Audia F, Shabahang S. Bone regeneration using rhBMP-2 induction in hemimandibulectomy type defects of elderly sub-human primates. *Cell Tissue Bank*. 2006;7(1):1-10.

Breitbart AS, Grande DA, Kessler R, Ryaby JT, Fitzsimmons RJ, Grant RT. Tissue engineered bone repair of calvarial defects using cultured periosteal cells. *Plast Reconstr Surg*. 1998;101(3):567-74.

Breitbart AS, Grande DA, Mason JM, Barcia M, James T, Grant RT. Gene-enhanced tissue engineering: applications for bone healing using cultured periosteal cells transduced retrovirally with the BMP-7 gene. *Ann Plast Surg*. 1999;42(5):488-95.

Brooks RA. A quantitative theory of the Hounsfield unit and its application to dual energy scanning. *J Comput Assist Tomogr*. 1977;1(4):487-93.

Chen B, Lin H, Wang J, Zhao Y, Wang B, Zhao W, Sun W, Dai J. Homogeneous osteogenesis and bone regeneration by demineralized bone matrix loading with collagen-targeting bone morphogenetic protein-2. *Biomaterials*. 2007;28(6):1027-35.

Currey JD. *Bones: Structure and Mechanics*. First Edition, Princeton: Princeton University Press, 2002

Cuvas P, de Paz V, Cuevas B, Marin-Martinez J, Picon-Molina M, Fernández-Pereira A, Giménez-Gallego G. Osteopromotion for cranioplasty: an experimental study in rats using acidic fibroblast growth factor. *Surg Neurol.* 1997;47(3):242-6.

Fini M, Motta A, Torricelli P, Giavaresi G, Nicoli Aldini N, Tschon M, Giardino R, Migliaresi C. The healing of confined critical size cancellous defects in the presence of silk fibroin hydrogel. *Biomaterials.* 2005;26(17):3527-36.

Gröger A, Kläring S, Merten HA, Holste J, Kaps C, Sittinger M. Tissue engineering of bone for mandibular augmentation in immunocompetent minipigs: preliminary study. *Scand J Plast Reconstr Surg Hand Surg.* 2003;37(3):129-33.

Havers, C. *Osteologia nova, or some new Observations of the Bones, and the Parts belonging to them, with the manner of their Accretion and Nutrition.* London: Thomlinson Library, 1691.

He H, Yan W, Chen G, Lu Z. Acceleration of de novo bone formation with a novel bioabsorbable film: a histomorphometric study in vivo. *J Oral Pathol Med.* 2008;37(6):378-82.

Henkel KO, Gerber T, Dietrich W, Bienengraber V. [Novel calcium phosphate formula for filling bone defects. Initial in vivo long-term results] Mund Kiefer Gesichtschir. 2004;8(5):277-81.

Henkel KO, Gerber T, Dörfling P, Gundlach KK, Bienengraber V. Repair of bone defects by applying biomatrices with and without autologous osteoblasts. J Craniomaxillofac Surg. 2005;33(1):45-9.

Henkel KO, Gerber T, Lenz S, Gundlach KK, Bienengraber V. Macroscopical, histological, and morphometric studies of porous bone-replacement materials in minipigs 8 months after implantation. Oral Surg Oral Med Oral Pathol Oral Radiol Endod. 2006;102(5):606-13.

Herford AS, Boyne PJ. Reconstruction of mandibular continuity defects with bone morphogenetic protein-2 (rhBMP-2). J Oral Maxillofac Surg. 2008;66(4):616-24.

Higuchi T, Kinoshita A, Takahashi K, Oda S, Ishikawa I. Bone regeneration by recombinant human bone morphogenetic protein-2 in rat mandibular defects. An experimental model of defect filling. J Periodontol. 1999;70(9):1026-31.

Hollinger JO, Kleinschmidt JC. The critical size defect as an experimental model to test bone repair materials. J Craniofac Surg. 1990;1(1):60-8.

Ibim SE, Uhrich KE, Attawia M, Shastri VR, El-Amin SF, Bronson R, Langer R, Laurencin CT. Preliminary in vivo report on the osteocompatibility of poly(anhydride-co-imides) evaluated in a tibial model. *J Biomed Mater Res.* 1998;43(4):374-9.

Issa JP, do Nascimento C, Iyomasa MM, Siéssere S, Regalo SC, Defino HL, Sebald W. Bone healing process in critical-sized defects by rhBMP-2 using poloxamer gel and collagen sponge as carriers. *Micron.* 2008;39(1):17-24.

Jung UW, Choi SY, Pang EK, Kim CS, Choi SH, Cho KS. The effect of varying the particle size of beta tricalcium phosphate carrier of recombinant human bone morphogenetic protein-4 on bone formation in rat calvarial defects. *J Periodontol.* 2006;77(5):765-72.

Kimura A, Watanabe T, Shimizu T, Okafuji N, Mori R, Furusawa K, Kawai T, Hasegawa H, Kawakami T. Bone repair of rabbit mandibular transection using rhBMP-2 and atelocollagen gel. *Eur J Med Res.* 2006;11(8):355-8.

Kirker-Head CA, Gerhart TN, Schelling SH, Hennig GE, Wang E, Holtrop ME. Long-term healing of bone using recombinant human bone morphogenetic protein 2. *Clin Orthop* 1995;(318):222-30.

Kleinheinz J, Wiesmann HP, Stratmann U, Joos U. [Evaluating angiogenesis and osteogenesis modified by vascular endothelial growth factor (VEGF)] *Mund Kiefer Gesichtschir.* 2002;6(3):175-82.

Kontaxis A, Abu-Serriah M, Ayoub AF, Barbenel JC. Mechanical testing of recombinant human bone morphogenetic protein-7 regenerated bone in sheep mandibles. *Proc Inst Mech Eng.* 2004;218(6):381-8.

Kubler NR, Wurzler K, Reuther JF, Faller G, Sieber E, Kirchner T, Sebald W. [EHBMP-2. Initial BMP analog with osteoinductive properties] *Mund Kiefer Gesichtschir.* 1999;3 Suppl 1:S134-9.

Laib A, Rügsegger P. Calibration of trabecular bone structure measurements of in vivo three-dimensional peripheral quantitative computed tomography with 28-microm-resolution microcomputed tomography. *Bone.* 1999;24(1):35-9.

Lagravère MO, Fang Y, Carey J, Toogood RW, Packota GV, Major PW. Density conversion factor determined using a cone-beam computed tomography unit NewTom QR-DVT 9000. *Dentomaxillofac Radiol.* 2006;35(6):407-9.

Lemperle SM, Calhoun CJ, Curran RW, Holmes RE. Bony healing of large cranial and mandibular defects protected from soft-tissue interposition: A comparative study of spontaneous bone regeneration, osteoconduction, and cancellous autografting in dogs. *Plast Reconstr Surg.* 1998;101(3):660-72.

Li Z, Yang Y, Wang C, Xia R, Zhang Y, Zhao Q, Liao W, Wang Y, Lu J. Repair of sheep metatarsus defects by using tissue-engineering technique. *J Huazhong Univ Sci Technolog Med Sci.* 2005;25(1):62-7.

Lu M, Rabie AB. The effect of demineralized intramembranous bone matrix and basic fibroblast growth factor on the healing of allogeneic intramembranous bone grafts in the rabbit. *Arch Oral Biol.* 2002;47(12):831-41.

Mao T, Wang C, Zhang S, Wang H, Zhao M, Chen F, Ma Q, Han L. An experimental study on rhBMP-2 composite bone substitute for repairing craniomaxillary bone defects. *Chin J Dent Res.* 1998;1(3):21-5.

Marukawa E, Asahina I, Oda M, Seto I, Alam MI, Enomoto S. Bone regeneration using recombinant human bone morphogenetic protein-2 (rhBMP-2) in alveolar defects of primate mandibles. *Br J Oral Maxillofac Surg.* 2001;39(6):452-9.

Marukawa E, Asahina I, Oda M, Seto I, Alam M, Enomoto S. Functional reconstruction of the non-human primate mandible using recombinant human bone morphogenetic protein-2. *Int J Oral Maxillofac Surg.* 2002;31(3):287-95.

Meijer GJ, van Dooren A, Gaillard ML, Dalmeijer R, de Putter C, Koole R, van Blitterwijk CA. Polyactive as a bone-filler in a beagle dog model. *Int J Oral Maxillofac Surg.* 1996;25(3):210-16.

Mistry AS, Mikos AG. Tissue engineering strategies for bone regeneration. *Adv Biochem Engin/Biotechnol* 2005;94:1-22

Mukherjee DP, Tunkle AS, Roberts RA, Clavenna A, Rogers S, Smith D. An animal evaluation of a paste of chitosan glutamate and hydroxyapatite as a synthetic bone graft material. *J Biomed Mater Res B Appl Biomater.* 2003;67(1):603-9.

Mulconrey DS, Bridwell KH, Flynn J, Cronen GA, Rose PS. Bone morphogenetic protein (RhBMP-2) as a substitute for iliac crest bone graft in multilevel adult spinal deformity surgery: minimum two-year evaluation of fusion. *Spine.* 2008;33(20):2153-9.

Nagao H, Tachikawa N, Miki T, Oda M, Mori M, Takahashi K, Enomoto S. Effect of recombinant human bone morphogenetic protein-2 on bone formation in alveolar ridge defects in dogs. *Int J Oral Maxillofac Surg.* 2002;31(1):66-72.

Norton MR, Gamble C. Bone classification: an objective scale of bone density using the computerized tomography scan. *Clin Oral Implants Res.* 2001;12(1):79-84.

Okafuji N, Shimizu T, Watanabe T, Kimura A, Kurihara S, Arai Y, Furusawa K, Hasegawa H, Kawakami T. Three-dimensional observation of reconstruction course of rabbit experimental mandibular defect with rhBMP-2 and atelocollagen gel. *Eur J Med Res.* 2006;11(8):351-4



Parfitt AM. The cellular basis of bone remodelling: the quantum concept re-examined in light of recent advances in the cell biology of bone. *Calcif Tissue Int.* 1984;36 Suppl 1:S37-45.

Park J, Ries J, Gelse K, Kloss F, von der Mark K, Wiltfang J, Neukam FW, Schneider H. Bone regeneration in critical size defects by cell-mediated BMP-2 gene transfer: a comparison of adenoviral vectors and liposomes. *Gene Ther.* 2003;10(13):1089-98.

Pekkarinen T, Jämsä T, Määttä M, Hietala O, Jalovaara P. Reindeer BMP extract in the healing of critical-size bone defects in the radius of the rabbit. *Acta Orthop.* 2006;77(6):952-9.

Ren T, Ren J, Jia X, Pan K. The bone formation in vitro and mandibular defect repair using PLGA porous scaffolds. *J Biomed Mater Res A.* 2005;74(4):562-9.

Revell PA. Histomorphometry of bone. *J Clin Pathol.* 1983;36(12):1323-31.

Rho JY, Kuhn-Spearing L, Zioupos P. Mechanical properties and the hierarchical structure of bone. *Med Eng Phys.* 1998;20(2):92-102.

Russell AP. The mammalian masticatory apparatus: an introductory comparative exercise. Tested studies for laboratory teaching, Proceedings of the 19th Workshop/Conference of the Association for Biology Laboratory Education, Karcher SJ. 1998;19:271-286.

Saadeh PB, Khosla RK, Mehrara BJ, Steinbrech DS, McCormick SA, DeVore DP, Longaker MT. Repair of a critical size defect in the rat mandible using allogenic type I collagen. *J Craniofac Surg.* 2001;12(6):573-9.

Schliephake H, Jamil MU, Knebel JW. Experimental reconstruction of the mandible using polylactic acid tubes and basic fibroblast growth factor in alloplastic scaffolds. *J Oral Maxillofac Surg.* 1998;56(5):616-26.

Schliephake H, Weich HA, Dullin C, Gruber R, Frahse S. Mandibular bone repair by implantation of rhBMP-2 in a slow release carrier of polylactic acid—an experimental study in rats. *Biomaterials.* 2008;29(1):103-10.

Sherris DA, Murakami CS, Larrabee WF Jr, Bruce AG. Mandibular reconstruction with transforming growth factor-beta1. *Laryngoscope.* 1998;108(3):368-72.

Shigeno K, Nakamura T, Inoue M, Ueda H, Kobayashi E, Nakahara T, Lynn AK, Toba T, Yoshitani M, Fukuda S, Kawanami R, Shimizu Y. Regenerative repair of the mandible using a collagen sponge containing TGF-beta1. *Int J Artif Organs.* 2002;25(11):1095-102.

Sikavitsas VI, Temenoff JS, Mikos AG. Biomaterials and bone mechanotransduction. *Biomaterials.* 2001;22(19):2581-93.

Srouji S, Rachmiel A, Blumenfeld I, Livne E. Mandibular defect repair by TGF-beta and IGF-1 released from a biodegradable osteoconductive hydrogel. *J Craniomaxillofac Surg.* 2005;33(2):79-84.

Thibodeau GA & Patton KT. *Anatomy & Physiology.* Sixth Edition, Missouri: Mosby Elsevier, 2007

Toriumi DM, Kotler HS, Luxenberg DP, Holtrop ME, Wang EA. Mandibular reconstruction with a recombinant bone-inducing factor. Functional, histologic, and biomechanical evaluation. *Arch Otolaryngol Head Neck Surg.* 1991;117(10):1101-12.

Toriumi DM, O'Grady K, Horlbeck DM, Desai D, Turek TJ, Wozney J. Mandibular reconstruction using bone morphogenetic protein 2: long-term follow-up in a canine model. *Laryngoscope.* 1999;109(9):1481-9.

Trantolo DJ, Sonis ST, Thompson BM, Wise DL, Lewandrowski KU, Hile DD. Evaluation of a porous, biodegradable biopolymer scaffold for mandibular reconstruction. *Int J Oral Maxillofac Implants.* 2003;18(2):182-8.

Ueki K, Takazakura D, Marukawa K, Shimada M, Nakagawa K, Takatsuka S, Yamamoto E. The use of polylactic acid/polyglycolic acid copolymer and gelatin sponge complex containing human recombinant bone morphogenetic protein-2 following condylectomy in rabbits. *J Craniomaxillofac Surg.* 2003;31(2):107-14.

Veronese FM, Marsilio F, Lora S, Caliceti P, Passi P, Orsolini P. Polyphosphazene membranes and microspheres in periodontal diseases and implant surgery. *Biomaterials*. 1999;20(1):91-8.

Wang H, Springer IN, Schildberg H, Acil Y, Ludwig K, Rueger DR, Terheyden H. Carboxymethylcellulose-stabilized collagenous rhOP-1 device-a novel carrier biomaterial for the repair of mandibular continuity defects. *J Biomed Mater Res A*. 2004;68(2):219-26.

Wheeler DL, Eschbach EJ, Hoellrich RG, Montfort MJ, Chamberland DL. Assessment of resorbable bioactive material for grafting of critical-size cancellous defects. *J Orthop Res*. 2000;18(1):140-8.

Wikesjö UM, Sorensen RG, Kinoshita A, Wozney JM. RhBMP-2/ $\alpha$ BSM induces significant vertical alveolar ridge augmentation and dental implant osseointegration. *Clin Implant Dent Relat Res*. 2002;4(4):174-82.

Wurzler KK, Heisterkamp M, Bohm H, Kubler NR, Sebald W, Reuther JF. [Mandibular reconstruction with autologous bone and osseoinductive implant in the Gottingen minipig] *Mund Kiefer Gesichtschir*. 2004;8(2):75-82.

Xu J, Meng Z, Yang Z. [Polylactic acid combined with recombinant human bone morphogenetic protein and basic fibroblast growth factor to repair the mandibular defects in rabbits] *Zhonghua Kou Qiang Yi Xue Za Zhi*. 1999;34(3):168-71.

Yaszemski MJ, Payne RG, Hayes WC, Langer R, Mikos AG. Evolution of bone transplantation: molecular, cellular and tissue strategies to engineer human bone. *Biomaterials*. 1996;17(2):175-85.

Zanchetta P, Lagarde N, Guezennec J. A new bone-healing material: a hyaluronic acid-like bacterial exopolysaccharide. *Calcif Tissue Int*. 2003;72(1):74-9.

Zellin G, Beck S, Hardwick R, Linde A. Opposite effects of recombinant human transforming growth factor-beta 1 on bone regeneration in vivo: effects of exclusion of periosteal cells by microporous membrane. *Bone*. 1998;22(6):613-20.

## **Abstracts**

## **Bone regeneration in critical-size bone defects using tissue engineering.**

**Preliminary Report.** K. Naudi, A. Ayoub, D. Lappin, J. McMahon, L. Di Silvio. University of Glasgow Research Seminar, 2008 (Awarded **First Prize** for best project presentation).

### **Aims**

To assess the quality of bone regeneration in a critical size osteoperiosteal mandibular discontinuity defect using BMP-7 on a tricalcium phosphate (TCP) scaffolding with mesenchymal stem cells. Would the quality of bone regeneration be better if mesenchymal stem cells or rhBMP-7 are used with the scaffolding for the reconstruction? Would the combination of mesenchymal stem cells, rhBMP-7 and TCP improve the quality of bone regeneration?

### **Materials and Methods**

Nine adult white New Zealand rabbits (3.0-4.0kg) were used. The rabbits were divided into two treatment groups; in 6 cases the defect was filled with rhBMP-7 in the TCP, in the remaining 3 cases the defect was filled with the TCP alone. Radiographic assessment with plain radiographs was carried out at 0, 4, 8, and 12 weeks. Three months post-operatively the animals were sacrificed, the mandibles were removed and the surgical sites assessed radiographically; with plans for histomorphometric analysis and mechanical testing.

### **Results**

Initial radiographic analyses demonstrated evidence of significantly better graft remodelling occurring within the group that received the rhBMP-7 and TCP.

**Bone regeneration in critical-size mandibular defects using tissue engineering**, K. Busuttill Naudi, A. Ayoub, J. McMahon, D. Lappin, L. Di Silvio. United Kingdom Society for Biomaterials Annual Conference, Liverpool 2008.

### **Introduction**

The gold standard for bone grafting is still autologous cortical and cancellous bone from the iliac crest due to its combined osteogenic, osteoinductive and osteoconductive properties. Autograft availability is, however, limited and often associated with donor site morbidity.

### **Aims**

The aim was to assess the quality of bone regeneration in a critical-size osteoperiosteal mandibular discontinuity defect using bone morphogenetic protein 7 (rhBMP-7) on a tricalcium phosphate (TCP) scaffolding. Would the quantity and shape of bone regenerate be better if rhBMP-7 had been used with scaffolding for mandibular reconstruction?

### **Materials & Methods**

This investigation was conducted on nine adult white New Zealand rabbits (3.0-4.0kg). In all the cases a critical size continuity defect was created in the anterior part of the mandible. Under general anaesthesia the mandible was exposed by raising a mucoperiosteal flap via a submandibular approach. A 12mm long 2.0mm diameter titanium screw was inserted through the body of the mandible in the region of the first premolars to reinforce the lower border



(Figure 1). A straight body osteotomy was performed anterior to the first premolar, and the second cut was made across midline in the region of the mandibular symphysis. The segment of bone was removed with the covering periosteum and incisor tooth (Figure 2 & 3).



Figure 1. Rabbit mandible



Figure 2. Surgical defect

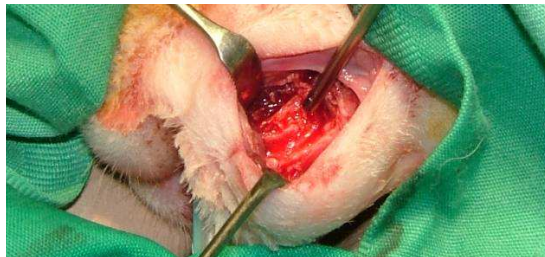


Figure 3. Surgical defect created in one of the cases

The rabbits were divided into two groups. In six cases the critical-size defect was filled with rhBMP-7 in a prefabricated scaffolding of TCP (Figure 4). In the remaining cases the defect was filled with the prefabricated scaffolding alone. Radiographic assessments with plain radiographs were carried out at 0, 4, 8, and 12 weeks follow-up.



Figure 4. Scaffolding in defect



Figure 5. Regenerated bone

Three months post-operatively the animals were sacrificed, the mandibles were removed and the areas where the critical-size defect was created were assessed with cone beam CT radiographs.

## Results

**Clinical Findings.** The regenerated bone (Figure 5) appeared to be continuous with the adjacent bone, and had remodelled to a size commensurate with the defect size and there was no incidence of infection.

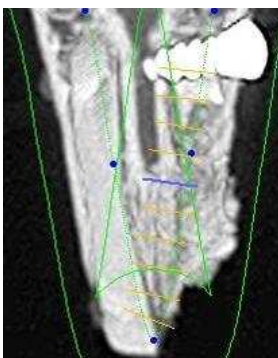


Figure 6. Axial CT

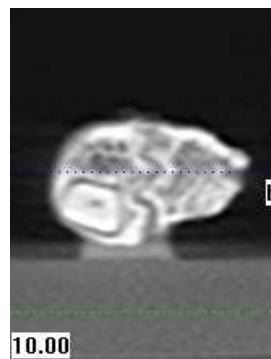


Figure 7. Coronal CT

**Radiographic Findings.** Both plain radiography & cone beam CT scanning (Figures 6&7) showed significant bone regeneration in the surgical defects

repaired with the TCP scaffolding containing rhBMP-7 when compared to the sites repaired with TCP scaffolding alone, where in the latter the healing was incomplete with no bridging of the surgical defect.

### **Conclusion**

The restoration of critical-size mandibular defects in rabbit mandibles using a combination of rhBMP-7 with TCP scaffolding was found to be a successful technique. This would suggest the possibility of future clinical applications.

**Bone regeneration in a critical-size mandibular defect using tricalcium phosphate and bone morphogenetic protein 7.** K. Busuttill Naudi, A. Ayoub, J. McMahon, D. Lappin, L. Di Silvio. Triennial Conference of the Royal College of Physicians and Surgeons of Glasgow 2008

### **Aims**

The aim was to assess the quality and quantity of bone regeneration in a critical-size osteoperiosteal mandibular discontinuity defect using bone morphogenetic protein 7 (rhBMP-7) on a tricalcium phosphate (TCP) scaffolding.

### **Methodology**

The investigation was conducted on nine adult white New Zealand rabbits (3.0-4.0kg). In all cases a unilateral straight body osteotomy was performed anterior to the first premolar following insertion of a titanium screw to reinforce the lower border. The segment of bone was removed with the covering periosteum and incisor tooth. In six cases the critical-size defect was filled with rhBMP-7 in a prefabricated scaffolding of TCP (Group 1). In the remaining three cases the defect was filled with the TCP alone (Group 2). Radiographic assessments with plain radiographs were carried out at monthly intervals. Three months post-operatively the animals were sacrificed and the mandibles were removed. The surgical sites were assessed with cone beam CT radiography, mechanical testing and histomorphometric analysis.

## **Results**

Clinically the regenerated bone appeared to be continuous with the adjacent bone and had remodelled to a size commensurate with the defect size. Both plain radiography & cone beam CT scanning showed significantly more bone regeneration in group 1, while in group 2 there was incomplete healing with no bridging of the surgical defect.

Results of the mechanical testing and histomorphometric analysis will follow.

## **Conclusions**

The restoration of critical-size mandibular defects in rabbit mandibles using a combination of rhBMP-7 with TCP scaffolding was found to be a successful technique. This could suggest the possibility of future clinical applications.

**Bone regeneration in a critical-size mandibular defect using bone morphogenetic protein 7 on tricalcium phosphate scaffolding.** K. Busuttill Naudi, A. Ayoub, J. McMahon, D. Lappin, L. Di Silvio. 19<sup>th</sup> International Conference on Oral and Maxillofacial Surgery, Shanghai China 2009

### **Objectives**

To assess radiographically, mechanically and histologically the quality and quantity of bone regeneration in a critical-size osteoperiosteal mandibular discontinuity defect following the application of bone morphogenetic protein 7 (rhBMP-7) on a tricalcium phosphate (TCP) scaffolding.

### **Methods**

The investigation was conducted on nine adult New Zealand white rabbits (3.0-4.0kg). In all cases a unilateral, osteoperiosteal mandibular continuity critical-size defect was created. In six cases the critical-size defect was filled with rhBMP-7 in a prefabricated scaffolding of TCP (Group 1). In three cases the TCP was used alone (Group 2). Plain radiographs were taken at monthly intervals. Three months post-operatively the animals were sacrificed, and the surgical sites were assessed with cone beam CT radiography, mechanical testing and histomorphometric analysis.

### **Results**

Clinically the regenerate appeared to be continuous with the adjacent bone and was remodelled to a size commensurate with the defect size. Both plain radiography & cone beam CT scanning showed significantly more bone

regeneration in group 1, while in group 2 there was incomplete healing with no bridging of the surgical defect. Mechanical testing gave variable results but the failure moments for group 1 were consistently higher.

### **Conclusions**

The restoration of critical-size mandibular defects in rabbit mandibles using a combination of rhBMP-7 with TCP scaffolding was successful. This would suggest the possibility of future clinical applications.

**Histomorphometric evaluation of bone regenerate in a critical-size defect in the rabbit mandible treated with tricalcium phosphate scaffolding loaded with bone morphogenetic protein 7.** K. Busuttill Naudi, A. Ayoub, D. Lappin, J. McMahon, L. Di Silvio, K. Hunter. United Kingdom Society for Biomaterials Annual Conference, Belfast 2009.

## **Introduction**

Bone defects in the human maxillofacial region which arise as a result of trauma, infection or tumour resection cause significant aesthetic, functional and psychological disabilities. The gold standard for reconstruction of these defects has been autologous cortical and cancellous bone graft. Autograft availability is, however, limited and often associated with donor site morbidity. Current trends have been to explore methods that move away from using autografts by using various bone substitutes.

## **Aims**

The aim was to evaluate the quality and quantity of bone regenerated in a critical-size mandibular defect in the rabbit model, reconstructed with tricalcium phosphate (TCP) scaffolding and bone morphogenetic protein 7 (rhBMP-7).

## **Materials and Methods**

Nine adult New Zealand white rabbits (3.0-4.0kg) were used; in six cases the critical-size defect was filled with the rhBMP-7 in a TCP scaffolding (Group 1), and in three cases the TCP was used alone (Group 2).



### *Surgical procedure*

In each case a unilateral osteoperiosteal mandibular body critical-size defect was created (Figure 1). The prefabricated tricalcium phosphate scaffolds, with or without rhBMP-7, were then secured in the surgical defect (Figure 2). Three months post-operatively the cases were sacrificed and the mandibles were surgically removed.



Figure 1. Dry mandible.

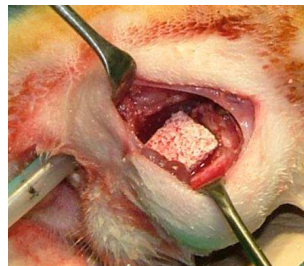


Figure 2. TCP in defect.

### *Specimen preparation*

The surgical areas were removed from the rest of the mandible. The mandibular sections were decalcified in 10 % formic acid for 1 week before sectioning them in a sagittal plane. The two halves of the mandible section were embedded separately and one section from each block was stained using haematoxylin and eosin (H&E).

### *Quantitative analysis of bone content*

The sections were viewed at 20x (Figure 3) and 40x magnification. Three fields were selected; the proximal end of the regenerated tissue, adjacent to the premolar tooth root, a mid surgical field and the distal end of the regenerated tissue, towards the symphysis.

These fields were captured digitally on a photo microscope (Olympus UK Ltd, Watford, UK) fitted with a Colourview IIIu camera using CellB software. The digital image was opened in Adobe Photoshop Elements 2.0 and after background correction was converted to greyscale. Using the threshold function, unstained areas (with no bone formation) were converted to white and then the eosin stained areas (with bone formation) were rendered black to create a binary image (Figure 4). The binary image was then imported into ImageTool image analysis software (version 3.00, UTHSCSA, Texas USA). The proportion of black and white pixels was counted and expressed as a percentage of the total image.

#### *Statistical analysis*

Statistical analysis of the results was conducted using the Student's t-test.



Figure 3. H&E (x20).



Figure 4. Binary image.

## **Results**

### *Gross histological appearance*

There was more bone regeneration within the cases of group 1, with evidence of both woven and lamellar types of bone (Figure 5). There was union at the surgical site with no cartilage formation. In group 1 some cases showed hints of outer cortex formation. No evidence of bone marrow formation was seen and

the regenerated bone was confined to the area that received the scaffold, with no calcification in the surrounding soft tissues. The TCP was also resorbed more completely in group 1. Very little bone was formed in the cases where the defect was filled with TCP alone (Group 2).

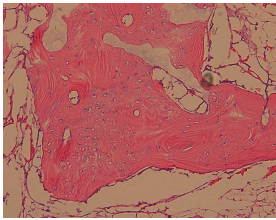


Figure 5. Lamellar bone.

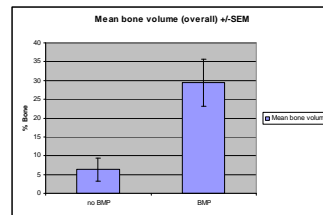


Figure 6. Chart of bone volume.

#### *Binary image analysis*

The overall mean of the percentage regenerated bone volume, in all the three fields tested, in group 1 was  $29.41\% \pm 6.25$ , while that for group 2 was  $6.35\% \pm 3.08$  (Figure 6). The difference between the groups was statistically significant,  $p = 0.014$ . If the percentage of regenerated bone volume in the mid surgical field alone was compared between groups, the value for group 1 was again statistically significantly higher than that of group 2,  $p = 0.009$  (Group 1,  $22.8\% \pm 5.0$ ; group 2,  $2.9\% \pm 1.8$ ).

#### **Conclusions**

Analysis of the regenerate in the treated critical-size defects in this rabbit model showed that TCP loaded with rhBMP-7 was significantly superior in its capacity for bone regeneration than TCP alone. This could have significant clinical applications.

## **Mechanical Testing of Bone Regenerated with BMP-7 in TCP Scaffolding.**

K. Busuttill Naudi, J. Barbenel, J. McMahon, D. Lappin, L. Di Silvio, A. Ayoub.

British Society for Dental Research Annual Conference, Glasgow 2009.

### **Introduction**

The gold standard for bone grafting is still autologous cortical and cancellous bone. This is due to the combined osteogenic, osteoinductive and osteoconductive properties of the graft. Autograft availability is, however, limited and often associated with donor site morbidity. The current trends are to explore other methods that move away from using autografts for the repair of these defects by using various bone substitutes.

### **Objectives**

The objective was to assess the physical properties of the bone regenerated in a critical-size unilateral mandibular defect in the rabbit model treated with bone morphogenetic protein 7 (rhBMP-7) in a tricalcium phosphate (TCP) scaffolding.

### **Methods**

Nine adult New Zealand white rabbits (3.0-4.0kg) were used; in six cases the critical-size defect was filled with the rhBMP-7 in a TCP scaffolding (Group 1), and in three cases the TCP was used alone (Group 2). Three months post-operatively the cases were sacrificed and the mandibles were surgically removed. The mandibles were divided into hemi-mandibles at the symphysis and mounted within custom made aluminium blocks that were mounted into a

BOSE Electroforce® 3300 test instrument. The mechanical properties of the regenerated bone in the surgical sites were then tested by applying the principle of cantilevers. The maximum load that occurred at fracture was recorded and the distance between the loading point and the site of failure on the dorsal surface of the specimen was measured. The failure moment was then calculated.

### **Results**

The failure moments for group 2 were found to be very low (0-48mNm) while those for group 1 were higher but there was considerable variation between the cases (55-2115mNm). Some of the cases in group 1 achieved failure moments comparable to normal untreated bone.

### **Conclusions**

The repair of critical-size mandibular defects with rhBMP-7 in TCP scaffolding could result in the regeneration of bone with mechanical properties similar to those of natural bone.

**Radiographic evaluation of the bony regenerate in a critical-size mandibular defect filled with mesenchymal stem cells on a tricalcium phosphate scaffolding.** K. Naudi, R. Alfotawei, A. Ayoub, D. Lappin, J. McMahon, K. Hunter, J. Barbenel, L. Di Silvio. Association of British Academic Oral and Maxillofacial Surgeons Annual Conference, Belfast 2009.

The gold standard for bone grafting is still autologous cortical and cancellous bone. This is due to the combined osteogenic, osteoinductive and osteoconductive properties of the graft. Autograft availability is, however, limited and often associated with donor site morbidity. The current trend is to explore methods that move away from using autografts to the repair of these defects by using various bone substitutes.

The aim of this project is to assess the radiographic properties of the bone regenerated in a critical-size unilateral mandibular defect in the rabbit model treated with mesenchymal stem cells seeded onto a tricalcium phosphate (TCP) scaffolding.

Eight adult New Zealand white rabbits (3.0-4.0kg) were used; in six cases the critical-size defect was filled with the mesenchymal stem cells seeded onto the TCP scaffolding (Group 1), and in two cases the TCP was applied alone (Group 2). Three months post-operatively the cases were sacrificed and the mandibles were surgically removed. The explanted mandibles were then scanned using an i-CAT<sup>®</sup> cone beam CT scanner.

The results were compared with our previous investigations where bone morphogenetic protein 7 and TCP were used for the repair of similar critical-size defects. In these cases there had been reasonable bone formation. The actual differences in the pattern of bone formation will be presented and its clinical significance will be discussed.